

~~CONFIDENTIAL~~

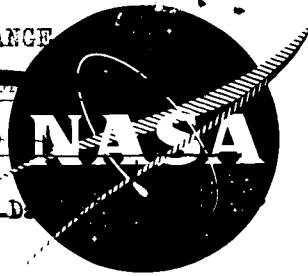
NASA CR-72047

CLASSIFICATION CHANGE

TO: UNCLASSIFIED

By authority of T.D. No. 73-2

Changed by E. R. Smith



DETERMINATION OF THE RESISTANCE OF TUNGSTEN-UO₂ COMPOSITES TO CYCLIC THERMAL STRAINS (U)


by
J.B. Conway and J. F. Collins

N73-71379

Unclas
54959

00/99

Prepared for
NATIONAL AERONAUTICS AND SPACE ADMINISTRATION
Contract NAS3-6213

NUCLEAR MATERIALS and PROPULSION OPERATION
NUCLEAR TECHNOLOGY DEPARTMENT
NUCLEAR ENERGY DIVISION
GENERAL  ELECTRIC

Cincinnati, Ohio 45215

~~CONFIDENTIAL~~

~~RESTRICTED DATA~~

THIS DOCUMENT CONTAINS INFORMATION OF
A TECHNICAL NATURE AND IS NOT TO BE
DISCLOSED TO THE PUBLIC OR TO AN UN-
AUTHORIZED PERSON WITHOUT PERMISSION.

ALL INFORMATION CONTAINED HEREIN IS UNCLASSIFIED
DATE 10/1/99 BY 60322 UCBAW/BK/DAK

(NASA-CR-72047) DETERMINATION OF THE
RESISTANCE OF TUNGSTEN-UO₂ COMPOSITES TO
CYCLIC THERMAL STRAINS Final Report
(General Electric Co.) 85 p

Unr 72047
(NASA CR OR TMX OR AD NUMBER)
(CATEGORY)
FACIL

NOTICE

This report was prepared as an account of Government sponsored work. Neither the United States, nor the National Aeronautics and Space Administration (NASA), nor any person acting on behalf of NASA:

- A.) Makes any warranty or representation, expressed or implied, with respect to the accuracy, completeness, or usefulness of the information contained in this report, or that the use of any information, apparatus, method, or process disclosed in this report may not infringe privately owned rights; or
- B.) Assumes any liabilities with respect to the use of, or for damages resulting from the use of any information, apparatus, method or process disclosed in this report.

As used above, "person acting on behalf of NASA" includes any employee or contractor of NASA, or employee of such contractor, to the extent that such employee or contractor of NASA, or employee of such contractor prepares, disseminates, or provides access to, any information pursuant to his employment or contract with NASA, or his employment with such contractor.

~~CONFIDENTIAL~~

066-7432
NASA CR-72047

INFORMATION
AFFECTED
STATE
LAWS
TRANS
IN AN
PROHIBIT

Final Report
DETERMINATION OF THE RESISTANCE OF TUNGSTEN-UO₂
COMPOSITES TO CYCLIC THERMAL STRAINS (U)

by
J. B. Conway and J. F. Collins

Prepared for
NATIONAL AERONAUTICS AND SPACE ADMINISTRATION
CONTRACT NAS 3-6213

August 30, 1966

Technical Management
NASA Lewis Research Center
Cleveland, Ohio
Materials and Structures Division
Neal T. Saunders

DOWN FROM AUTOMATIC
CONFIRMATION

NUCLEAR MATERIALS and PROPULSION OPERATION
NUCLEAR TECHNOLOGY DEPARTMENT
NUCLEAR ENERGY DIVISION

GENERAL  ELECTRIC

Cincinnati, Ohio 45215

~~CONFIDENTIAL~~

~~CONFIDENTIAL~~

DETERMINATION OF THE RESISTANCE OF TUNGSTEN- UO_2
COMPOSITES TO CYCLIC THERMAL STRAINS

by

J. B. Conway and J. F. Collins

X 66-51641

ABSTRACT

Tungsten clad composites containing 10, 20, and 30 volume percent of a $\text{UO}_2\text{-Y}_2\text{O}_3$ phase dispersed in tungsten as the core material were subjected to a thermal cycling treatment between room temperature and 2500°C in helium. Each of fifteen test specimens was subjected to fifty thermal cycles with inspections after every five cycles. No clad cracking was observed in any of the specimens. However, in all but two of the tests, a decrease in specimen diameter occurred. It appears that some additional sintering has taken place to bring about the observed diameter decrease.

Linear thermal expansion data for the three core compositions are presented to 2500°C .

Author

~~CONFIDENTIAL~~

TABLE OF CONTENTS

	Page
I. SUMMARY	1
II. INTRODUCTION	3
III. SPECIMEN FABRICATION	5
General Specimen Description	5
Materials.....	5
Fuel Preparation.....	7
Core Fabrication.....	9
Machining of Cores	10
Cladding Preparation	10
Specimen Assembly and Bonding	10
Fabrication of Thermal Expansion Specimens	14
Fabrication of Type D Specimens	14
IV. EXPERIMENTAL TESTING PROCEDURES.....	19
Thermal Expansion Measurements	19
Thermal Cycling Tests	21
V. RESULTS AND DISCUSSION	25
Thermal Expansion Data	25
Thermal Cycling Results.....	27
a) Type A, B, and C Specimens	27
b) Type D Specimens	36
c) End-Plate Growth Studies	38
Post-Test Metallographic Evaluation	39
a) Type A, B, and C Specimens.....	39
b) Type D Specimens	41
VI. SPECIAL PROGRAM HIGHLIGHTS	45
VII. CONCLUSIONS AND RECOMMENDATIONS.....	47
VIII. REFERENCES	49
IX. SUPPLEMENTARY INFORMATION	51
Appendix A - Raw Materials Analyses	52
Appendix B - Evaluation of Fuel Types	53
Appendix C - Gas Pressure Bonding Studies	57
Appendix D - Alternate Fabrication Procedures for Type D Specimens ..	58
Appendix E - Thermal Cycling Test Procedures and Test Data	60

FIGURES

	Page
1 - Configuration and dimensions of Type A, B, C, and D specimens	6
2 - Fabrication procedure for clad composite specimens	8
3 - Photomicrographs of cores of Types A, B, and C specimens as-sintered at 2500°C	11
4 - Photomicrographs of core-cladding interface of specimens showing normal bonding achieved by autoclaving and abnormal separation of cladding after proof testing a defective specimen at 2500°C	13
5 - Photomicrograph of transverse section of specimen D-5 in as-fabricated condition showing W-30 percent fuel core, W-20 percent fuel sleeve, and vapor deposited tungsten coating	17
6 - Special specimen assembly for use in making diameter measurements optically in thermal expansion apparatus	21
7 - Linear thermal expansion characteristics of unclad 80 W-20 (UO ₂ -Y ₂ O ₃) measured in helium	26
8 - A comparison of the linear thermal expansion data for unclad Type A, B, and C compositions measured in helium	26
9 - Six tungsten clad W-(UO ₂ -Y ₂ O ₃) specimens after being subjected to 50 thermal cycles between room temperature and 2500°C in helium	28
10 - Effect of number of thermal cycles on percent change in diameter of Type A, B, and C specimens cycled between room temperature and 2500°C in helium; 10-minute dwell at high temperature	29
11 - Effect of number of thermal cycles on percent change in diameter of Type A, B, and C specimens cycled between room temperature and 2500°C in helium; 1-hour dwell at high temperature	29
12 - Effect of total exposure time at 2500°C on diameter changes in Type A, B, and C specimens	30
13 - Effect of number of thermal cycles between room temperature and 2500°C on the sample length for Type A, B, and C specimens	31
14 - A comparison of some diameter changes as influenced by exposure time at 2500°C for Type A, B, and C specimens	34
15 - Photograph showing Type D specimens, two in the as-fabricated condition, and three (D-2, D-3, and D-4) after test	37
16 - Change in specimen diameter as a function of number of thermal cycles (10-minute dwell) from room temperature to 2500°C for Type D specimens..	37
17 - Percent increase in thickness as a function of the number of thermal cycles from room temperature to 2500°C for W - 25Re - 30Mo end-plates...	38
18 - Photomicrographs of core-cladding interface of Type A, B, and C specimens after 50 thermal cycles to 2500°C using the Type 1 cycle	40
19 - Photomicrographs of core-cladding interface of Type A, B, and C specimens after 50 thermal cycles to 2500°C using the extended cycle	42
20 - Photomicrographs of core-sleeve interface area of specimen D-2 after 50 thermal cycles to 2500°C using fast cycle	44

	Page
B-1 - UO_2 - 10 mole percent Y_2O_3 , solutioned at 2000°C for 8 hours in H_2 . Crushed and screened to -270/+400 mesh. Particle range 30 to 180 microns.	54
B-2 - W - 20 v/o (UO_2 - Y_2O_3) core structure as sintered at 2200°C for 2 hours. Density was 92.3% of theoretical.	54
E-1 - Tungsten heating element used in thermal cycling furnace	60
E-2 - Photograph of high temperature thermal cycling furnace and associated equipment.....	61
E-3 - Typical temperature - time relationship obtained during thermal cycling test with 10-minute dwell at 2500°C	63

TABLES

	Page
1 - Yttria content of various lots of agglomerated fuel and corresponding cores prepared	9
2 - History of specimens of Types A, B, and C.....	12
3 - Inspection data obtained for Type D specimens as coated with tungsten by vapor deposition.....	15
4 - Measurements of control specimen D-5 in the as-fabricated condition	16
5 - Schedule of thermal cycling tests for specimen Types A, B, C, and D	23
6 - Summary of inspection results obtained after 50 thermal cycles between room temperature and 2500°C	32
B-1 - Sintered densities of W- UO_2 - Y_2O_3 core composites containing high fired fuel particles	55
B-2 - Sintered densities of W- UO_2 - Y_2O_3 core composites containing agglomerated fuel particles	56
E-1 - Summary of inspection results obtained in thermal cycling tests	65

[REDACTED]

DETERMINATION OF THE RESISTANCE OF TUNGSTEN- UO_2 COMPOSITES TO CYCLIC THERMAL STRAINS

by

J. B. Conway and J. F. Collins

Nuclear Materials and Propulsion Operation
General Electric Company
Cincinnati, Ohio 45215

I. SUMMARY

A study was made to determine the effect of up to 50 thermal cycles between room temperature and 2500°C in helium on the dimensional stability and general integrity of several tungsten clad tungsten-uranium dioxide-yttrium oxide composites. Four tungsten clad specimens of each of three core compositions, W-10, 20, and 30 volume percent ($\text{UO}_2\text{-Y}_2\text{O}_3$), were evaluated in two different types of thermal cycling treatments, one involving a 10-minute dwell time at maximum temperature and one employing a 1-hour dwell time. In addition, three tungsten clad specimens consisting of a W-30 v/o ($\text{UO}_2\text{-Y}_2\text{O}_3$) core with a 0.020 inch thick sleeve of the W-20 v/o ($\text{UO}_2\text{-Y}_2\text{O}_3$) composition were evaluated in the 10-minute dwell tests.

Inspections after every five thermal cycles, up to 50 cycles, failed to identify any cracks in the specimen cladding. It was noted, however, that in all twelve specimens of the W-10, 20, and 30 v/o ($\text{UO}_2\text{-Y}_2\text{O}_3$) compositions a decrease in diameter had occurred. While these decreases were a function of the number of thermal cycles imposed, no obvious relationship with composition was observed. However, the percentage decrease in specimen diameter was greater in the 1-hour dwell tests than in the 10-minute dwell tests suggesting that additional specimen sintering was responsible for the observed diameter decreases. Supplementary tests of pure tungsten specimens substantiated the additional sintering concept.

As the rate at which the diameter decreased was higher in thermal cycling tests than in isothermal tests at the same test temperature, it was concluded that higher sintering rates and higher final sintered densities appear to be obtainable at 2500°C if the temperature is cycled during the sintering operation.

Results obtained with the special specimen construction involving the composite core-sleeve combination indicated no specimen cracking but the dimensional changes were not consistent within themselves nor did they agree with the results obtained with the other specimens. In two of the three specimens tested, an increase in specimen diameter was observed. No current explanation of the behavior is available.

Measurements of the linear thermal expansion characteristics of the unclad core compositions of W-10, 20, and 30 v/o ($\text{UO}_2\text{-Y}_2\text{O}_3$) to 2500°C in helium showed the W-10 v/o ($\text{UO}_2\text{-Y}_2\text{O}_3$) composition to be essentially identical to the data for pure tungsten. Slightly higher expansions were obtained as the fuel content increased above 10 percent.

~~CONFIDENTIAL~~

II. INTRODUCTION

Many fuel element designs for use in nuclear reactors are based on the dispersion concept in which particles of UO_2 are intimately blended with fine metal powder. Usually, the metal forms the continuous matrix in these constructions with the fuel particles uniformly distributed throughout the matrix. In this way, the fuel-bearing portion of the element is strengthened due to the metal matrix and the very low thermal conductivity of UO_2 is partially offset by employing small particle sizes and having these completely surrounded by a high conductivity metal phase.

Recent studies of high temperature nuclear power plants have identified a need for special dispersion-type fuel elements using refractory metals as the continuous matrix. These metals, such as W, Mo, Ta, Re and alloys of these metals, offer the advantage of high melting points and high temperature strength. For rocket propulsion systems, for example, the desired performance levels are achieved only by operating temperatures close to 2500°C ; and, hence, these refractory metals offer one of the few practical alternatives.

In a space propulsion system being investigated by NASA Lewis Research Center, a dispersion-type fuel element employing uranium dioxide (with small additions of yttrium oxide) dispersed in a continuous tungsten matrix is suggested (Reference 1). Current estimates indicate that operation for about 10 hours at 2500°C (4532°F) in hydrogen will be required. In one NASA fuel element design configuration, a honeycomb-type structure with 0.020 inch thick walls of a tungsten-uranium dioxide composition separating hexagonal flow channels 0.125 inch wide is under study. Since the nuclear heating which will take place in this structure will induce thermal gradients, some evaluation of the ability of the fuel material to accommodate these gradients is required. It also is pertinent to investigate the ability of the W- UO_2 material to withstand the thermal strains induced in a thermal cycling type of operation.

In the present study certain tungsten-uranium dioxide-yttrium oxide compositions, clad with tungsten, were subjected to repeated thermal cycles to determine the ability of these materials to withstand this type of treatment. Previous experience at GE-NMPO (Reference 2), as well as at other laboratories, has indicated that these types of materials are not dimensionally stable when subjected to a number of thermal cycles (Reference 3). In most cases an increase in specimen diameter has been observed, the magnitude of which has been a function of the specimen materials, the maximum temperature employed in the thermal cycling test, and the rate at which the temperature is changed during the thermal cycling. Since these dimensional changes represent plastic deformation of the cladding material, the possibility of cracks developing in the clad is always present. Particularly was this true in the case of the specimens proposed for use in the present program since the ductility of tungsten is not considered sufficient to allow much deformation without cracking.

Evaluations of the ability of the specimens used in this investigation to withstand a thermal cycling treatment were made by cycling between room temperature and 2500°C in helium. All the specimens were heated in a resistively heated tungsten tube furnace employing a

~~CONFIDENTIAL~~

heating rate of about 40°C/minute and a cooling rate of some 14°C/minute. Each specimen was inspected after every five (5) thermal cycles and changes in length, diameter, volume and weight were measured. In addition, the specimens were inspected for cracks in the tungsten cladding which may have resulted from induced thermal strains. Contract specifications had indicated that all specimens were to be tested either until cracking was observed or for fifty (50) thermal cycles, whichever occurred first. Actually no cracking (except in blisters in a few specimens) was observed and hence every specimen tested received the full fifty thermal cycles.

ACKNOWLEDGMENTS

Throughout the course of this program special contributions were made by the Metallographic and Crystallographic Unit, the Analytical Chemistry Unit, and the Manufacturing Operation of GE-NMPO. These efforts were pertinent to the successful completion of the many aspects of this extensive study. In addition, special acknowledgement is given to N. P. Fairbanks and R. E. Seibert for fuel and specimen preparation, to D. G. Salyards and C. P. Johnstone for furnace design and specimen testing, to R. A. Hein for thermal expansion measurements, to W. R. Yario and C. A. Asaud for metallographic evaluations and to J. P. Clark for nondestructive inspection of tested specimens.

III. SPECIMEN FABRICATION

GENERAL SPECIMEN DESCRIPTION

In this investigation of the effect of a thermal cycling treatment on clad fueled composites, four specimen types were employed. In the first three types, selected core compositions were employed as follows:

<u>Specimen Type</u>	<u>Core Composition, vol. percent</u>
A	90W-10(UO_2 - Y_2O_3)
B	80W-20(UO_2 - Y_2O_3)
C	70W-30(UO_2 - Y_2O_3)

where the fueled phase was a solid solution of UO_2 and Y_2O_3 , containing 10 mole percent (8.5 weight percent) Y_2O_3 * dispersed in a continuous tungsten matrix. It was specified that the core material be sintered to at least 95 percent of theoretical density† and have the dimensions given in Figure 1, approximately 0.84 inch in diameter by 2.75 inches in length. Cladding material for the cylindrical surfaces was unfueled tungsten 0.020 ± 0.001 inch thick which was to be metallurgically bonded to the core material. In addition, the ends of the specimens were fitted with refractory metal (W-25Re-30Mo alloy, atomic percent) end caps to minimize fuel vaporization during exposure to the high test temperatures.

A fourth specimen type, Type D (see Figure 1), consisted of a Type C core, approximately 0.78 inch in diameter, surrounded (except at the ends) by a Type B sleeve, 0.020 ± 0.001 inch thick, and then clad with a layer of unfueled tungsten 0.0015 ± 0.0005 inch thick. Metallurgical bonding between core and sleeve and between sleeve and cladding was specified.

MATERIALS

All materials used in the fabrication of the test specimens were of the highest purity that was commercially available. Furthermore, precautions were taken during processing to prevent contamination.

The UO_2 was depleted UO_2 powder prepared by the ammonium diuranate process (ADU) by a commercial fuel supplier. The analysis of the UO_2 powder is given in Appendix A.

The Y_2O_3 powder was high purity material requisitioned from a large lot of commercially produced powder on hand in the GE-NMPO laboratories. It had the analysis given in Appendix A.

*The Y_2O_3 was added to the UO_2 to help stabilize the UO_2 and minimize the degree of UO_2 decomposition at the high test temperature. Without this "fuel stabilizer," UO_2 would partially decompose ($\text{UO}_2 \rightarrow \text{UO}_{2-x} + \text{O}$) at high temperatures and precipitate excess uranium ($\text{UO}_{2-x} \rightarrow \text{UO}_2 + \text{U}$) at lower temperatures. This uranium could greatly change the properties of the core.

†Based on pure component data the theoretical densities of the 10, 20, and 30 v/o compositions are 18.4, 17.4, and 16.5 g/cm³ respectively.

~~CONFIDENTIAL~~

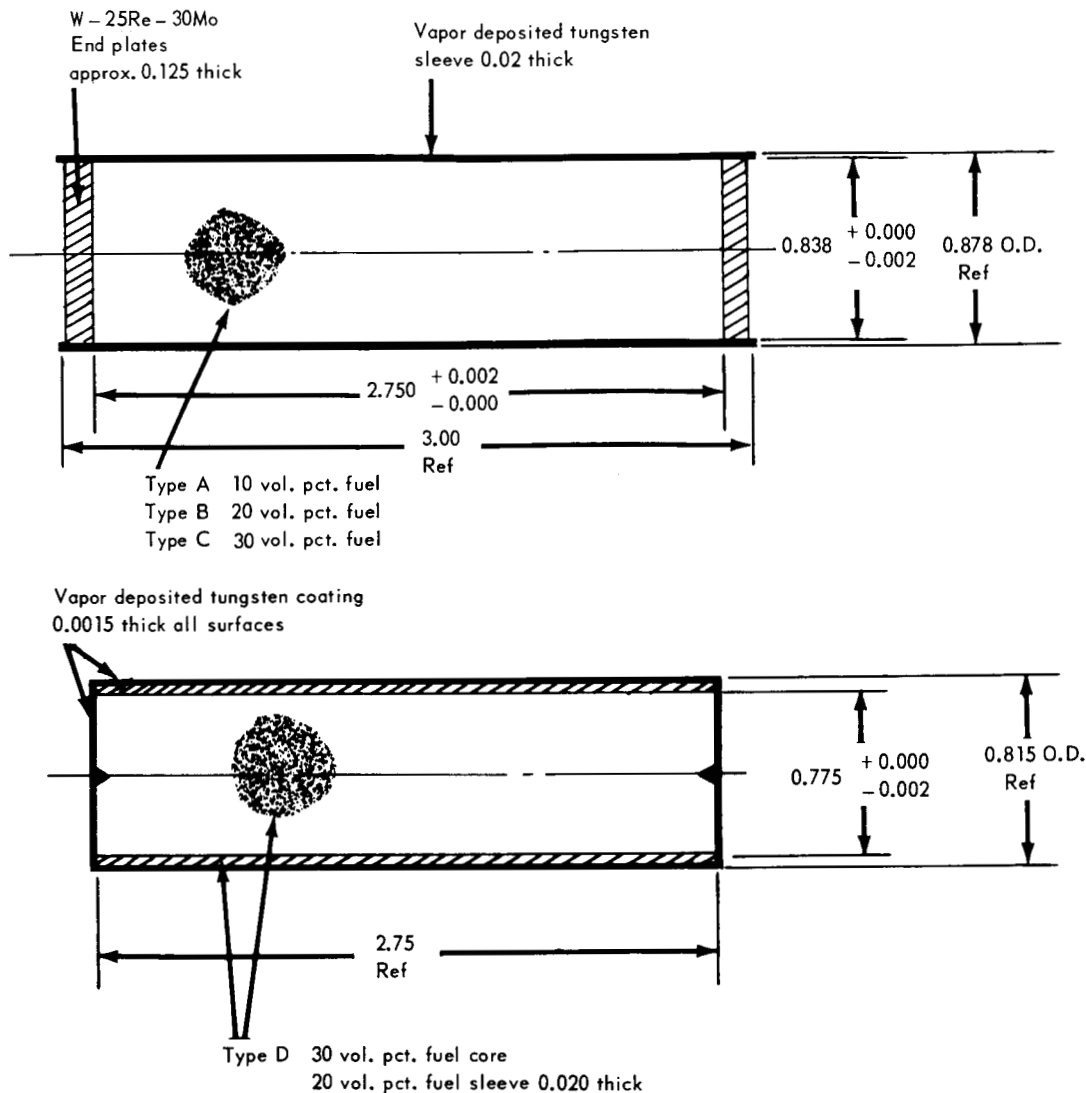


Figure 1 - Configuration and dimensions of Type A, B, C, and D specimens
(dimensions in inches)

The tungsten powder was 1 to 3 micron particle size material obtained commercially. The vendor's analysis of this powder is given in Appendix A.

Tungsten cladding to be used in specimen fabrication was obtained as tubing formed to size by the vapor deposition of tungsten by the hydrogen reduction of tungsten hexafluoride. A total of 30 pieces of tungsten tubing was purchased from a commercial supplier with dimensions of 0.840 inch ID by 0.890 inch OD by 3.25 inches long.

Chemical analysis for fluorine content of the vapor deposited tungsten was performed on the as-received material and after treatment in vacuum (3×10^{-4} Torr) at 2500 °C for 1 hour. The as-deposited tungsten contained 6 ppm fluorine* and the vacuum treated tungsten

*Also contained 14 ppm oxygen.

~~CONFIDENTIAL~~

~~CONFIDENTIAL~~

contained 2 ppm fluorine. Analysis of a second lot of vapor deposited tungsten tubing purchased at a later date indicated 37 ppm of fluorine. No porosity was noted in the microstructure of the low fluorine material after the 2500 °C treatment but the high fluorine tungsten showed considerable porosity in the nature of gas bubbles which collected at the grain boundaries after the high temperature treatment. No dimensional distortion was measured in either tube after the thermal treatment.

FUEL PREPARATION

The original work statement of the NASA Contract specified that the UO_2 should be high-fired and should contain 10 mole percent Y_2O_3 in solid solution. It was further specified that the fuel particles should be in the range of -270/+400 mesh. Efforts during the first month of the contract were devoted to preparation of high-fired fuel and the sintering of W- UO_2 - Y_2O_3 cores containing such fuel. Not only was the preparation of the solutioned UO_2 - Y_2O_3 material in the particle size range of -270/+400 mesh difficult and tedious but also the cores did not sinter to the high densities required and the fuel distribution was poor because of the angular shape of the fuel particles. The details of the high-fired fuel work and the data obtained are given in Appendix B.

Based on previous experience with W- UO_2 composites at GE-NMPO, it was felt that the final sintered densities of at least 95 percent of theoretical could be achieved by using agglomerated instead of high-fired fuel. Hence, the use of agglomerated fuel particles was suggested by GE-NMPO and a Technical Directive was issued by NASA authorizing the preparation of test specimens containing agglomerated fuel.

The fuel was processed in batches of about 2 kilograms of the UO_2 - Y_2O_3 blend. Twelve (12) batches were processed in the course of the core fabrication work with an average yield of about 27 percent based on the desired particle size.

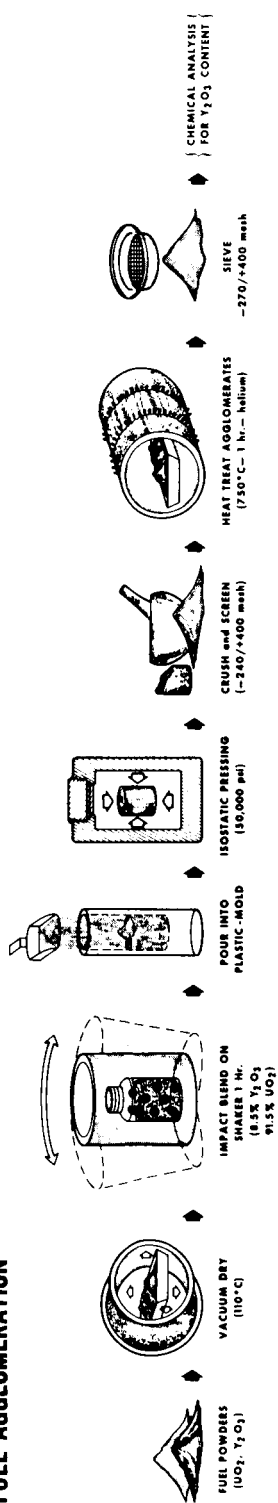
The agglomeration process is shown schematically in Figure 2. Prior to blending the Y_2O_3 was calcined by heating at 1000 °C for 2 hours in air, and the UO_2 was dried in a vacuum oven at 110 °C for 4 hours.

In 500 gram lots, 91.5 weight percent UO_2 and 8.5 weight percent Y_2O_3 were thoroughly mixed by impact blending using a shaker. These powder blends were then placed in plastic molds and were isostatically pressed at 50,000 psi into cylindrical compacts. These were hand crushed and screened to obtain the particle size of -270/+400 mesh. This material was heated to 750 °C in helium for 1 hour to strengthen the agglomerates and then rescreened to remove any fines that may have been generated.

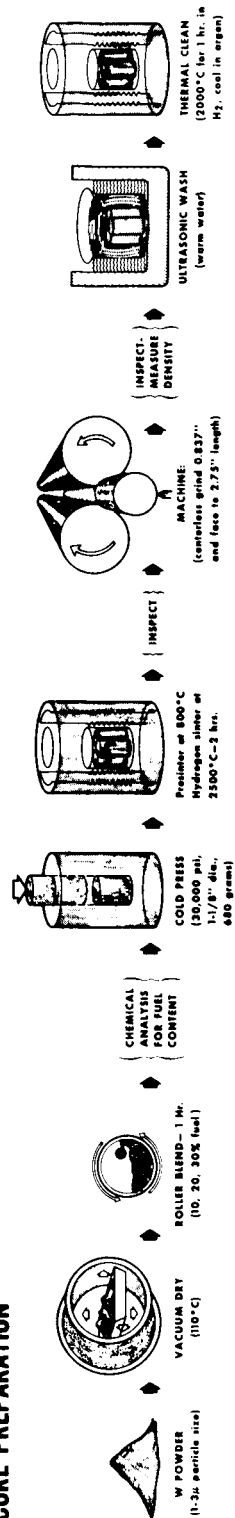
Each lot of prepared fuel was sampled and analyzed for Y_2O_3 content. The analytical results are shown in Table 1 for the 12 lots used in the fabrication of the test specimens as well as in the cores used for thermal expansion specimens. All lots show a lower retention of Y_2O_3 than the 8.5 weight percent (10 mole percent) addition. It was found by analysis that the fine fuel screened from both the green agglomerates and the fired fuel was high in Y_2O_3 content (8.83 weight percent). This indicated that complete homogeneity was not achieved in blending of the UO_2 and Y_2O_3 , and the Y_2O_3 , which had the finer particle size, tended to drop out in the screening operations. It can be noted from Table 1 that the 8 lots of fuel used in the fabrication of the 15 test specimens of Types A, B, and C (underlined) had an average Y_2O_3 content of 7.29 weight percent or 8.6 mole percent.

~~CONFIDENTIAL~~

FUEL AGGLOMERATION



CORE PREPARATION



ASSEMBLY AND BONDING OF CLADDING

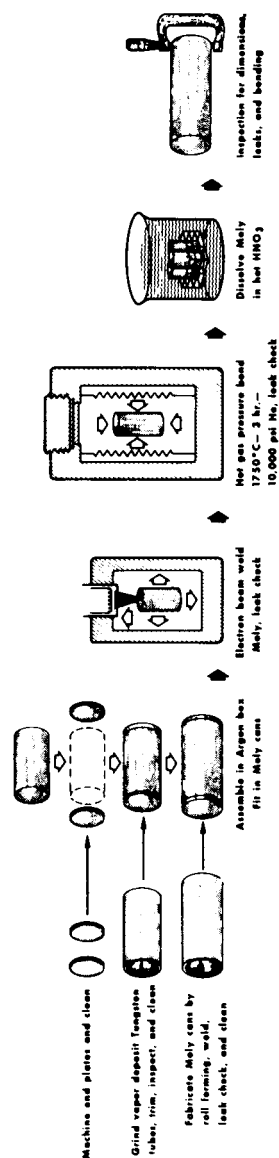


Figure 2 - Fabrication procedure for clad composite specimens

CONFIDENTIAL

CONFIDENTIAL

~~CONFIDENTIAL~~

TABLE 1
YTTRIA CONTENT OF VARIOUS LOTS OF AGGLOMERATED
FUEL AND CORRESPONDING CORES PREPARED

Fuel Lot No.	Net Weight, gms	Y ₂ O ₃ Content, wt %	Cores Prepared*
AFY - 153	345	7.18	<u>C-7</u> , <u>C-8</u>
- 154	238	7.56	<u>C-5</u> , <u>C-6</u>
- 155	146	6.91	A-5, A-6, A-7
- 158	410	7.46	B-9, <u>B-10</u> , <u>B-11</u>
- 159	156	7.59	A-8, <u>A-9</u> , A-10
- 160	260	7.44	<u>B-12</u> , B-13, <u>B-14</u>
- 161	400	7.71	<u>C-9</u> , <u>C-10</u> , <u>C-11</u>
- 162	385	7.46	<u>C-13</u> , <u>A-11</u> , <u>A-12</u> B-15, B-16, C-12
- 163	280	7.13	A-15, A-13, <u>A-14</u> <u>B-17</u> , B-18
- 166	98	6.87	<u>B-19</u>
- 189	315	7.11	C-15, C-16, C-17
- 190	217	7.12	
Green Fines		8.83	
Fired Fines (-400 mesh)		8.22	

*Underlined specimens were used in Type A, B, and C evaluations;
others were used in making thermal expansion specimens, in making
Type D specimens, or for control purposes.

CORE FABRICATION

In all, 32 cores of Types A, B, and C were fabricated using agglomerated fuel. The procedure used, which is common to all thermal cycle test specimens, is shown schematically in Figure 2.

The tungsten powder of 1 to 3 micron particle size was dried in a vacuum oven at 110°C for 4 hours. It then was blended with the agglomerated fuel in compositions of 10, 20, and 30 volume percent fuel, using a roller mill blending technique designed to minimize fracturing of the agglomerated fuel particles. Chemical analysis for fuel content was performed on each of three blends and showed 10.47, 20.54 and 30.33 volume percent fuel, respectively. Charges of 675 grams of the blended powders were cold pressed in a 1.25 inch diameter steel die to form green cores 3.5 inches long. No binder was used in any cold pressed compact.

These green compacts were pre-sintered by slowly heating to 800°C in hydrogen and holding for 15 minutes before cooling. This was a precaution taken to avoid possible cracking of the large compact when heating to sintering temperatures; the pre-sinter was later shown to be unnecessary.

In the sintering operation three cores were loaded together in a tungsten crucible which was placed in a 4-inch diameter vertical tungsten tube furnace. All sintering was accomplished using the following cycle: heat in 1 hour to 1200°C, hold at 1200°C for 1.5 hours, heat to 2200°C in 1 hour, hold at 2200°C for 1 hour, heat to 2500°C in 1 hour, hold at 2500°C for 2 hours, cool to 2000°C; then change the furnace atmosphere from hydrogen to argon before furnace cooling to room temperature.

This sintering cycle was designed to not only achieve high density but also to accomplish solutioning of the UO₂-Y₂O₃ fuel particles in situ. X-ray diffraction analyses of the fuel

~~CONFIDENTIAL~~

~~CONFIDENTIAL~~

in cores sintered by this procedure indicated that solutioning was achieved since no Y_2O_3 or UO_2 were present as separate identities. (See Appendix B for X-ray diffraction analyses).

The microstructures of sintered cores of Types A, B, and C are shown in Figure 3. These show good fuel dispersion, few fine fuel particles, and well rounded particles of high density. In the etched condition, the tungsten matrix is seen to have a relatively coarse grain structure as a result of the 2500°C sintering. No free uranium was observed in the fuel of any of the specimens examined.

MACHINING OF CORES

The as-sintered cores weighed about 675 grams and had nominal dimensions of 0.95 inch diameter by 3 inches in length. These were centerless ground to a diameter of 0.837 inch and the ends were face ground to a length of 2.75 inches. A special grinding fixture was used on the ends to prevent chipping of the corners.

The machined cores were cleaned ultrasonically in hot water to remove machining lubricants. They then were dried and heated in argon to 1500°C and in dry hydrogen to 2000°C for one hour to prepare the surface for cladding, and then they were cooled in argon and stored in argon-filled containers until ready for assembly with the cladding material. The precaution to store these specimens in argon-filled containers was suggested by recent (Reference 4) tests in which UO_2 - Y_2O_3 was found to oxidize in air at room temperature following heating to high temperature in hydrogen.

CLADDING PREPARATION

Specimen cladding was in the form of vapor deposited tungsten tubes (see II. Materials). These tubes were cylindrically ground on centers at GE-NMPO to 0.879 inch OD to produce a uniform wall thickness of 0.020 inch and were cut to lengths of approximately 3 inches. All sleeves then were given fluorescent penetrant inspection for cracks or pits and then were inspected ultrasonically at a reject level of 10 percent of wall thickness.

After machining and inspection all tungsten sleeves were cleaned ultrasonically in Freon 10 solvent and then treated in dry hydrogen at 1400°C for 18 hours.

End-plates for the specimens were machined from an extruded rod of W-25Re-30Mo alloy prepared at GE-NMPO. The carbon content of this alloy was 20 ppm. The blanks cut from the rod were surface ground to 0.125 inch thickness and cylindrically ground to 0.837 inch \pm 0.001 inch diameter. Some of the first lot of end-plates had grooves cut in one face by EDM machining to prepare a weld bead, but this was omitted in later end-plates after welding of the specimen cladding was abandoned. A few end-plates were ground to 0.080 inch to remove the weld preparation material. Specimens having these thinner end-plates are indicated in Table 2. All end-plates were ultrasonically cleaned in Freon 10 and treated in dry hydrogen at 1400°C like the tungsten sleeve material.

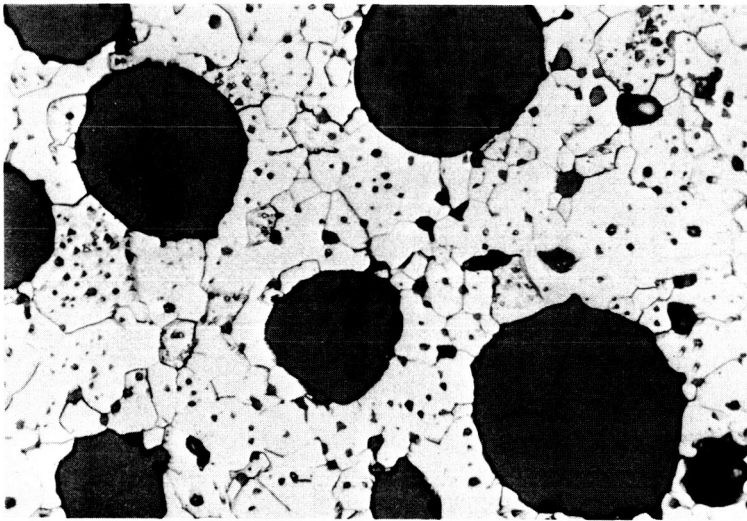
SPECIMEN ASSEMBLY AND BONDING

Assembly of the fueled core with the cladding components was performed in an argon-filled dry box to avoid possible oxidation of the yttria-stabilized fuel particles. Steps in the assembly and bonding process are shown schematically in Figure 2.

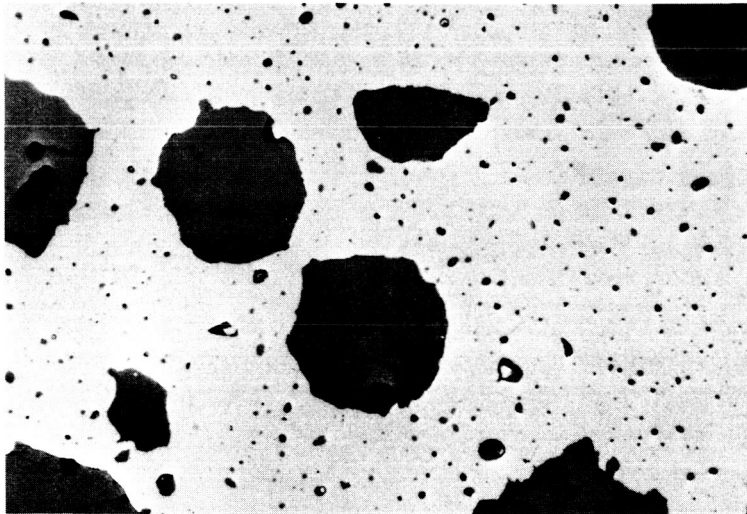
Molybdenum cans were roll formed of arc-melted grade sheet, 0.017 inch thick and seam welded. One end was welded in place and the can was leak checked. The assembled specimen with cladding and end-plates was fitted into the molybdenum can, the molybdenum end-closure was pressed in place, and the can was evacuated and sealed by electron beam welding.

~~CONFIDENTIAL~~

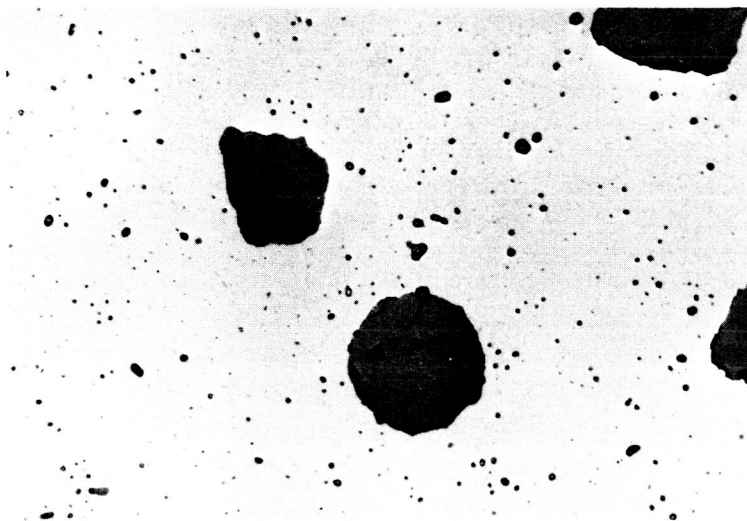
CONFIDENTIAL



Specimen C-7; 30% fuel; 97% T.D.
Neg. 6219, etched in Murakami's reagent



Specimen B-9; 20% fuel; 97% T.D.
Neg. 6270, as-polished



Specimen A-5; 10% fuel; 96.5% T.D.
Neg. 6254, as-polished

Figure 3 - Photomicrographs of cores of Types A, B, and C specimens as-sintered at 2500°C (500X)

CONFIDENTIAL

~~CONFIDENTIAL~~

TABLE 2
HISTORY OF SPECIMENS OF TYPES A, B, AND C

Specimen No.	Sintered Density, % Theor.	Fuel Lot No.	Typical Fuel Content, v/o	End Plate thk., in.	Autoclave Cycles	Percent Bonded ^a	Metall. Mount No.	Disposition
A-6	96.6	155	10.47	unclad	—	—	—	Thermal expansion measurement
A-7	96.6	155		0.125	3	92	9726	Thermal cycle test
A-8	96.6	159		0.080	2	98	—	
A-9	96.6	159		0.125	2	—	{ 9267 9268	Metallographic standard
A-10	96.5	159		{ 0.125 0.080	3	99	9994	Thermal cycle test
A-14	96.2	163		0.125	1	—	—	Thermal cycled 5 times — blistered
A-15	96.8	163		0.125	1	99	—	Thermal cycle test
B-9	97.1	158	20.54	unclad	—	—	—	Thermal expansion measurement
B-10	97.2	158		0.125	3	—	—	Thermal cycle test
B-11	97.2	158		0.125	1	—	{ 9666 9681	Thermal cycled 3 times — blistered
B-12	96.0	160		0.125	1	98	{ 9667 9794	Thermal cycle test
B-13	95.6	160		{ 0.125 0.080	2	—	—	Isothermal test; leaked
B-14	95.8	160-163		{ 0.125 0.080	2	98	—	Thermal cycle test
B-19	96.9	166		0.080	1	99	9995	Thermal cycle test
C-6	95.5	153-154	30.33	unclad	—	—	—	Thermal expansion measurement
C-7	96.9	153		0.125	3	—	8732	Thermal cycle test; later tested at NASA-Lewis in fast cycle
C-8	96.9	153		0.125	2	98	{ 9727 8961	Thermal cycle test
C-9	96.9 ^b	161		0.125	1	98	MA-28	Thermal cycle test
C-10	96.7	161		0.125	1	98	{ 9992 9993	Thermal cycle test
C-11	96.6	161		0.125	1	—	—	Tested at NASA-Lewis in fast cycle with C-7

^aBond measured by longitudinal Vidigage scan at four locations.

^bCladding stripped after testing and density measured as 99.4% of theoretical.

These canned specimens were processed in an autoclave at 1750 °C under 10,000 psi helium pressure for 3 hours. About one half of the specimens were given multiple autoclave cycles as indicated in Table 2. These specimens were originally processed before the over-clad of molybdenum was adopted and were not successfully bonded on the initial autoclave attempt. In most cases, it was necessary to replace the tungsten sleeve and end-plates and reassemble in molybdenum cans for successful autoclaving.

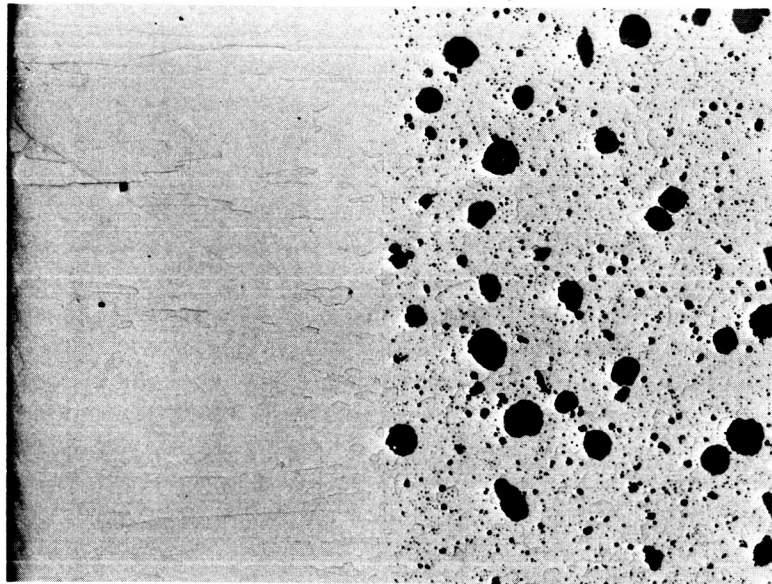
After processing in the autoclave the specimens were given a leak check by the helium bubble method and if gas-tight, they were assumed to be bonded. The molybdenum then was removed by immersing in hot concentrated nitric acid for 1 to 2 hours. The acid did not attack either the tungsten cladding or the W-Re-Mo end-plates.

Non-destructive inspection was performed on the completed specimen and included leak check, fluorescent penetrant inspection for cladding defects, bond check by Vidigage, and dimensional and volume measurements. The specimens that passed these quality control measures were ready for thermal cycle testing. The data pertinent to the processing history of each of the test specimens are given in Table 2.

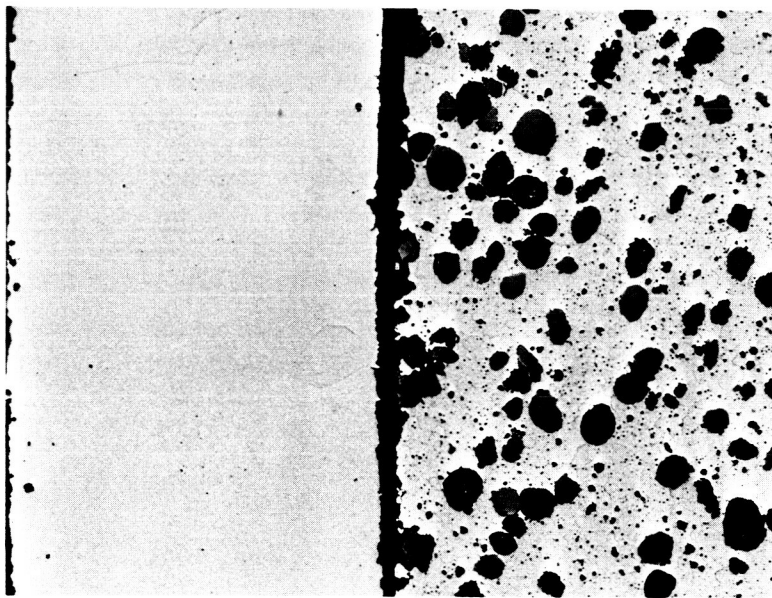
The as-fabricated condition of specimen A-9 which was prepared as a control standard was evaluated metallographically. A typical section of the core-clad interface is shown in Figure 4. This shows that an excellent metallurgical bond between the vapor deposited tungsten sleeve and the core matrix was achieved by autoclaving. Also shown in Figure 4 is a section of specimen B-11 which had a defective bond and developed a blister after three thermal cycles to 2500 °C. This separation of cladding from the core occurred on one side

~~CONFIDENTIAL~~

CONFIDENTIAL



Specimen A-9 after gas pressure bonding at 1750°C (Neg. 7584)



Specimen B-11 after 2500°C proof test (Neg. 7585)

Figure 4—Photomicrographs of core-cladding interface of specimens showing normal bonding achieved by autoclaving and abnormal separation of cladding after proof testing a defective specimen at 2500°C (100X, unetched)

CONFIDENTIAL

of the specimen only. This is an extreme example of poor bonding and was observed to a lesser extent in only two other specimens, A-10 and A-14, after thermal cycle testing.

FABRICATION OF THERMAL EXPANSION SPECIMENS

In the first measurements of the thermal expansion characteristics of unclad W-UO₂-Y₂O₃ composites, the specimens employed were 2.5 inches in length and had a 0.25 inch square cross section. These samples were ground to size from core specimens of the same dimensions fabricated for use in the thermal cycling evaluations. In each case two thermal expansion specimens were obtained from one core sample. Considerable difficulty was encountered in the grinding of these thermal expansion specimens in that sound samples were not always achieved. Some specimens cracked in two prior to the attainment of the desired dimensions. While a few sound specimens were produced and used successfully in making some of the necessary thermal expansion measurements, it was felt that too many of the core specimens would be consumed in preparing all the thermal expansion specimens required. For this reason, some additional core material was prepared in the form of solid cylinders, 0.4 inch in diameter and 3.0 inches in length. These were fabricated in the same manner as the core specimens prepared for use in the thermal cycling specimens. A centerless grinding operation then led to sound thermal expansion specimens 0.313 inch in diameter and 2.5 inches in length. These were found to be easily fabricated and satisfactory thermal expansion specimens were prepared with little difficulty.

FABRICATION OF TYPE D SPECIMENS

The Type D specimen was of the same general configuration as those discussed above, and the composition of the core was that of Type C specimens (30 v/o fuel). However, the outer sleeves for the Type D specimens were formed from the Type B core composition. This fueled sleeve was 0.020 inch in thickness as shown in the drawing of Figure 1. To prevent vaporization of fuel, the cylindrical surfaces and ends of the specimen were coated with tungsten, 0.0015 inch thick, applied by a vapor deposition process.

Several approaches* to the fabrication of this Type D specimen were evaluated, and because of some difficulties with each method the fabrication work fell behind schedule. Initially, it was proposed that the fueled sleeve be machined from a Type B core and the sleeve be fitted over a Type C core. Problems of cracking of the sleeve were encountered during the drilling of thin-walled sleeves in lengths of 3 inches. However, it was demonstrated that the joints between sections of short sleeves could be completely healed in the autoclave bonding process and hence it became acceptable to machine the sleeves in short lengths. This is the approach that was taken.

Type D cores were isostatically pressed and sintered to densities of 96 percent of theoretical in the same manner as the previous Type C cores. The dimensions of these cores after sintering were about 0.810 inch diameter by 2.75 inches long. They were mounted on centers and cylindrically ground to clean up at diameters ranging from 0.760 to 0.775 inch.

Sleeves of the Type B material were isostatically pressed around a mandrel in short lengths. After sintering at 2500 °C the dimensions of these sleeve sections were about 0.730 inch ID, 0.880 inch OD, and 2 inches long. These sleeves were custom ground in pairs on the ID to fit the ground cores with a clearance of 0.003 inch on the diameter. The diameters of these sleeves then were cylindrically ground to 0.900 inch leaving a wall thickness of about 0.065 inch. The ends were faced to make a tight joint at the middle of the core specimen and to adjust the length so the two sleeve sections would just cover the center core.

*See Appendix D.

The cores and sleeves were ultrasonically cleaned in warm water to remove machining coolants. They then were heat treated at 2000°C in hydrogen for 1 hour and cooled in argon. The sleeve sections were fitted over their respective cores and the assemblies were canned in previously prepared tantalum containers of 0.910 inch diameter. To permit retention of the centers in the ends of the cores, discs of molybdenum were placed over each end. The tantalum cans were sealed by electron beam welding, and the sleeves were hot gas pressure bonded to the cores by autoclaving at 1750°C for 3 hours under 10,000 psi helium pressure.

After leak checking the cans to insure that pressure bonding had occurred, the tantalum end-plates were ground away exposing the molybdenum discs. The molybdenum then was dissolved from the center holes using concentrated nitric acid. Some fuel particles may have been dissolved also in the immediate vicinity of the center hole but not to any appreciable depth in the short time (approximately 20 minutes) that the molybdenum was dissolved.

The cores were mounted on the original centers and cylindrically ground removing the tantalum overclad and sufficient sleeve material to leave approximately 0.019 inch thickness of fueled sleeve over the core. This sleeve thickness was confirmed by grinding the ends of the core to a smooth finish so the interface could be defined and microscopically measuring the thickness of the sleeve.

The core-sleeve specimens were inspected by dye penetrant techniques and no defects or evidence of the joint between the two sleeve sections was found on any of the specimens. They were then ultrasonically cleaned in warm water, dried, and subsequently heated to 1800°C and held for 1 hour in hydrogen to prepare the surface for vapor deposition of tungsten. The five specimens were cooled in argon and then sealed in argon-filled plastic bags for shipment to a vendor for vapor deposition.

Using hydrogen reduction of tungsten hexachloride, a tungsten coating, 0.002 inch thick, was applied over the entire surface of the five specimens. Inspection by dye penetrant techniques revealed no defects in the tungsten coating of three specimens and minor defects in one end of two specimens. The results of these inspections are given in Table 3. Neither leak-check nor bond check appeared feasible for this type of coating, and hence such inspections were not performed.

TABLE 3
INSPECTION DATA OBTAINED FOR TYPE D SPECIMENS AS COATED WITH TUNGSTEN BY VAPOR DEPOSITION

Specimen No.	Weight, gms		Diameter, in.		Length, in.	As-Sintered Density, % Theor.		Average Sleeve Thickness, ^b in.	Average Coating Thickness, in.	Surface Defects
	Before Coating	After Coating	Before Coating	After Coating ^a		Core	Sleeve			
D-1	416.2	420.8	0.826	0.8302	2.92	—	—	0.019	0.0021	Longitudinal seam and small defect in end
D-2	336.8	340.4	0.811	0.8155	2.46	95.8	96.5	0.019	0.0023	None
D-3	338.8	342.8	0.811	0.8162	2.51	95.3	96.3	0.019	0.0026	None
D-4	342.6	346.8	0.796	0.8010	2.65	96.1	96.1	0.019	0.0025	None
D-5	318.2	321.8	0.796	0.8004	2.47	96.1	96.5	0.019	0.0022	Small defects in one end

^aMaximum taper from end to end 0.0024 inch.

^bMeasurements performed using metallurgical microscope; sleeve thickness measurements varied between 0.0185 and 0.020 inch.

The selection of two specimens for thermal cycle testing was based on dimensional tolerances, and as shown by the data in Table 3, specimens D-2 and D-3 most closely met the specifications. However, specimen D-4 was subsequently used as a replacement for D-3 which developed a blister on one end.

~~CONFIDENTIAL~~

Specimen D-5 was sectioned for metallographic analysis in the as-fabricated condition and to determine the dimensional control that was achieved in the fabrication process. A transverse section was cut from the middle of the specimen, and longitudinal sections were prepared of each of the end pieces by grinding away half of the diameter.

Measurements were made microscopically at three points on the longitudinal and transverse sections to determine the thickness of the sleeve and the tungsten coating. These measurements are given in Table 4. These data show the core diameter is unchanged from the original ground size of 0.760 inch. The sleeve thickness measured 0.019 inch \pm 0.001 inch over the length of the specimen. The tungsten coating thickness averaged 0.0017 inch and was uniform within the tolerance of \pm 0.0005 inch. Because of difficulty in differentiating the interfaces between the core, sleeve, and coating, the accuracy of these measurements is not better than \pm 0.0003 inch.

TABLE 4
MEASUREMENTS^a OF CONTROL SPECIMEN D-5 IN THE
AS-FABRICATED CONDITION

	(Measurements Made Across Diameters)					
	Longitudinal Section			Transverse Section		
	1	2	3	1	2	3
W coating thickness, inch	0.0016	0.0016	0.0018	0.0018	0.0016	0.0015
Sleeve thickness, inch	0.0178	0.0188	0.0182	0.0195	0.0187	0.0192
Core diameter, inch	0.7598	0.7598	0.7598	0.7560	0.7598	0.7598
Sleeve thickness, inch	0.0184	0.0182	0.0180	0.0199	0.0180	0.0177
W coating thickness, inch	0.0018	0.0020	0.0019	0.0013	0.0021	0.0016

^aThese measurements were made on the polished metallographic specimens using a microscope stage which had micrometers on the x and y translations. A filar eyepiece was used for indexing purposes.

Generally the quality of the tungsten coating was good with no porosity observed. The bond to the tungsten matrix of the sleeve was excellent as shown in Figure 5.

~~CONFIDENTIAL~~

~~CONFIDENTIAL~~

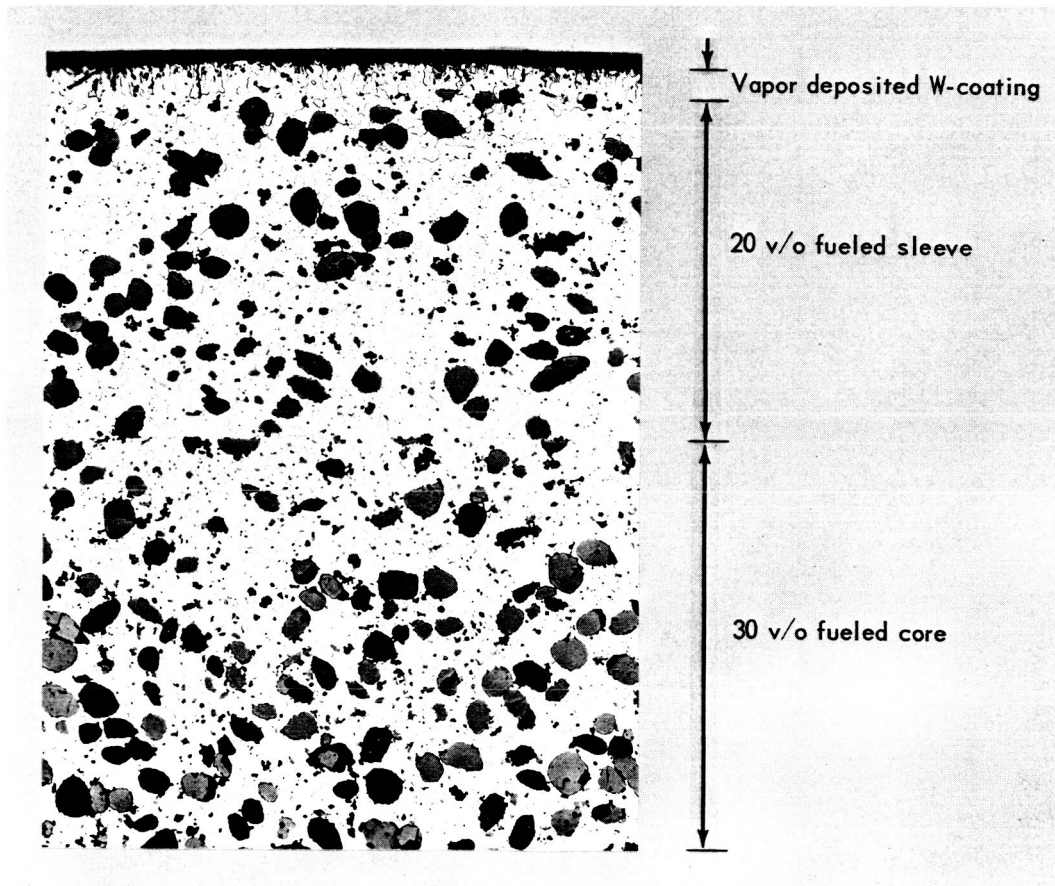


Figure 5—Photomicrograph of transverse section of specimen D-5 in as-fabricated condition showing W-30 percent fuel core, W-20 percent fuel sleeve, and vapor deposited tungsten coating (Neg. 7586, unetched, 100X)

~~CONFIDENTIAL~~

CONFIDENTIAL

IV. EXPERIMENTAL TESTING PROCEDURES

THERMAL EXPANSION MEASUREMENTS

Measurements of the linear thermal expansion characteristics of unclad composite specimens of W-10 v/o ($\text{UO}_2\text{-Y}_2\text{O}_3$), W-20 v/o ($\text{UO}_2\text{-Y}_2\text{O}_3$) and W-30 v/o ($\text{UO}_2\text{-Y}_2\text{O}_3$) were made in helium to 2500°C using a technique which has been employed rather extensively in recent expansion measurements of various refractory metals (Reference 5).

In these measurements, a resistively heated tungsten tube furnace was employed. The heating element in this furnace was 20 inches in length, 4 inches in diameter with a 20 mil wall thickness, and operated in the vertical position. With this arrangement, a hot zone some 8 inches in length was obtained to insure temperature uniformity during the thermal expansion measurements. Specimens, 2.5 inches in length and either 0.313 inch in diameter or with a 0.25 inch square cross section, were employed and were positioned horizontally in a special holding fixture (Reference 5), at the longitudinal midpoint of the furnace heating element.

Expansion measurements were made by sighting paired filar micrometer microscopes on fiducial marks located near the ends of the specimen. These fiducial marks were in the form of 0.008 inch holes and viewed against the low temperature background provided by the lower regions of the tube furnace. A clear and distinct view of these holes made it very convenient to focus the paired microscopes on these fiducial marks in making the thermal expansion measurements.

A thermal radiation shield formed to fit around the specimen holder provided a temperature uniformity which was well within 10°C at maximum temperature over the 2.5 inch specimen length.

Temperatures to 1000°C were measured by a platinum/platinum-10 percent rhodium thermocouple positioned in the small central hole in the specimen holder. Above 1000°C , temperatures were measured by means of an optical pyrometer sighted through a quartz window in the top of the furnace into the black body hole either in the specimen or in the specimen holder midway between the two microscope sight holes. Optical pyrometer corrections for the quartz window were obtained in previous calibration tests.

Prior to each test, a microscope calibration was performed by employing a standard linear scale etched on a glass slide. After removing the complete microscope system from the top of the furnace, it was placed on a special table, and the glass scale then was placed directly below the microscopes. At this time, the vertical distance between this scale and the microscopes was set equal to that between the specimen and microscope during furnace operation. The eyepiece cross hairs then were moved to be coincident with the extremities of the 2-inch scale, and the two eyepiece micrometer readings were recorded. Following this measurement the microscope system then was repositioned atop the furnace, and an electrically heated tungsten coil within the top of the furnace then was energized to illuminate the specimen. In this manner, the room temperature value of the distance between the fiducial marks on the sample was measured by adjusting the eye-

CONFIDENTIAL

~~CONFIDENTIAL~~

piece cross hairs until they were coincident with the fiducial marks. Readings taken from the eyepiece micrometers then enabled the cold length to be easily calculated based on the above calibration. Measurements made as the furnace temperature was increased were referred to this initial length in the usual manner to enable percent elongation to be calculated. At furnace temperatures below 900°C, the resistively heated tungsten coil provided the necessary illumination of the fiducial marks for the elongation measurements.

Previous measurements with this thermal expansion technique have confirmed that the reproducibility of repeated measurements is within ± 3 percent. Measurements using sapphire, tungsten, and molybdenum specimens established the accuracy of this technique since it was shown that agreement with accepted published data for these materials was within experimental error.

In the proposal associated with this contract, GE-NMPO suggested a special use of the above thermal expansion technique in measuring any diametral strains resulting from the thermal cycling of composite materials. Previous experience at GE-NMPO with this thermal expansion technique was concerned in a few cases with the identification of phase transformations in various materials and with the study of densification rates of W-UO₂ composites during sintering at various temperatures. These experiences suggested that this technique could be modified to provide an instantaneous measurement of the diameter of a specimen as the temperature was increased and then decreased. In such a test, the ordinary thermal expansion curve should result. However, it was reasoned that if any dimensional instability results from a thermal cycling treatment, deviations from the expansion curve obtained in the first heating could then be interpreted as the deformation resulting from subsequent heatings and coolings. It was felt that since diametral measurements were made at every temperature during the heating and cooling process, the temperature at which the plastic deformation would first begin could be identified. It was proposed, therefore, that these diametral measurements be made in 10 test cycles in which the specimen was heated to 2500°C and then returned to room temperature. Such an approach should allow the identification of whether any dimensional instability was a function of the number of heating cycles.

In order to effect the diametral measurements proposed for this phase of the program, some specimen modification was necessary. It was necessary to devise some type of fiducial mark either on or attached to the specimens so that a diametral measurement could be made. Furthermore, since the micrometer microscopes employed in conjunction with these thermal expansion measurements were spaced some 2 inches apart, it was clear that these fiducial marks could not be positioned on the surface of the 0.89 inch diameter specimens employed in this program. After some consideration then, the configuration shown in Figure 6 was adopted in which 0.60 inch diameter tungsten rods about 0.6 inch in length were welded into small tungsten tabs, 0.12 inch x 0.25 inch x 0.06 inch. Two of these rod-tab constructions were electron beam welded to opposite sides of a specimen whose diametral changes were to be measured, taking care to assure that these rods were in good alignment and exactly perpendicular to the surface of the specimen. Small holes, 0.010 inch in diameter and 2 inches apart, were then drilled in these rods to serve as the fiducial marks for making the diameter measurements optically. Using a solid tungsten rod (shown in Figure 6) of the same diameter as the specimens proposed for use in this program, the reliability of this technique was demonstrated when the thermal expansion curve obtained for the arrangement shown in Figure 6 was identical to that obtained in the usual measurement procedure employing 0.25 inch diameter rods 2.5 inches in length. It was felt that any plastic deformation which would cause any diameter changes in this specimen could be detected as deviations from the expansion

~~CONFIDENTIAL~~

~~CONFIDENTIAL~~

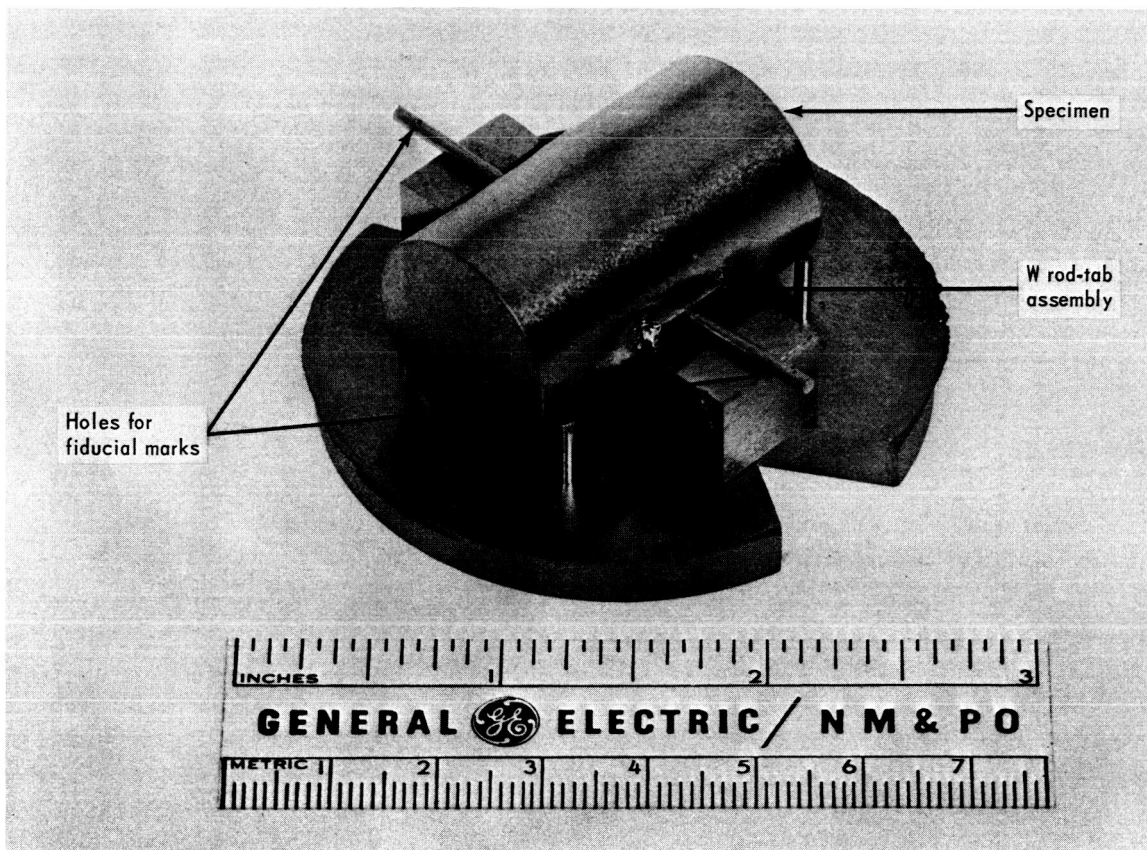


Figure 6 - Special specimen assembly for use in making diameter measurements optically in thermal expansion apparatus (Neg. P66-1-28)

curve measured for this material. While this measurement was made only with a sample of pure tungsten, it was felt that the principle of this approach was established and could be applied to the case of clad composite specimens.

Early in the thermal cycling test program associated with this contract, it was observed that the diameter changes which were taking place after 10 thermal cycles were extremely small and of the order of -0.1 to -0.2 percent corresponding to diameter changes from 0.8 to 1.6 mil. These changes were smaller than those expected and were close to the lower limit of detection of the optical technique being employed. For this reason it did not seem desirable to pursue the portion of the program dealing with diametral measurements and, with the concurrence of the NASA Contracting Officer, these measurements were then deleted from the program.

THERMAL CYCLING TESTS

Special high temperature thermal cycling furnaces have been developed and fabricated by GE-NMPO over the past several years for use in the evaluation of the high temperature capabilities of various materials. These furnaces (see Appendix E) are based on the use of a resistively heated, thin-wall refractory metal tube which can operate in either hydrogen, inert gas, or vacuum and can attain temperatures up to 3000°C . Test specimens positioned within this tubular heating element are heated by radiant energy at rates

~~CONFIDENTIAL~~

which can be readily controlled by the rate at which power is supplied to the furnace. Cooling rates can be similarly controlled. Operation has been made completely automatic to allow the use of any pre-selected heating or cooling rate, any test temperature, and any dwell time at the maximum test temperature. After a cycle has been completed, the same sequence of events is automatically repeated until the desired number of test cycles has been imposed.

In this study, three specimens were tested simultaneously, all positioned in the same plane of the furnace, with the long axis of the specimens parallel to the axis of the furnace heating element. Prior to each test a furnace degassing procedure (see Appendix E) was employed following which the furnace was filled with helium to a pressure of 5 psig to provide the test atmosphere for the specimens.

Temperature measurements were made using an optical pyrometer which had been calibrated by reference to a standard pyrometer which was calibrated and certified by the National Bureau of Standards. Based on this type of calibration, temperature measurements to 2500°C were considered accurate within $\pm 10^\circ\text{C}$.

In some pre-test evaluations, a relationship between specimen temperature and furnace power input was established. It was found permissible, therefore, to employ this concept to produce the desired temperatures during the thermal cycling tests. Also identified in these pre-test studies was the fact that at 2500°C the specimen temperature was uniform longitudinally within 50°C.

In the thermal cycling evaluations, two specimens each of Types A, B, and C were subjected to 50 thermal cycles using Test Type 1 (10-minute dwell at 2500°C); two additional specimens of each of these types were then subjected to 50 thermal cycles using Test Type 2 (1-hour dwell at 2500°C). Also, three of the Type D specimens were subjected to 50 thermal cycles using the Type 1 thermal cycling test procedure. In general, no cracking of the outer cladding was detected, and hence each specimen tested was subjected to the maximum number of thermal cycles (50) as specified.

As discussed in Appendix E, it was possible to test three specimens simultaneously in the furnace employed in these thermal cycling evaluations. In the first four furnace loadings, one each of specimen Types A, B, and C were employed (see Table 5) whereas in the fifth and final furnace loading, three of the Type D specimens were tested together.

During the course of the thermal cycling tests, each sample was inspected periodically to detect any changes which might result from the thermal cycling treatment. At the beginning of this test program, inspections were scheduled after every five (5) cycles for the first twenty (20) cycles and then after every two (2) cycles for the remainder of the test. These frequent inspections proved fairly time consuming and when it was considered that the objectives of this study could be achieved just as accurately with less frequent inspections a modification was made to perform inspections after every five (5) cycles. It can be noted in footnote (e) of Table E-1 (see Appendix E) that this revision in the inspection schedule went into effect following the fortieth cycle of the specimens (A-7, B-12, and C-8) involved in the first furnace loading.

When the specimens were removed from the test furnace for each scheduled inspection (and this applies to the specimens prior to test as well), the following measurements and evaluations were performed:

Visual Inspection

Each specimen was inspected visually to assess the general condition of the outer surface with particular attention being given to surface discoloration and localized blisters.

TABLE 5
SCHEDULE OF THERMAL CYCLING TESTS FOR
SPECIMEN TYPES A, B, C, AND D

(Room Temperature to 2500°C in Helium)					
Furnace Loading	Specimens Involved	Type of* Thermal Cycling Test	No. of Thermal Cycles Imposed	Testing Started	Testing Completed
1	A-7 B-12 C-8	1	50	10-3-65	12-4-65
2	A-15 B-10 C-7	1	50	10-29-65	12-16-65
3	A-8 B-14 C-9	2	50	12-14-65	1-25-66
4	A-10 B-19 C-10	2	50	12-16-65	1-26-66
5	D-2 D-3 D-4	1	50	5-18-66	6-2-66

*Type 1 employed 10-minute dwell at 2500°C.

Type 2 employed 1-hour dwell at 2500°C.

Dimensional Measurements

Diameter measurements were made using a micrometer caliper at five equally spaced locations along the length of the specimen. One location was chosen at the longitudinal midpoint while two others corresponded to the end points of the sample. The other two locations were chosen at the midpoint between the center and end positions. These measurements were made at the same position each time by proper indexing of the specimen. Following these measurements, the specimen was rotated 90° and another set of diameter measurements was obtained. In evaluating the percentage change in the specimen diameter, the two diameter measurements at the longitudinal midpoint were averaged and used in conjunction with the average midpoint diameter obtained in the pre-test condition. All measurements of the percent change in diameter are considered accurate within 0.02 percentage units.

Length measurements were made using a micrometer caliper contacting the exact center of each end-plate of the specimen. Percentage changes in length were then calculated by referencing these measurements to the pre-test length. Measurement accuracy is within 0.01 percentage units.

Volume Measurement

Sample volume was measured by weighing the specimen in air and then submerged in toluene. This procedure has been used consistently at GE-NMPO and allows a direct calculation of sample volume. Percent changes in volume then were calculated by referencing these measurements to the pre-test specimen volume. Obviously, these measurements reflect over-all or external volumes and do not give any information pertaining to the core or matrix volume.

~~CONFIDENTIAL~~

Percentage changes in specimen volume are considered accurate within 0.003 percentage units.

Weight Measurement

Each specimen was weighed, and these data then were referenced to the pre-test data to yield a value for the percent change in specimen weight. Percentage changes in specimen weight are accurate within 0.0004 percent.

Leak Test

Each specimen was pressurized to 500 psi in helium and held at this pressure for 15 minutes. The pressure then was released and the sample was quickly transferred to a vacuum chamber connected to a mass spectrometer which is capable of detecting a leak rate of about 1×10^{-10} cc of helium per second. If no helium was detected, the capsule was considered leak-free. In general, no leaks were detected in any of the specimens either before or after test although the blistered D-3 specimen did exhibit a large leak at the blister, as detected by submersion of the specimen in methanol after pressurization. Gas bubbles formed by the escaping helium provide a clear indication of the actual leak.

Crack Detection

A standard Zyglo inspection was performed to determine if any cracks developed in any surface of the specimens. In this test, a commercial penetrant was employed, and inspection of the specimen surfaces under ultraviolet light was employed in the usual manner to see if any cracks were present. In general, no cracking was observed in any of the specimens tested except, of course, the blistered Type D specimens.

Bond Integrity

Prior to test and after every 25 thermal cycles, the integrity of the bond between the material was evaluated. In this determination, a specially constructed instrument was employed using a broad band, pulse echo technique. This instrument supplies short pulses of about one-half cycle duration to a 17.5 megacycle lithium sulfate transducer, which serves as the frequency determining component of the system. During actual operation, this transducer was used to generate a sound beam with a focal spot 8 mil in diameter and with a 0.5 inch focal distance when immersed in water. With the focal point at the core-clad interface, a total of eight (8) longitudinal scans were made on each specimen. Reflections from the core-clad interfaces were received by the transducer and displayed on an oscilloscope to allow determination of both amplitude and transient time. Since reflections only occur in the case of an unbonded area, a plot was generated showing the location of these unbonded areas as a function of specimen length for each scan. From this type of plot, an estimate of the percentage of unbonded area was obtained. Before test, each sample inspected was found to be bonded over at least 98 percent of the surface. In the post-test condition, it was found that while some loss of bonding occurred the percentage of bonding was above 90 percent in all but two cases and never less than 85 percent.

~~CONFIDENTIAL~~

~~CONFIDENTIAL~~

V. RESULTS AND DISCUSSION

THERMAL EXPANSION DATA

In a few cases, both round and square thermal expansion specimens were available and tested. It was found that the expansion characteristics were the same, independent of specimen geometry.

Typical thermal expansion data obtained in this study are shown in Figure 7 for an unclad Type B composition. Measurements in triplicate reveal the reproducibility obtainable in these evaluations. Also, the specimen was found to return to its original length following each heating. Similar data were obtained for the Type A and C cores, and in each case a least squares computer analysis yielded the following expressions for the thermal expansion characteristics:

Type A:

$$\frac{L_T - L_{25^\circ\text{C}}}{L_{25^\circ\text{C}}} \times 100 = 3.978 \times 10^{-3} + 3.591 \times 10^{-4}T + 9.870 \times 10^{-8}T^2$$

Type B:

$$\frac{L_T - L_{25^\circ\text{C}}}{L_{25^\circ\text{C}}} \times 100 = -5.585 \times 10^{-3} + 4.319 \times 10^{-4}T + 1.027 \times 10^{-7}T^2$$

and for Type C:

$$\frac{L_T - L_{25^\circ\text{C}}}{L_{25^\circ\text{C}}} \times 100 = -1.214 \times 10^{-2} + 3.457 \times 10^{-4}T + 1.610 \times 10^{-7}T^2$$

where L_T refers to the specimen length at temperature $T^\circ\text{C}$. These least squares equations are shown as the solid curves in Figures 7 and 8.

Thermal expansion data for the three core compositions studied are presented in terms of the least squares curves in Figure 8. Some slight crossover of the data for Type B and Type C compositions is noted at 1500°C but no particular significance is attached to this behavior. In view of the reproducibility of the data, the differences involved are considered well within measurement error; and hence, in the lower temperature regime the data for the Type B and Type C compositions are considered essentially identical. In the temperature range above 1700°C , the data are positioned as expected with the percent expansion for the Type A composition lower than either the Type B or Type C specimens. As noted, the difference between the Type B and Type C data is small but this is the same type of effect observed by Taylor (Reference 6) in a study of similar compositions (no Y_2O_3 in the Taylor study). It is interesting that the data for the Type A composition are identical to those for pure tungsten (Reference 7). This conclusion is the same as that reached in the Taylor study.

A comparison of the data in Figure 8 with those of Taylor (Reference 6) reveals excellent agreement for the Type A composition over the entire temperature range. For the

~~CONFIDENTIAL~~

CONFIDENTIAL

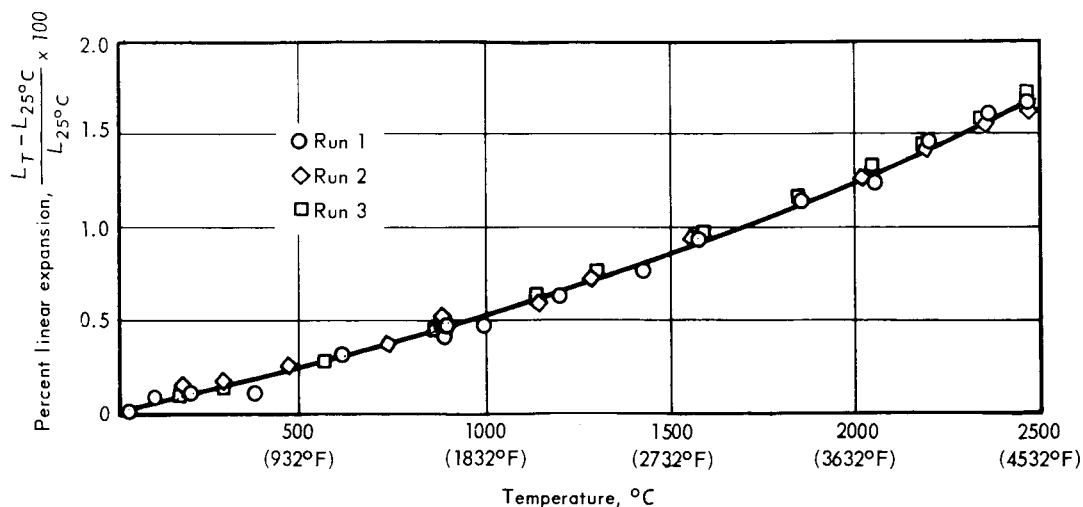


Figure 7—Linear thermal expansion characteristics of unclad 80W-20(UO₂-Y₂O₃) measured in helium. (Specimen dia. 0.313 inch; specimen sintered at 2500°C to 97.4 percent of theoretical density.)

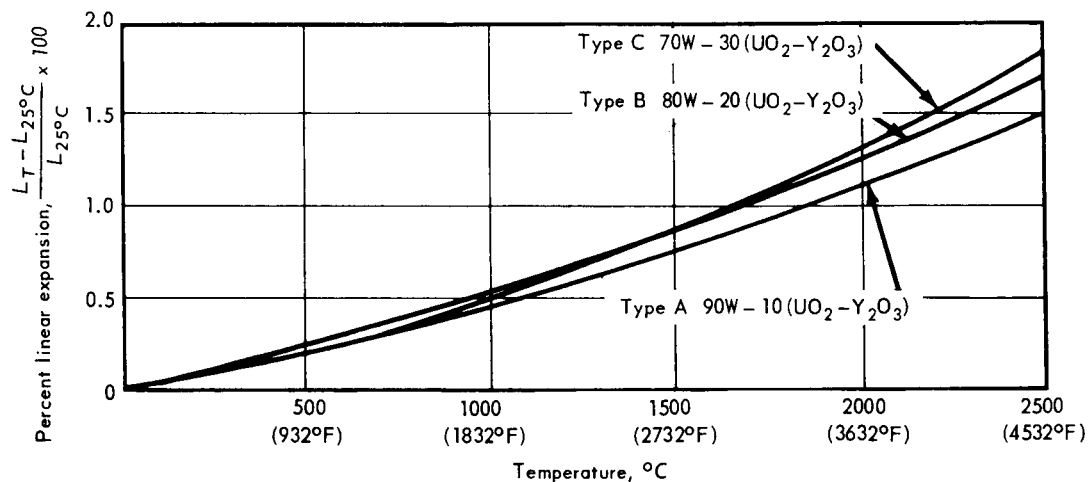


Figure 8—A comparison of the linear thermal expansion data for unclad Type A, B, and C compositions measured in helium. (All specimens sintered at 2500°C to densities of 96 to 97 percent of theoretical density.)

other two compositions, good agreement exists up to about 1500°C. Above this temperature, the Figure 8 data are positioned slightly higher (up to 10 percent) than the corresponding data published by Taylor. In general, it is considered that the agreement between these two independent studies is quite good considering the slightly different material compositions involved and the small differences in the measurement techniques employed. Each thermal expansion measurement given in Figure 8 was performed in triplicate as indicated in the discussion of Figure 7. Following the third heating of each specimen, weight measurements were made to determine if any weight loss of the specimen was occasioned by the repeated exposures to 2500°C in these expansion measurements. It was found that

CONFIDENTIAL

weight losses of 0.07, 0.16, and 0.5 percent were experienced by the unclad Type A, B, and C compositions, respectively. These percentages are based on a total specimen weight of 40 to 53 grams. These weight losses would not be expected to significantly affect the thermal expansion measurements.

THERMAL CYCLING RESULTS

A summary of the inspection data obtained for the fifteen specimens tested in this program is presented in Table E-1 (see Appendix E). Also presented in this table are the inspection data obtained in special tests of two unclad tungsten specimens and a special test of specimen B-13 (tests discussed below). It will be noted that in Table E-1 the specimen number is given in the first column and the number of thermal cycles in the second column. In this case, these numbers represent the points at which the specimens were removed from the test furnace and inspected. In the third column, the cumulative hours on test are given reflecting the total time during which the specimens were above room temperature. Reference to Figure E-3 reveals that some 60 minutes were required to heat the specimens from room temperature to 2500°C, and after a 10-minute hold at 2500°C, the cooling to room temperature required a period of some 200 minutes. In all then, the total cycle time amounted to 270 minutes or 4.5 hours. Hence, the first entry in Table E-1 indicates an accumulated time at temperature of 22.5 hours corresponding to 5 thermal cycles.

Data obtained during the specimen inspection are presented in the last four columns of Table E-1. Expressed as percent change from the pre-test values, data are presented for specimen diameter, length, volume and weight.

(a) Type A, B, and C Specimens

A photograph of the six Type A, B, and C specimens tested using a 10-minute dwell at 2500°C is presented in Figure 9. After 50 thermal cycles, no noticeable specimen deterioration was observed. As a matter of fact, no change in surface appearance could be noted and any observed surface spots or markings were present in the pre-test condition. Specimen A-15 was particularly striking in that the post-test appearance was essentially identical to that observed in the pre-test inspection. A slightly different end-plate configuration is noted in the Type C specimens. This design was employed when it was felt that end closure would require an electron beam welding operation. Actually, the two specimens shown in Figure 9 were the only ones made with this type of end-plate. In subsequent fabrications (Type C specimens were fabricated first in this program), an autoclaving operation provided an adequate end closure and the end-plate design shown in these Type C specimens was no longer utilized.

One of the first observations made during the thermal cycling tests of specimens A-7, B-12, and C-8 (first samples tested) was that the specimen diameter was decreasing as the number of thermal cycles increased. In other words, the specimen was undergoing a slight densification or shrinkage. It also was noted that in every case the specimen length was increasing slightly. Subsequent testing of the remainder of the specimens (excluding the Type D samples) indicated a similar behavior, and hence, it was found that a decrease in diameter and an increase in length were observed on every specimen tested. Volumes and weight changes were not as consistent for, as seen in Table E-1, there are nine instances of a volume decrease and 3 instances of a volume increase in the tests of the Type A, B, and C specimens. A similar situation is found in the case of weight changes where nine increases and three decreases were observed.

~~CONFIDENTIAL~~

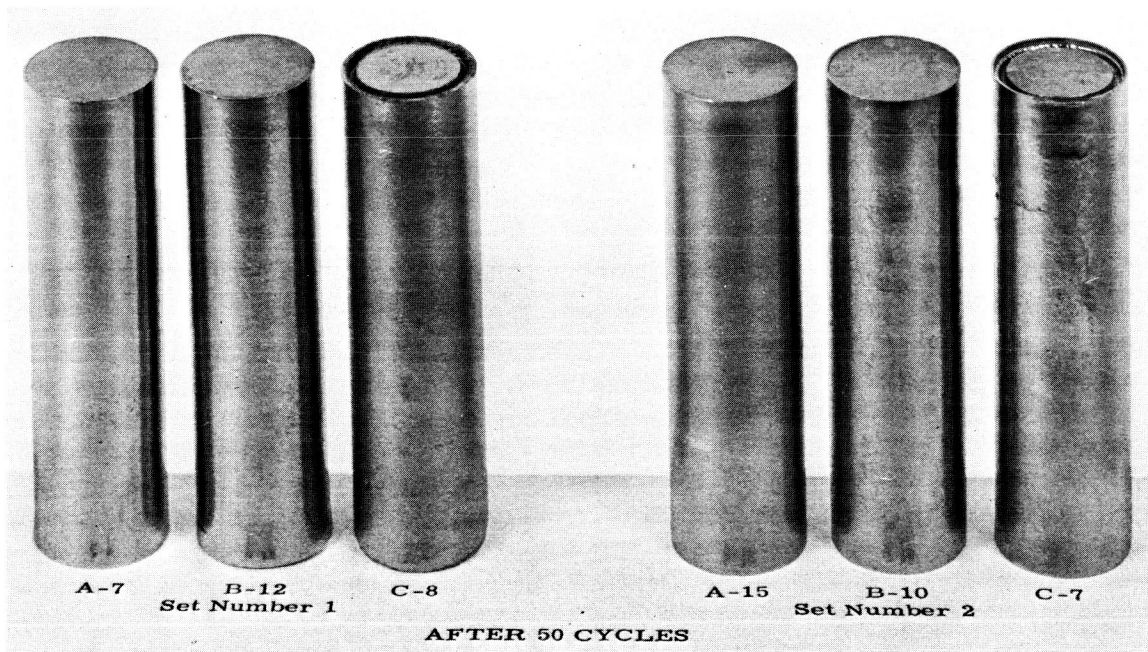


Figure 9 - Six tungsten clad $W-(UO_2-Y_2O_3)$ specimens after being subjected to 50 thermal cycles between room temperature and $2500^\circ C$ in helium (Neg. P65-12-26)

Plots of the percentage changes in specimen diameter observed after various thermal cycles are shown in Figure 10 for the Type 1 testing and in Figure 11 for the Type 2 tests. As already mentioned, a decrease in diameter was observed for every specimen, but as is noted in Figures 10 and 11, no general trend is discernible. Specimen C-7 exhibited the best dimensional stability of all the samples tested in terms of diameter change although the length change observed in this sample was somewhat larger than that observed in several other samples. Figures 10 and 11 also reveal that no trend with fuel loading seems to exist. In Furnace Loading No. 1, the Type A and C specimens exhibited about the same diameter change whereas the Type B specimen had the largest change in diameter noted for this one group of specimens. A definite change in this sequence was observed in Furnace Loading No. 2 where the largest diameter change was noted for the Type A specimen while the Type B and C specimens had about the same diameter change. Specimen Type B is seen to have experienced the largest diameter change in Furnace Loading No. 3 while the Type C specimen had the greatest diameter change in Furnace Loading No. 4. Obviously, it would be difficult if not impossible to identify any trend with fuel loading based on these results.

It is important to note that the data in Figure 11 indicate, on the average, much greater diameter changes after 50 thermal cycles than those given in Figure 10 (see Table 6 for summary of data after 50 thermal cycles). Since the only difference between the tests in these two figures is the dwell time at $2500^\circ C$, it seems necessary to conclude that the dimensional changes observed are a function of the exposure time at the high temperature. For this reason the data from Figures 10 and 11 were replotted in Figure 12 to indicate diameter changes as related to the total exposure time at the high temperature (50 cycles in the Figure 10 tests represents 500 minutes or 8.33 hours at $2500^\circ C$). While only the data for specimens A-15, B-10, and B-12 from Figure 10 are shown, it is clear

~~CONFIDENTIAL~~

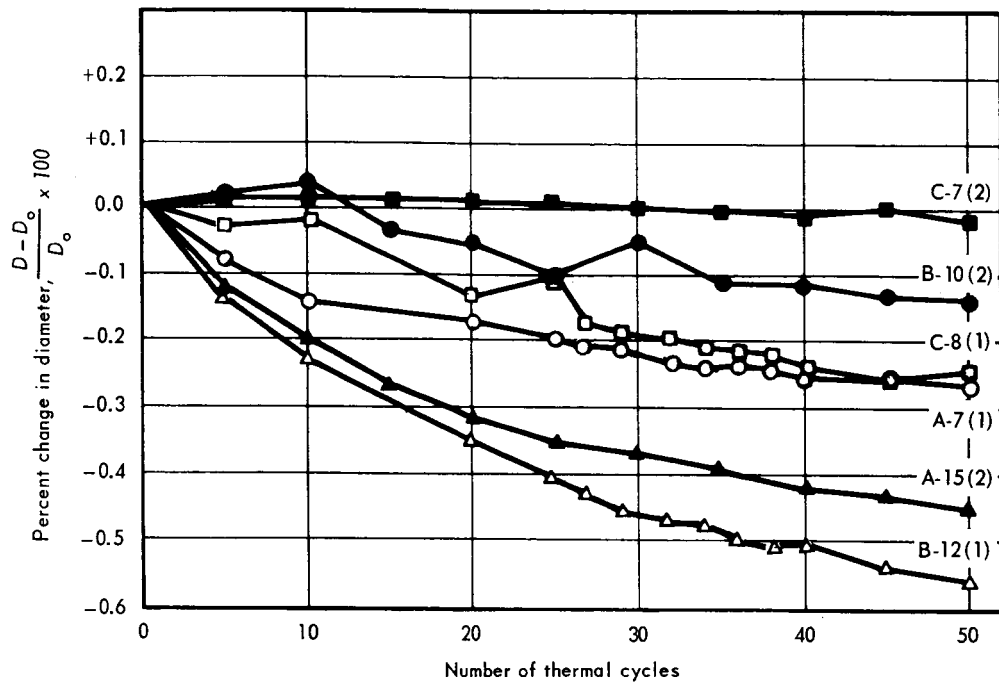


Figure 10 - Effect of number of thermal cycles on percent change in diameter of Type A, B, and C specimens cycled between room temperature at 2500°C in helium; 10-minute dwell at high temperature.

(1) Furnace loading No. 1
(2) Furnace loading No. 2

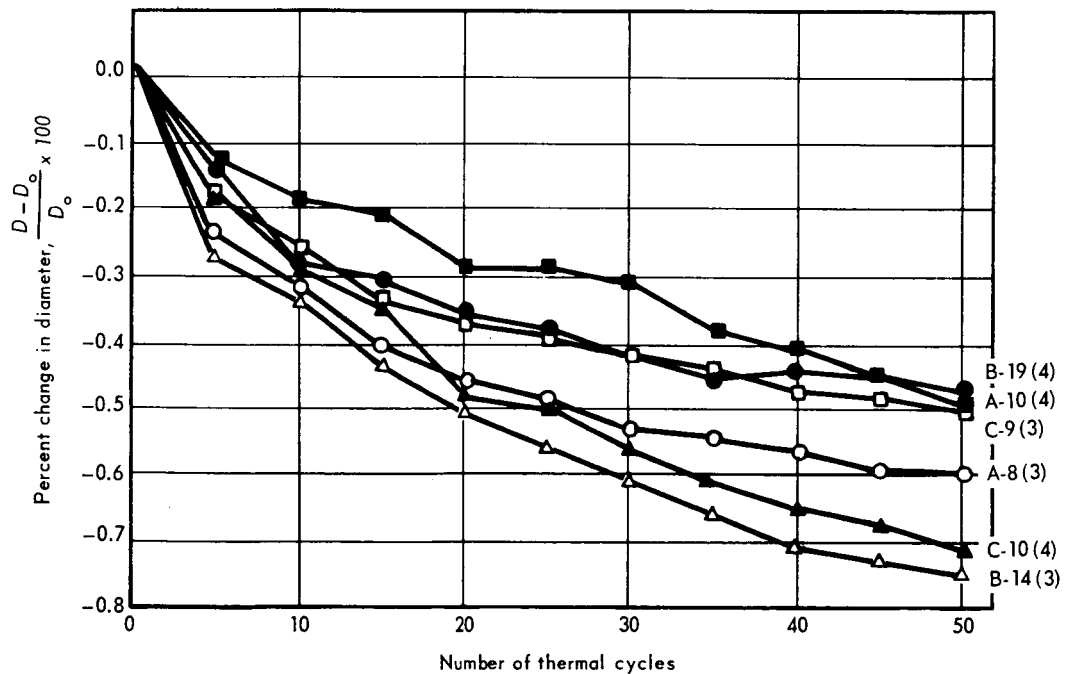


Figure 11 - Effect of number of thermal cycles on percent change in diameter of Type A, B, and C specimens cycled between room temperature and 2500°C in helium; 1-hour dwell at high temperature.

(3) Furnace loading No. 3
(4) Furnace loading No. 4

~~CONFIDENTIAL~~

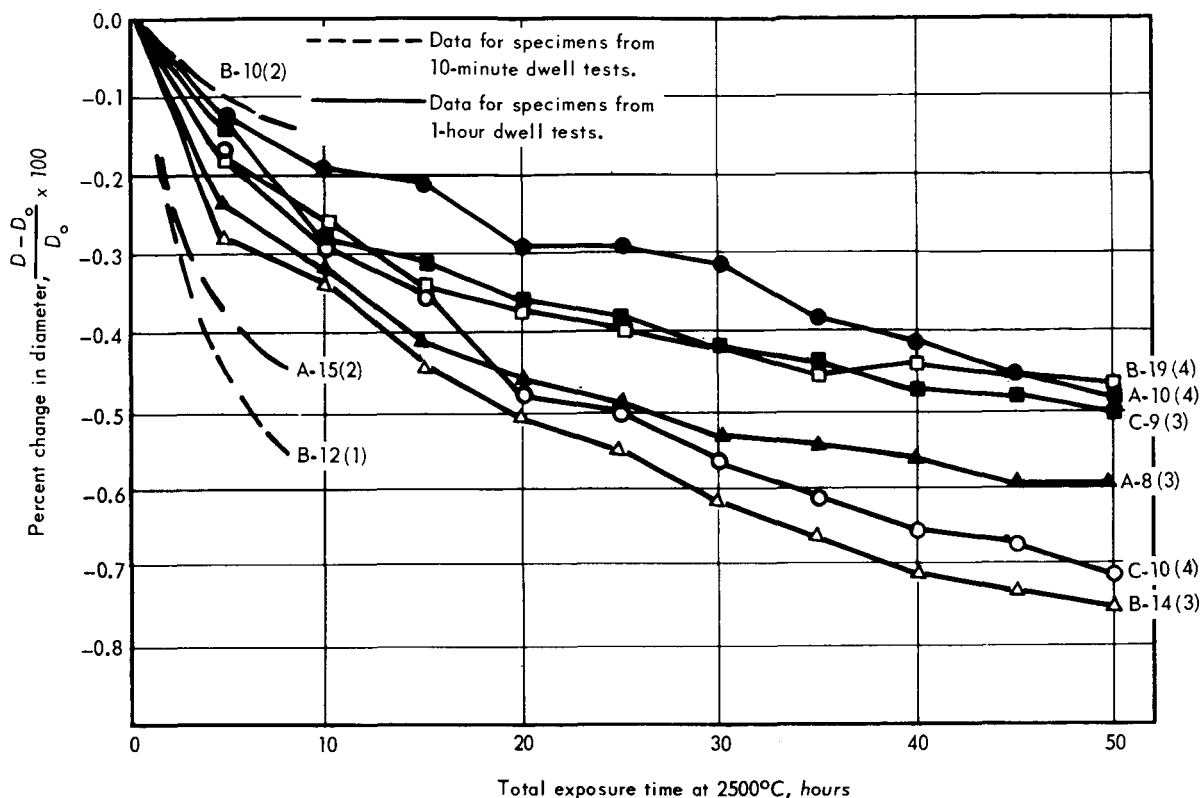


Figure 12 - Effect of total exposure time at 2500°C on diameter changes in Type A, B, and C specimens

that the Figure 11 data are bracketed by those of Figure 10. Furthermore, it is interesting that specimens A-15 and B-12 experienced a diameter change which occurred at a much higher rate than any of the specimens in Figure 11. It is possible that had A-15 and B-12 been exposed to 2500°C for a total of 50 hours in such thermal cycling tests, the total change in diameter would be comparable to that observed in specimens B-14 and C-10. No explanation for this behavior can be given at this time. It was presented only because this effect is not immediately obvious from a direct comparison of Figures 10 and 11.

A brief summary of the length changes is presented in Figure 13. In every case, a length increase was noted after 50 thermal cycles and it will be observed that the length changes in the 1-hour dwell tests are, on the average, greater than those observed in the 10-minute dwell tests. This, too, seems to suggest an effect of total time at maximum temperature on the dimensional stability of the specimen. A comparison similar to that shown in Figure 12 indicates consistent behavior for all the curves presented in Figure 13 for the 10-minute dwell time would be bracketed by the data obtained in the longer dwell tests.

It will be observed that the specimens which exhibited the greatest change in diameter are not necessarily those in which the greatest changes in length were observed. A brief study of Figures 10, 11, and 13 will reveal that while specimen B-14 had the greatest diameter change of the 1-hour dwell specimens, it had the smallest increase in length; specimen C-9 on the other hand, which had one of the smallest diameter changes, had

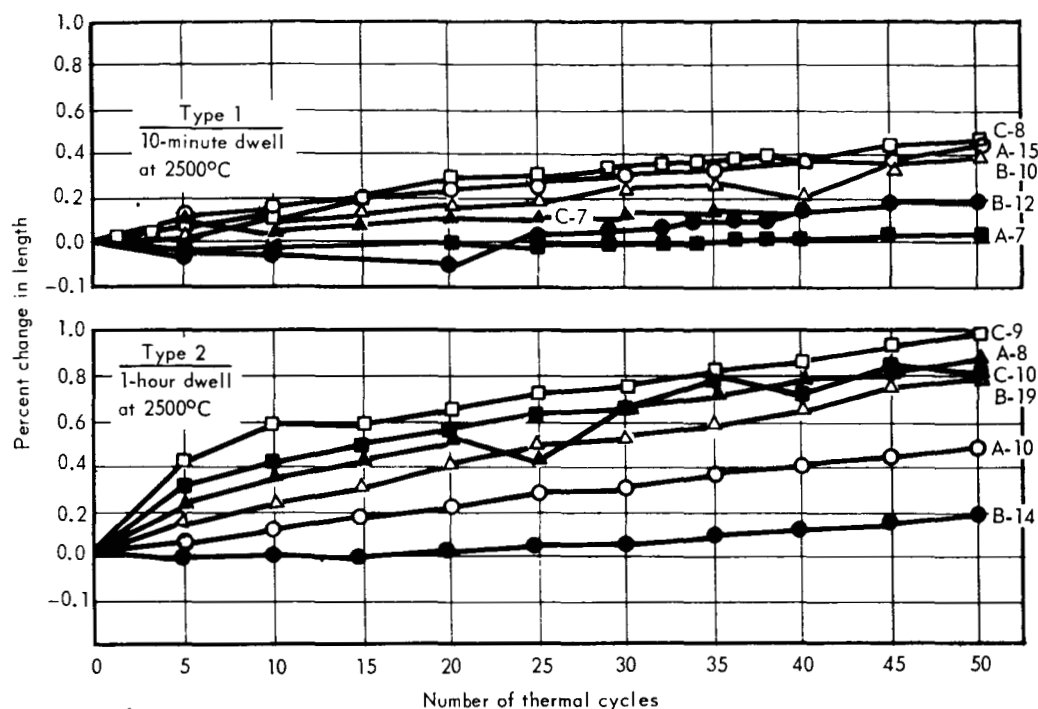


Figure 13—Effect of number of thermal cycles between room temperature and 2500°C on the sample length for Type A, B, and C specimens

at the same time the greatest increase in length. A similar pattern can be noted in the 10-minute dwell tests where specimen B-12 had the largest diameter change and yet the smallest length change; specimen B-10, on the other hand, had one of the smallest changes in diameter and one of the largest increases in length.

Measured changes in diameter were not found to be uniform over the entire length of the specimens. Hence, while the data in Figures 10 and 11 reflect the changes in diameter at the longitudinal midpoint of the specimen, they are definitely not to be interpreted as applying over the entire length of the samples. Diameters at the specimen ends, for example, were found to follow a particularly irregular pattern. Data for the percentage change in end diameters, corresponding to the inspection after 50 thermal cycles, are given in columns 2 and 3 of Table 6. It is seen that these data deviate markedly from the midpoint diameter measurements. In some cases, both the top and bottom diameter increased; in some cases they both decreased; and in other cases, the top diameter increased while the bottom diameter decreased; whereas some specimens experienced an increase in the bottom diameter and a decrease in the top diameter. It also can be observed that in some specimens the decreases observed in the end diameters were larger than those measured at the specimen midpoint. No particular explanation can be offered for this erratic behavior although it is felt that end diameter increases are associated with growth of the end-plates used in making the specimens. Subsequent tests, to be described below, indicated that powder metallurgy W-Re-Mo alloy, of the composition used for these end-plates, exhibits an appreciable change in both diameter and thickness when thermally cycled to 2500°C in helium. It is interesting, and this too will be described later, that little or no such dimensional changes were observed when arc-cast material was used in these subsequent evaluation tests.

~~CONFIDENTIAL~~

TABLE 6
SUMMARY OF INSPECTION RESULTS OBTAINED AFTER
50 THERMAL CYCLES BETWEEN ROOM TEMPERATURE
AND 2500°C

Specimen	Percent Change in Diameter		Percent Change in			
	Top	Bottom	Midpoint Diameter	Length	Volume	Weight
1) - Type Number 1, 10-minute Dwell Tests						
A-7	0.14	0.57	-0.26	0.06	-0.47	3.1×10^{-2}
B-12	0.08	0.9	-0.56	0.20	-0.87	3.8×10^{-2}
C-8	0.50	-0.19	-0.25	0.47	-0.17	-2.0×10^{-2}
B-10	-0.057	-0.11	-0.14	0.40	0.16	2.8×10^{-2}
C-7	0.08	0.19	-0.02	0.20	0.17	1.6×10^{-2}
A-15	-0.27	-0.57	-0.45	0.45	-0.36	3.0×10^{-2}
2) - Type Number 2, 1-hour Dwell Tests						
A-8	-0.58	-0.85	-0.59	0.83	-0.16	4.0×10^{-3}
B-14	0.21	0.14	-0.75	0.19	-1.09	4.0×10^{-2}
C-9	-0.3	-0.12	-0.50	1.0	0.36	5.0×10^{-2}
A-10	-0.4	0.31	-0.35	0.49	-0.02	-8.0×10^{-3}
B-19	-0.47	0.58	-0.47	0.81	-0.01	-5.0×10^{-3}
C-10	-0.24	-0.76	-0.71	0.88	-0.48	2.0×10^{-2}

It was usually found that the diameter measurements at the two locations between the ends of the specimen and the longitudinal midpoint were in agreement with the midpoint measurements. Only in cases where the changes in the end diameters were pronounced did this effect extend along the specimen to affect these locations.

A fair amount of consistency can be observed in the diameter, length, and volume measurements for a particular specimen. If, for example, the specimen volume change is calculated from the measured length and diameter changes, good agreement with the measured volume change is noted in all but a few cases. Based on data after 50 thermal cycles, such calculations yielded the data given in parentheses in the sixth column of Table E-1 enabling a direct comparison to be made with the measured parameter. Some discrepancy is to be expected in view of the non-uniformity of the diameter change along the length of the sample. However, despite this effect the agreement must be considered fairly good.

In view of the statement made previously that specimen diameter always decreased while specimen length always increased, some specimen anisotropy appears to be suggested. The end-plate growth (3 to 4 mils in thickness in each end-plate measured in supplementary tests) can account for a portion of this effect, but it cannot account completely for this unexpected result. Even allowing for the increase in end-plate thickness, it still is observed that the diameter decrease is not accompanied by an associated decrease in length. That a certain amount of anisotropy might be present seems to be confirmed, at least partially, by the results obtained (see Table E-1) in the test of specimen W-1, an unclad sample of pure tungsten, having the same dimensions as the fuel samples used in this study. In this test (only 20 thermal cycles), a diameter decrease occurred consistent with the data obtained with the fueled sample. While no length increase was noted, it is interesting that the length change is much less than that corresponding to completely isotropic behavior (percent length decrease should be equal to the percent diameter decrease for purely isotropic behavior). Hence, even in pure

~~CONFIDENTIAL~~

tungsten, in this configuration, subjected to a thermal cycling treatment, the dimensional changes suggest anisotropic behavior. It would seem, then, that the behavior of the Type A, B, and C specimens is consistent with that of the pure tungsten sample. Of course, the observed difference in the diameter and length changes might be due to some type of thermal stress ratcheting (Reference 3) mechanism and not to what is usually considered as anisotropy but with the data available in this investigation no clear distinction can be made.

In another test of an unclad specimen of pure tungsten (W-2), the sample was exposed to 2500°C in helium for 67 hours and hence underwent only one thermal cycle in this treatment. Interestingly enough, this specimen experienced a diameter decrease of 0.36 percent and a length decrease of 0.35 percent. This is essentially isotropic behavior. Based on these limited data, it would seem that the only conclusion available is that tungsten behaves isotropically in isothermal treatments at high temperatures (i. e., 2500°C) but anisotropically when subjected to a thermal cycling treatment.

When this program was first initiated it was felt that the thermal expansion differences between the clad and matrix materials would lead to clad cracking in the thermal cycling evaluations. It also was felt that increases in specimen diameter would be observed inasmuch as this has been a fairly standard observation in various thermal cycling evaluations of the type of material being used in this study (Reference 3). However, no clad cracking was observed and no increase in specimen diameter was noted. Instead, as discussed in some detail on previous pages, a diameter decrease was observed. This ranks, perhaps, as the first time such an observation has been made for such materials in this type of thermal cycling test. Of course, the temperature of the testing in this study is higher than that used in most evaluations, and hence it must be concluded that this factor almost alone is responsible for the observed diameter decrease. As a matter of fact, it seems fairly probable that the high temperature involved has caused additional sintering of the specimens and this has caused the observed diameter decreases. Since a length decrease also should be expected if only additional sintering were taking place, it must be concluded that whereas additional densification due to sintering may be taking place, it cannot be the only operating phenomenon. Since this program was designed to evaluate the performance of a given number of specimens when subjected to a certain thermal cycling treatment, it could not supply enough data to allow an identification of the exact mechanisms which were operating to effect the dimensional changes which were observed.

One comparison of the data obtained in this study is presented in Figure 14 where the percent change in diameter is plotted against total time at 2500°C. Curves for specimens A-10 and B-14 are presented to bracket the data obtained in the 1-hour dwell tests of Figure 11. Following the completion of the full 50 thermal cycles, specimen B-14 was given a 67-hour isothermal soak treatment at 2500°C. It was observed, as shown in Figure 14, that essentially no further change in the diameter was noted. However, when the thermal cycling tests were resumed, further diameter decreases were found to occur. Such behavior appears to suggest that, after a certain amount of thermal cycling treatment, specimens of this type do not experience any noticeable dimensional change when exposed to high temperatures in isothermal treatments. Following this isothermal treatment, however, additional thermal cycling will cause additional dimensional changes. Hence, the further decrease in diameter observed in specimen B-14 following the 67-hour isothermal soak identifies thermal cycling effects as being fairly predominant in causing the diameter decreases noted in this specimen. It seems reasonable to conclude

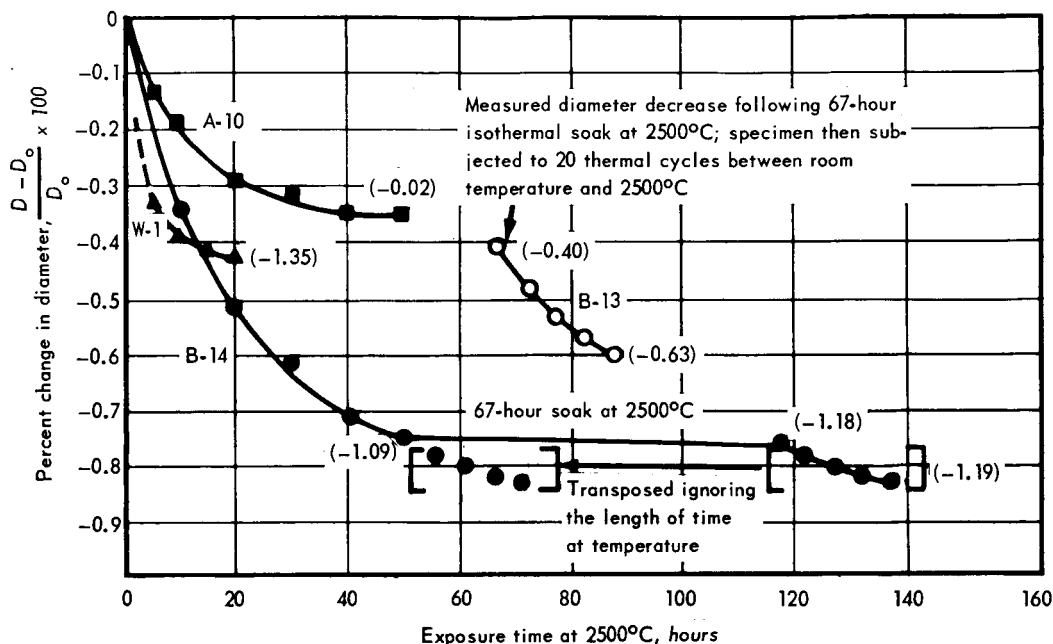


Figure 14—A comparison of some diameter changes as influenced by exposure time at 2500°C for Type A, B, and C specimens (values in parentheses represent percent volume change)

that had no additional thermal cycling been imposed little change in the diameter of specimen B-14 would have been noted in isothermal tests at 2500°C. Considering the 67-hour soak as one thermal cycle, the last four thermal cycling data points for specimen B-14 can, as shown in Figure 14, be transposed to the left to form a fairly exact continuation of the curve corresponding to the first 50 thermal cycles. Such behavior indicates again the stability of the specimen during the 67-hour isothermal treatment.

In another special evaluation, untested specimen B-13 was subjected to an isothermal exposure to 2500°C in helium for 67 hours. As noted in Figure 14, a fairly substantial diameter decrease was obtained indicating that isothermal treatment at 2500°C preceding any thermal cycling tests has a decided effect on specimen stability. This must be compared to the behavior of specimen B-14 where no, or certainly very little, effect of isothermal treatment is obtained once the specimen has been subjected to 50 thermal cycles. It was interesting though that when specimen B-13 was subjected to Type 2 (one-hour dwell) thermal cycling tests following this 67-hour isothermal treatment, diameter decreases were found to occur at fairly high rates. No data are available relating the diameter decrease with time during the first 67 hours of the test of specimen B-13; however, it seems reasonable to expect that the shape of this curve would approximate that of specimen A-10. In other words, the rate of change of diameter with respect to time would decrease continually approaching a percent diameter change of -0.40 percent. Hence, it is clear that the thermal cycling tests immediately following the isothermal treatment of this specimen have caused the rate of diameter change with respect to time to increase markedly. There seems no other conclusion but that thermal cycling has a pronounced effect on the dimensional stability of these specimens. Such behavior is so consistent with that observed in the last 20 thermal cycles of specimen B-14 that this effect must be considered of some importance. As a matter of fact, this behavior suggests that this approach of applying a thermal cycling treatment might well have merit in sintering operations where high densification rates and high final densities are desired.

CONFIDENTIAL

In another special thermal cycling test, a pure tungsten specimen, W-1, having the same dimensions as the composite specimens was employed. Results of this test also are shown in Figure 14 where it is noted that after 20 thermal cycles the tungsten specimen experienced a diameter decrease of some 0.43 percent. It also should be noted that the 1.35 percent decrease in volume of this specimen during this cycling treatment represents a noticeable densification. This densification of pure tungsten must be considered consistent with the dimensional changes observed in the composite specimens used in this thermal cycling program.

A few studies of the core density after test have been made. A grinding operation was employed to remove the clad material from specimens B-11, B-12, and C-9. Measurements then were made of the density of the cores of these samples with the results shown in the following table:

Specimen	No. of Thermal Cycles	Percent Change In			Measured Core Density	
		Diameter	Length	Volume	Percent of Theoretical Before Test	After Test
B-11*	3	—	—	—	97.2	97.42
B-12 (10-min. dwell)	50	-0.56	0.20	-0.87	96.0	97.6
C-9 (1-hr. dwell)	50	-0.50	1.0	0.36	96.9	99.4

*Blistered after 3 cycles and was removed from the test program.

It is interesting that for the two specimens subjected to 50 thermal cycles the core material has undergone additional densification. On the other hand, in specimen B-11 which was subjected to only 3 thermal cycles only a very nominal increase in density was observed. Admittedly the before-test densities are those measured before the specimens were autoclaved in the cladding operation, but then very little density increase is expected during this process. This effect is confirmed to some extent by the data for specimen B-11. It must be concluded, therefore, that the core material seems to have undergone additional densification during these thermal cycling tests. Such behavior obviously is consistent with the diameter decreases which have been measured following the thermal cycling tests but, of course, is inconsistent with the measured increases in specimen length.

At this moment, no explanation of this phenomenon can be offered. It should be expected that increases in length accompanied by core shrinkage would result in the formation of voids within the capsule. Actually such voids have been detected in several samples by radiographic techniques, but recent measurements to provide estimates of the volume occupied by these voids led to values much below those required to provide a consistent interpretation. These voids occurred at the end (usually only at one end) of the capsule between the core and clad and were found to almost completely encircle the core.

A comparison of the W-1 and W-2 data provides another confirmation of the effect of thermal cycling on specimen density. It will be noted that after 5 thermal cycles (i.e., 5 hours at 2500°C), the diameter decrease of specimen W-1 is essentially equal to that observed in specimen W-2 after 67 hours at 2500°C. Since diameter and densities are related,

CONFIDENTIAL

~~CONFIDENTIAL~~

this information seems once again to confirm the observation made previously that faster sintering rates are obtainable when a temperature cycling treatment is employed.

(b) Type D Specimens

Testing of the Type D specimens (using 10-minute dwell test) was initiated using specimens D-2 and D-3. After 5 thermal cycles, two blisters developed, one on each of the end-faces of specimen D-3. This distorted the length measurements being made, but since it was felt that the diameter measurements would probably still be representative, the sample was continued on test. However, specimen D-4 was added to the test program in the event that specimen D-3 would not yield meaningful results. This specimen also developed a blister on one end-face after 5 thermal cycles, but as in the case of specimen D-3 the testing was continued since the diameter measurements were felt to be unaffected by this localized blistering.

Measurements of specimen D-3 after 5 thermal cycles revealed that the blister on the top end-face was about 0.035 inch in height and seemed to affect the entire specimen diameter at this location while the blister on the bottom end-face was about 0.015 inch in height and about 0.2 inch in diameter. Both these blisters increased in size during the thermal cycling tests, and at the end of 50 thermal cycles, the top blister was some 0.140 inch in height while the bottom blister was about 0.040 inch in height. Severe cracking was noted in the large blister on the top end-face. After 45 cycles a small blister, 0.010 inch in height and about 0.1 inch in diameter, was noticed on the side of specimen D-3 located 0.1 inch below the top end-face. It is likely that this formation was linked to the formation of the large top face blister.

Only one blister formed in specimen D-4 and this after 5 thermal cycles. Located on the top end-face, this blister was 0.012 inch in height and about 0.25 inch in diameter. It did not seem to grow as additional thermal cycles were imposed.

A photograph of the five Type D specimens employed in this evaluation is shown in Figure 15. Specimens D-1 and D-5 are shown in the as-fabricated condition along with specimens D-2, D-3, and D-4 following exposure to 50 thermal cycles to 2500 °C in helium. Clearly shown is the severely blistered and fissured end of specimen D-3. Also apparent is the small blister which developed in the end-face of specimen D-4. Specimen D-2 still appears in excellent condition and is essentially identical to the pre-test shape and form.

These specially fabricated specimens were found to behave somewhat differently than the Type A, B, and C specimens (see data in Table E-1). While no specimen cracking was observed, the dimensional changes were somewhat different from those observed in the previous tests. In specimen D-2, a diameter decrease was observed whereas a diameter increase was noted in specimens D-3 and D-4. Only specimen C-7 had a diameter decrease smaller than that observed in specimen D-2. Of course, since no diameter increases were observed in the tests of the Type A, B, and C specimens, the behavior of specimens D-3 and D-4 is unique. A plot of the diameter variation with the number of thermal cycles is shown in Figure 16. Even for the D-2 specimen, the slope of this plot appears to be different from any shown in Figures 10 and 11 particularly insofar as the slope appears to be steeper in the range following 30 cycles than that observed in the 0 to 30 cycle range.

Since a diameter decrease was noted in specimen D-2 while increases were observed in specimens D-3 and D-4, it is difficult to draw any definite conclusions regarding material behavior. However, it does seem interesting, although this might be fortuitous, that the increase in diameter noted in specimens D-3 and D-4 is very close to that corresponding

~~CONFIDENTIAL~~

CONFIDENTIAL

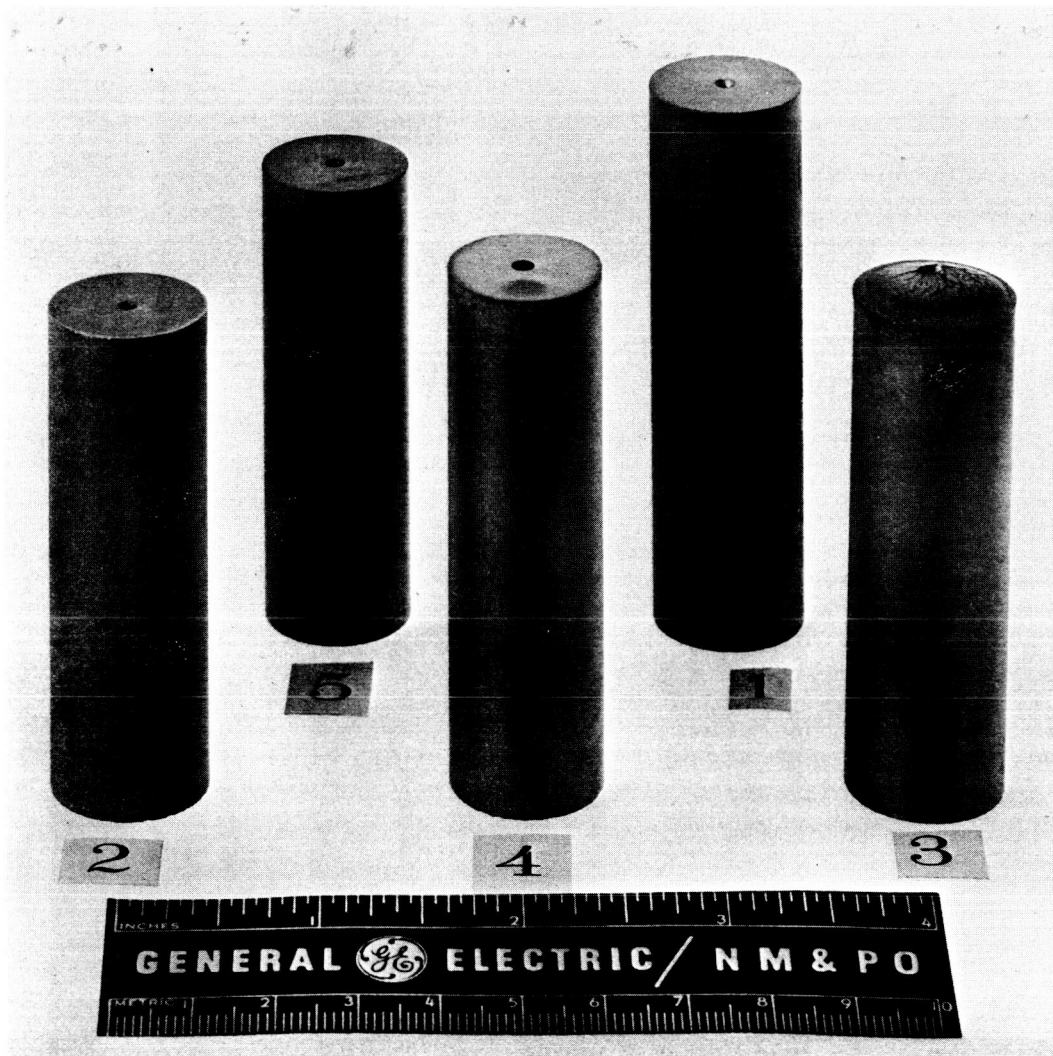


Figure 15 – Photograph showing Type D specimens, two in the as-fabricated condition and three (D-2, D-3, and D-4) after test (Neg. P66-6-13A)

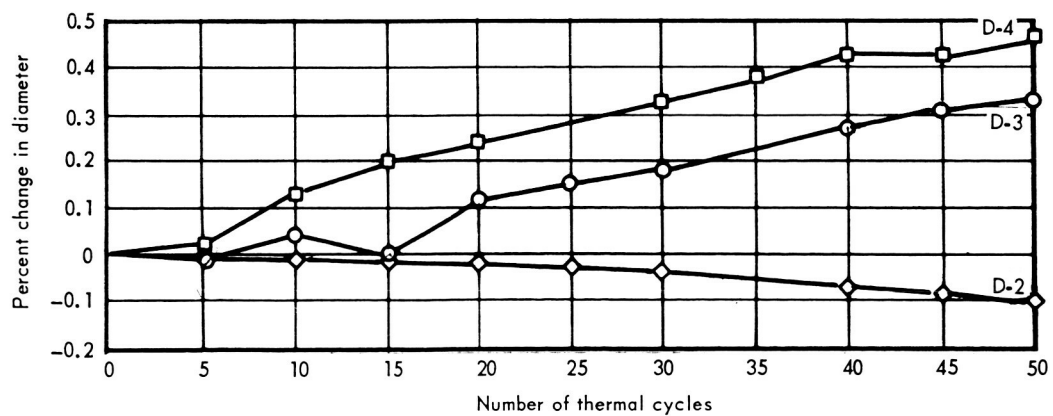


Figure 16 – Change in specimen diameter as a function of number of thermal cycles (10-minute dwell) from room temperature to 2500°C for type D specimens

CONFIDENTIAL

to the difference between the thermal expansion characteristics at 2500°C for the core and sleeve compositions (see Figure 8). Certainly more confirmation of this effect will be required before this interpretation can be accepted as factual.

(c) End-Plate Growth Studies

During a post-test metallographic evaluation of specimen B-12, there was some indication that the W-25Re-30Mo end-plates had experienced an increase in thickness. Since this observation seemed consistent with the length increases observed in the thermal cycling tests of all the Type A, B, and C specimens some supplementary tests of end-plate material were suggested. Two W-25Re-30Mo (powder metallurgy material) end-plates were obtained, one 0.080 inch in thickness and another 0.131 inch thick. Both of these specimens then were subjected to the same thermal cycling treatment given the clad composite specimens. It was found that both end-plates did indeed increase in thickness as shown by the data in Figure 17. After fifty thermal cycles to 2500°C, increases in thickness of 1.8 percent (1.5 mil) and 2.5 percent (3.3 mil) were observed in the 0.080 and 0.131 inch end-plates, respectively. Hence, some dimensional instability exists in this end-plate material upon exposure to temperatures in the range of 2500°C. A simple calculation will reveal that end-plate changes of this magnitude are not sufficient to explain all of the length increases noted in the tests of the Type A, B, and C specimens (see Table E-1) but certainly these supplementary data do indicate that a portion of the length increases noted in the tested composite specimens must be the result of this material instability.

Data obtained using arc-melted W-25Re-30Mo end-plate material also are shown in Figure 17. It is clear that this material has excellent dimensional stability in that little or no increase in end-plate thickness was observed. It is felt that the decreased impurity level in the arc-melted material is primarily responsible for the increased dimensional stability.

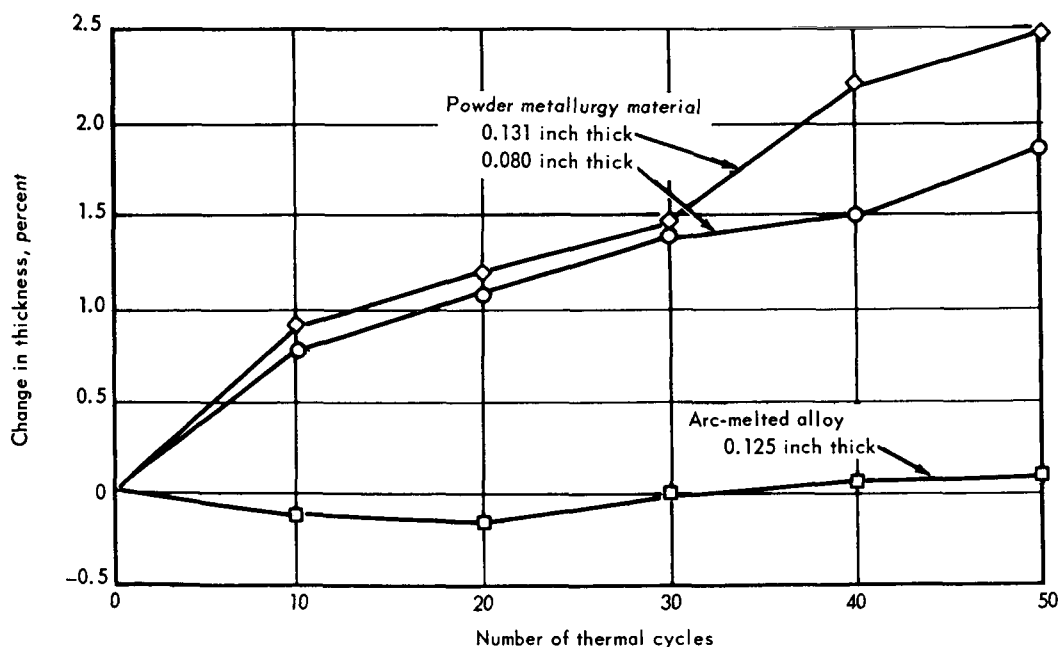


Figure 17 – Percent increase in thickness as a function of the number of thermal cycles from room temperature to 2500°C for W – 25Re – 30Mo end-plates

POST-TEST METALLOGRAPHIC EVALUATIONS

(a) Type A, B, and C Specimens

Representative specimens A-7, B-12, and C-8, of the three fuel loadings investigated were examined metallographically after testing using the fast cycle (Type 1; 10 minute dwell) while A-10, B-19, and C-10 were examined after testing using the extended cycle (Type 2; 1 hour dwell). Usually one transverse section was taken from each specimen although in a few cases longitudinal sections were taken as well. The microstructure of the tested specimens was compared with that of as-fabricated specimens of the same composition to determine the changes caused by the thermal cycling test.

Examination was primarily concerned with (1) core-clad bonding; (2) fuel stability; (3) fuel particle density, shape, and distribution; (4) the presence of free uranium or other metallic phases in the $\text{UO}_2\text{-Y}_2\text{O}_3$ fuel; (5) condition of the tungsten matrix; and (6) the porosity of the vapor deposited tungsten cladding.

Typical microstructures of the three specimens given the Type 1 thermal cycling test are shown in Figure 18. (The as-fabricated microstructures, typical of A, B, and C type specimens, were presented in Section III, Figures 3 and 4.) Generally, the specimens were in good condition. For the most part, the bond between the core and the vapor-deposited tungsten cladding was intact although a few small areas were observed where a void was present at the core-clad interface.

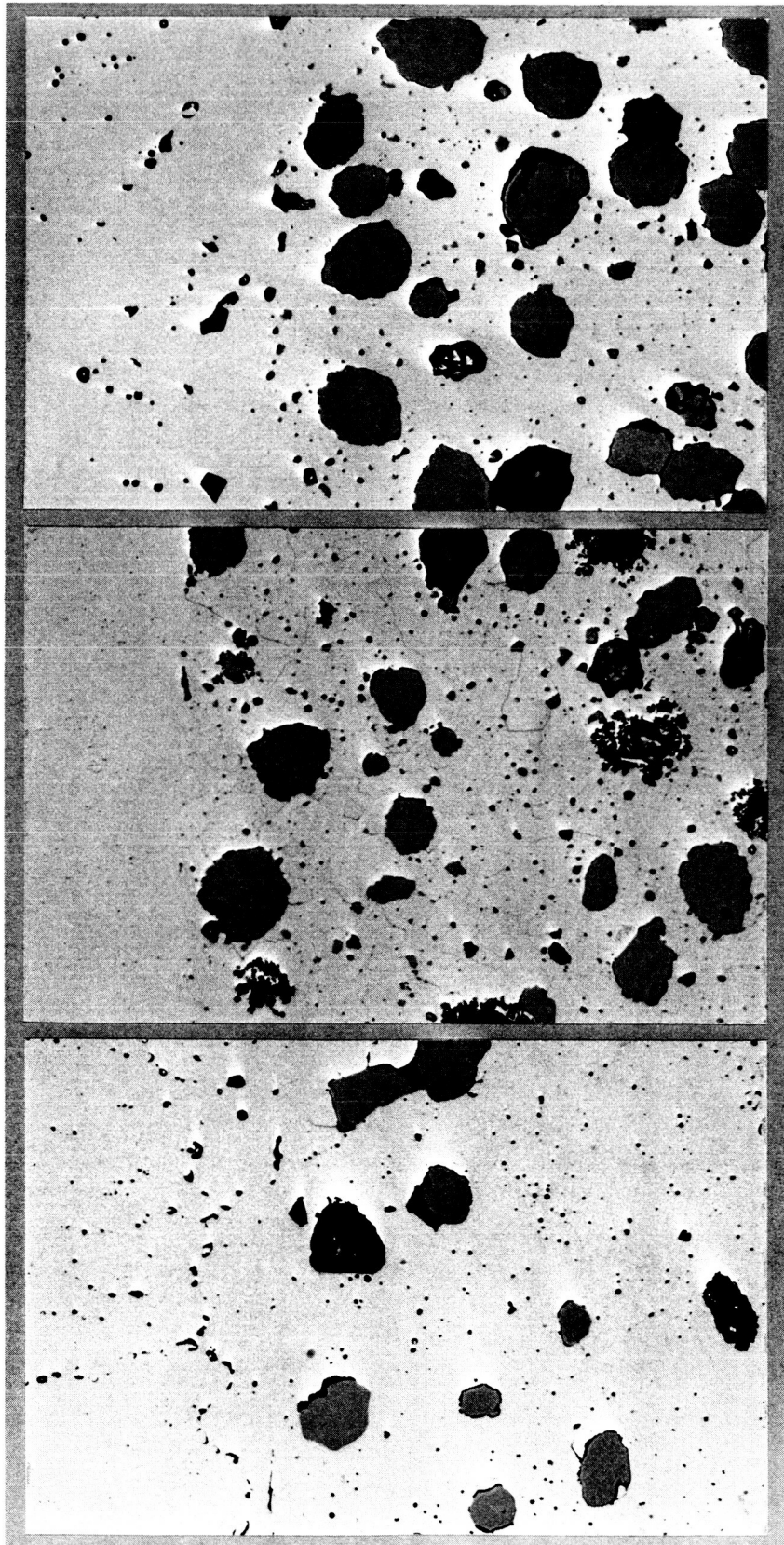
Some void formation was noted between each fuel particle and the tungsten matrix. Although not confirmed, such voids are usually caused by an increase in fuel particle density resulting from the high temperature testing. Because of this void formation, many of the fuel particles fell out during metallographic mounting and polishing of these samples.

Particularly noteworthy in this metallographic analysis was the lack of fuel migration into the tungsten matrix. The migration of fuel into the grain boundaries of the tungsten matrix, termed fuel channeling, has been observed frequently at GE-NMPO upon testing specimens containing hypostochiometric fuel.

Two specimens (C-8 and C-10) were analyzed chemically after testing to determine the amount of free U and free Y present. The analytical procedure (Reference 7) depends on the hydriding of the metallic phases at one temperature, the decomposition of the hydrides formed at some higher temperature, and the subsequent measurement of the volume of hydrogen liberated. Using this technique, it was found that the 30 v/o fuel specimens contained essentially no free U or Y within the limits of the analytical procedure. The hydrogen measured corresponded to less than 0.005 w/o U or Y. This observation along with the absence of fuel migration mentioned above indicates that the Y_2O_3 addition to the fuel apparently was effective in stabilizing the fuel under these test conditions.

No evidence of microcracking was observed in the tungsten matrix or the cladding. The grain size of the tungsten matrix increased only slightly since the fuel fines tend to pin the grain boundaries. It was noted though that a relatively large amount of porosity developed in the vapor-deposited tungsten cladding as a result of the test. This porosity, which is typical of vapor-deposited material prepared by the fluoride process heated to high temperatures, was present both within grains and intergranularly. The pores tended to be aligned along grain boundaries or were grouped together in a cluster. Only a moderate amount of grain growth occurred but the orientation difference between neighboring grains seemed to be enhanced by the test. Hence, the tested specimens had more sharply delineated grain boundaries.

CONFIDENTIAL



Specimen A-7; W-clad, W-10 v/o $\text{UO}_2\text{-Y}_2\text{O}_3$ (Neg. 6993)

Specimen B-12; W-clad, W-20 v/o $\text{UO}_2\text{-Y}_2\text{O}_3$ (Neg. 6973)

Specimen C-8; W-clad, W-30 v/o $\text{UO}_2\text{-Y}_2\text{O}_3$ (Neg. 6994)

Figure 18 - Photomicrographs of core-cladding interface of Type A, B, and C specimens after 50 thermal cycles to 2500°C using the Type 1 cycle (Unetched, 250X)

CONFIDENTIAL

CONFIDENTIAL

In Specimen B-12 (shown in Figure 18), many of the fuel particles appeared quite different from those observed in the other as-fabricated or tested specimens. At some sites a cluster of fine non-metallic particles which were identified as $\text{UO}_2\text{-Y}_2\text{O}_3$ fuel by microprobe analysis was present. In other areas a cluster of fine voids was observed. It appears that both conditions are related; i. e., the cluster of voids is the result of pull-out of the fine fuel particles during metallographic preparation. Possibly a small amount of fuel particles consisting of a cluster of finer particles was present in the fuel batch used to make this specimen. This condition did not seem to affect the performance of specimen B-12.

The yttrium content of the fuel particles, determined by microprobe analysis, was not uniform in specimen B-12 after testing nor in specimen A-9 in the as-fabricated condition. On the electron image, the variation in mass density between the various particles was readily observed. In specimen A-9, the yttrium content of the fuel particles ranged from 5 to 12 w/o. Generally, the yttrium content within a given particle was uniform. The variation in yttrium content between fuel particles in specimen B-12 was about the same as the yttrium distribution within a particle. This shows that the segregation occurred in blending and was not due to inadequate solutioning during sintering. Larger fuel particles of -100/+200 mesh prepared previously at GE-NMPO using similar procedures did not show as much variation in yttrium content.

There was no significant difference between the specimen held for one hour at 2500°C (extended cycle) and those held for 10 minutes (fast cycle). Typical microstructures of specimens given the extended cycle test are shown in Figure 19. The fuel and the matrix remained dense and there was no evidence of a fuel-matrix reaction and only a trace of fuel channeling. Possibly the tungsten matrix of the extended cycle specimens was more dense due to some additional sintering that occurred as a result of the one-hour hold at 2500°C with each cycle. However, the amount of porosity in the vapor-deposited tungsten cladding was about the same as in the fast cycle test series. An examination of a longitudinal section taken from specimen C-10 revealed that the W-25Re-30Mo end-plate material developed considerable porosity as a result of the test. It is thought that the increase in porosity is due either to the volatilization of impurities or the solutioning of sigma phase.

Generally, the tungsten cladding remained bonded to the core throughout the test. The area of specimen A-10 shown in Figure 19 is an example of the unbonded areas that were present over about 2 percent of the interface area of the specimens. This unbonded area is not related to the fuel particles in the core. Possibly the voids that form in the vapor-deposited material contribute to this bond failure.

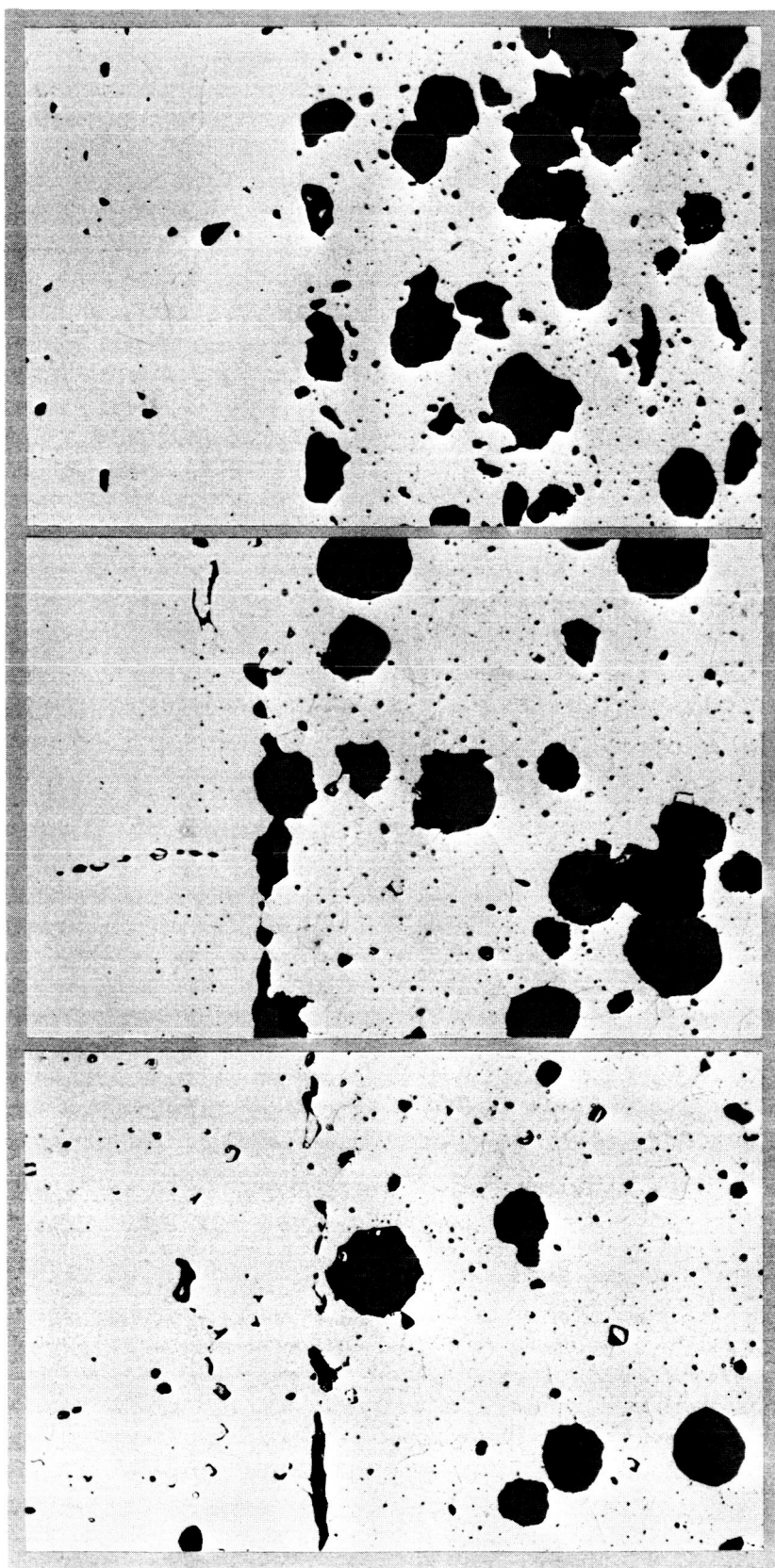
(b) Type D Specimens

The typical as-fabricated condition of the Type D specimens was described previously in Section III, Figure 5. The post-test condition was evaluated using metallographic sections of specimens D-2 and D-4.

A 3/4-inch long transverse section was cut from the middle of the tested specimens and longitudinal sections were prepared from the end pieces by grinding away nearly half of the diameter and polishing down to the center line of the specimens. Although the grinding was done slowly on these longitudinal sections, it appeared to have been too harsh for the brittle structure. The grinding produced cracks and increased polishing pull-out of both the fuel particles and the elongated grains of the vapor-deposited tungsten coating. Therefore, the metallographic evaluations to be discussed in this section were based primarily on the transverse sections.

CONFIDENTIAL

CONFIDENTIAL



Specimen A-10; W-clad, W-10 v/o $\text{UO}_2\text{-Y}_2\text{O}_3$ (Neg. 7037) Specimen B-19; W-clad, W-20 v/o $\text{UO}_2\text{-Y}_2\text{O}_3$ (Neg. 7619) Specimen C-10; W-clad, W-30 v/o $\text{UO}_2\text{-Y}_2\text{O}_3$ (Neg. 7036)

Figure 19 - Photomicrographs of core-cladding interface of Type A, B, and C specimens after 50 thermal cycles to 2500°C using the extended cycle (Unetched, 250X)

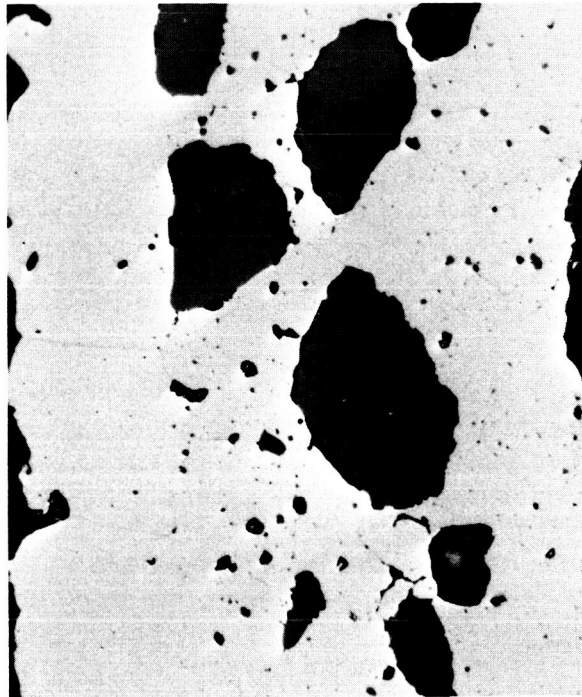
CONFIDENTIAL

Specimen D-2 which decreased slightly in diameter and volume as a result of the thermal cycle testing had a microstructure (see Figure 20) which was essentially unchanged from the pre-test condition. The bond of the core to the fueled sleeve was generally good and in some areas interdiffusion masked the original interface. Some porosity in the form of fine voids was evident in the tungsten matrix. In the etched condition, the tungsten matrix was composed of large grains and the porosity was located in the grain boundaries. The rounded fuel particles were generally of high density and were well distributed. Very few fuel fines were observed. No metallic phase was visible at high magnifications in the $\text{UO}_2\text{-Y}_2\text{O}_3$ fuel particles, and no evidence of fuel migration into the tungsten matrix was found.

The tungsten coating also was well bonded to the sleeve, although it appeared to be broken at some points as a result of pull-out of large grains during polishing. The vapor-deposited tungsten coating, which was applied by the chloride process and was reported to contain less than 10 ppm total halides, developed none of the porosity that normally results in coatings with high fluorine contents. By comparison, the Type A, B, and C specimens that were clad with tungsten tubing prepared by the hexafluoride process and contained up to 37 ppm fluorine, developed considerable porosity in the grain boundaries of the tungsten cladding when cycled to 2500 °C.

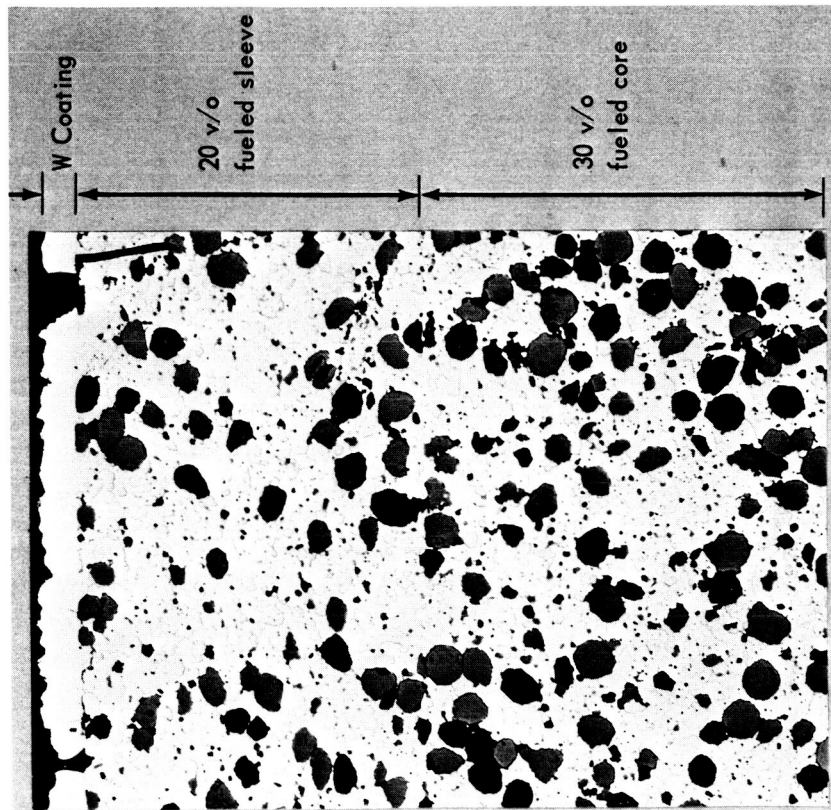
Specimen D-4 which increased in diameter and volume as a result of thermal cycling had a microstructure similar to that of specimen D-2. The major difference was scattered voids or areas of separation at the interface between the core and the fueled sleeve. These were extensive enough around the circumference of the transverse section that they could account for the increase in diameter measured in specimen D-4. Similar areas of separation were noted in the longitudinal sections.

A small blister developed in one end of specimen D-4 early in the thermal cycling test. A longitudinal section was cut through the blister area so it could be examined metallographically. The void associated with the blister was located within the core matrix well below the interface with the tungsten coating. It may be associated with some volatile impurity in the core, but no evidence was found that would establish the cause of the blister. A similar conclusion was reached in the analysis of the large blister on specimen D-3: as in D-4 the void was located within the core well below the core-cladding interface.



Neg. 7616, unetched, 500X

Figure 20 - Photomicrographs of core-sleeve interface area of specimen D-2 after 50 thermal cycles to 2500°C using fast cycle



Neg. 7615, unetched, 100X

~~CONFIDENTIAL~~

VI. SPECIAL PROGRAM HIGHLIGHTS

During the fabrication and testing portions of this program several observations were made which are believed worthy of special consideration. These special items are:

1. Dimensional measurements have indicated that tungsten clad, W- $\text{UO}_2\text{-Y}_2\text{O}_3$ core compositions involving 10, 20, and 30 volume percent of the fuel phase undergo a decrease in diameter when exposed to a thermal cycling treatment between 2500 °C and room temperature in helium. Previous experience with such materials had indicated that a diameter increase was to be expected. It appears, therefore, that this is the first observation involving a decrease in diameter for these materials subjected to a high temperature thermal cycling treatment.
2. It has been found that the use of relatively low density agglomerated fuel particles of $\text{UO}_2\text{-Y}_2\text{O}_3$ allows the attainment of high density (95 to 98 percent of theoretical) W- $\text{UO}_2\text{-Y}_2\text{O}_3$ cores in the as-sintered condition. When high fired (solution treated) $\text{UO}_2\text{-Y}_2\text{O}_3$ fuel was employed, densities less than 93 percent were the best that could be achieved in sintered compacts.
3. A combined sintering and solutioning procedure has been developed for use with W - ($\text{UO}_2\text{-Y}_2\text{O}_3$) compacts. In this special heat treatment cycle, the $\text{UO}_2\text{-Y}_2\text{O}_3$ agglomerates are solutioned in place, core cracking is avoided, and maximum core density is achieved.
4. Studies of the sintering characteristics of W - ($\text{UO}_2\text{-Y}_2\text{O}_3$) compacts have revealed that greater sintering rates and higher final sintered densities can be obtained by cycling the temperature during the sintering process. A patent disclosure has been written covering this particular phenomenon. This disclosure is identified as GE Docket No. 14D-NM-1076.
5. Hot gas pressure bonding techniques have been found successful in the application of a 0.020 inch thick vapor deposited sleeve of tungsten to serve as a cladding for tungsten - UO_2 cores. In this technique, expendable molybdenum cans served as gas-tight containers during the autoclave process.
6. Using hot gas pressure bonding techniques, sintered composites of different fuel contents have been diffusion bonded so well that no evidence of the original interface remains. Furthermore, cracks and joints between two sleeve sections were completely healed as a result of the high temperature deformation and densification of the sintered material. Using this method of fabrication, graduated fuel loading of cores proved feasible and the control of sleeve dimensions to very close tolerances was accomplished.

~~CONFIDENTIAL~~

~~CONFIDENTIAL~~

~~CONFIDENTIAL~~

VII. CONCLUSIONS AND RECOMMENDATIONS

Based on the results obtained in this investigation, several conclusions are suggested. In the first place, it is not correct to expect categorically that a thermal cycling treatment of refractory metal clad, tungsten-urania-yttria composites will lead to an increase in specimen diameter and to clad cracking. Such behavior was expected in this study and yet almost the opposite result was obtained. In almost every case, a decrease in specimen diameter was observed, and this was a function not only of the number of thermal cycles imposed but also of the hold time at maximum temperature. Furthermore, no specimen cracking was observed even after fifty thermal cycles. This behavior suggests that the high temperature (2500°C) employed in these thermal cycling tests has resulted in a certain amount of additional sintering of the specimens. Certainly, the effect of dwell time at maximum temperature in causing more pronounced diameter decreases can be interpreted in no other way. Furthermore, when tests using sintered tungsten specimens were found to yield similar diameter decreases, the additional sintering concept seemed to be confirmed. It would be interesting to perform similar tests of composite specimens in which the pre-test sintering operation is conducted over a sufficiently long time to preclude, or at least minimize, any additional sintering of the test specimens during the thermal cycling evaluation.

Another conclusion suggested by these thermal cycling tests is that sintering rates and final sintered densities are increased by causing the temperature to cycle during the sintering operation. Tests of tungsten clad composites and of pure tungsten specimens revealed similar behavior in that the rate of the diameter decrease (which is related to specimen density) is greater in a thermal cycling test to 2500°C than in an isothermal test at the same temperature. Final specimen densities also appear to be greater in the thermal cycling type of operation. This interesting observation suggests that some attention should be given to a more extensive evaluation of this phenomenon. Perhaps various test temperatures, heating and cooling rates, hold times at maximum temperature, and specimen geometry could all be investigated to determine the conditions which are most conducive to the attainment of maximum sintering rates and maximum final sintered densities.

Fabrication experience with the Type D specimens has indicated that specimens with graded (radially) fuel concentrations can be produced to very close tolerances. In addition this experience has proven that fueled sleeve segments can be assembled around a central fueled core and hot gas pressure bonding techniques employed to yield a final specimen in which no evidence of the original longitudinal or transverse interfaces remains.

A final recommendation pertaining to material reproducibility appears in order inasmuch as the measurements obtained in this program have indicated that duplicate tests of what were thought to be identical specimens failed to yield consistent behavior. If a reasonable interpretation of the effects of a thermal cycling treatment is to be developed for these clad composite materials, it would seem necessary to make certain that the specimens employed are characteristic of a given composition and yield similar behavior when subjected to certain test conditions. Once material uniformity is established and it is demonstrated

~~CONFIDENTIAL~~

that consistent test results are obtainable, it then would appear that a more meaningful interpretation of thermal cycling effects would be made possible. This recommendation is made with special reference to testing at temperatures above 2000 °C for in this temperature range a complete understanding of material stoichiometry, sintering effects, etc., is not available.

~~CONFIDENTIAL~~

~~CONFIDENTIAL~~

VIII. REFERENCES

1. "Nuclear Rocket Technology Conference, Pt. II - Tungsten Water-Moderated Nuclear Rocket," NASA SP-123, April 1966.
2. W. R. Yario, "Dimensional Stability of Refractory Metal Fuel Elements Under Thermal Cycling Conditions," GE-TM 66-4-17, 1966.
3. J. E. McConnelee, "Thermal Stress Ratchet Mechanism," GE-TM 65-5-31, May 4, 1965.
4. S. F. Bartram, E. F. Juenke, and E. A. Aitken, "Phase Relations in the System $\text{UO}_2\text{-UO}_3\text{-Y}_2\text{O}_3$," J. Am. Chem. Soc., Vol. 47, No. 4, 171, 1964.
5. J. B. Conway and A. C. Losekamp, "Thermal Expansion Characteristics of Several Refractory Metals to 2500°C," Trans. Met. Soc. AIME, Vol. 236, 702-709, 1966.
6. R. E. Taylor, "Final Report, Thermal Properties of Tungsten-Uranium Dioxide Mixtures," Confidential Report, NASA CR-54141, A1-64-153, September 1, 1964.
7. J. O. Hibbits and E. A. Schaefer, "The Determination of Uranium and Thorium Metal in Fuel Element Core Materials," GE-TM 65-9-14, June 1965.

~~CONFIDENTIAL~~

~~CONFIDENTIAL~~

~~CONFIDENTIAL~~

~~CONFIDENTIAL~~

IX. SUPPLEMENTARY INFORMATION

APPENDIX A

APPENDIX B

APPENDIX C

APPENDIX D

APPENDIX E

~~CONFIDENTIAL~~

CONFIDENTIAL

APPENDIX A RAW MATERIALS ANALYSES

Uranium Dioxide: Ceramic grade UO_2 powder prepared by ADU process.

Aver. Particle Size: 0.58 micron

Bulk Density: 0.93 g/cc.

Tap Density: 2.21 g/cc.

Uranium percent: 87.75

O/U: 2.06

Moisture percent: 0.16

Spectrographic Analysis: ppm

B	0.35	Fe	63	Pb	<1
Cd	0.10	F	<10	Si	80
C	37	Mn	<5	Ti	2.5
Ca	<20	Mo	<1	Co	<5
Cr	9	Ni	16	Total R. E.	<2 EBC

Yttrium Oxide: High purity Y_2O_3 powder

Chemical Analysis: percent

Y 78.51

C 0.097

S <0.001

Spectrographic Analysis: ppm

Ca Strong trace: 50 to 500

Mg Trace: <100

Na Trace: <100

Si Trace: <100

Not detected: Ag, Al, As, B, Bi, Cb, Cd, Co, Cr, Cu, Fe, Mn,
Mo, Ni, Pb, Sb, Sn, Sr, Ti, V, W, Zn, Ba, Li, K.

Tungsten Powder: High purity material of 1 to 3 micron particle size.

Spectrographic Analysis: ppm

Al <6 Fe 46 Mn <6

Ca 16 Cr 12 Mg 7

Si <7 Ni 20 Sn <6

Mo 98 Cu 7

Flame Photometry Analysis, ppm

Na 15 K 74

Leco Analysis, ppm

O_2 1190 C 11

Fisher Sub-Sieve Size Analysis

as supplied 1.26 micron 0.716 porosity

lab milled 1.25 micron 0.516 porosity

Particle Size Distribution by Photometer, weight percent

as lab milled 0-1 micron 32.7

1-2 micron 50.8

2-3 micron 13.5

3-4 micron 2.8

APPENDIX B

EVALUATION OF FUEL TYPES

High-Fired Fuel: The required fuel particles were to be a solid solution of UO_2 - 10 mole percent Y_2O_3 (8.5 wt. %) in the size range of -270/+400 mesh (37 to 53 micron diameter). Solutioning of Y_2O_3 in UO_2 is usually accomplished by heating the blended powders above 2000°C in dry hydrogen. The first procedure used in fuel preparation was as follows: six kilograms of depleted UO_2 powder were vacuum dried at 110°C for 4 hours; one kilogram of yttria powder was calcined at 1000°C in air and furnace cooled; blends of 91.5 weight percent UO_2 and 8.5 weight percent Y_2O_3 were thoroughly mixed by shaking in plastic bottles for 1 hour; each blend was analyzed for homogeneity and the Y_2O_3 content ranged from 6.9 to 8.8 weight percent with an average for six blends of 7.6 weight percent Y_2O_3 .

These powder blends were placed in rubber molds and isostatically pressed at 50,000 psi into cylindrical compacts. These compacts were then heated at 2000°C for 8 hours in dry hydrogen as a solutioning treatment. This material was crushed and screened to obtain the particle size of -270/+400 mesh. The crushing was accomplished by either dry milling with tungsten carbide balls or by passing the material through a roll crusher. Both methods were slow and produced a low yield of the required particle size. Furthermore, the particles were angular in shape, as shown in the photomicrograph of Figure B-1, and of high density, which is an undesirable property for sintering with a tungsten matrix.

X-ray diffraction analysis of the fuel indicated that complete solutioning had been accomplished at 2000°C; no oxide existed either as urania or yttria.

To determine the sinterability of this high density fuel in large core compacts of tungsten, trial runs were made using the W - 20 volume percent (UO_2 - Y_2O_3) composition. The powder blend was cold pressed in a 1.25-inch diameter die, without use of binder material, to a green density of 55 percent of theoretical. These compacts were sintered at 2200°C for 2 hours in hydrogen and a maximum density of 92 percent of theoretical was attained. The microstructure of one of these trial specimens is shown in Figure B-2 and is typical of the unfavorable core structure that results from the high fired, angular fuel particles. A total of 12 fueled core compacts were prepared of Types A, B and C using the high density, angular fuel particles and various sintering cycles were employed in an effort to achieve high density core bodies. The results of these experimental sinterings are shown in Table B-1. Also shown are data for an unfueled tungsten compact which was similarly sintered for comparison. The higher the fuel loading the lower the sintered density. Using the optimum sintering cycle, densities greater than 90 percent of theoretical were difficult to attain; yet, the unfueled tungsten compact sintered to better than 94 percent of theoretical.

Two of these experimental cores (B-4 and B-7) were sealed in expendable tantalum cans and were autoclaved in 10,000 psi helium pressure at 1750°C for 1.5 hours. This resulted in densification to 94.7 percent of theoretical density (T.D. = 17.45 g/cm³). For fabrication of test specimens, the core density should be at least 95 percent of theoretical prior to autoclave bonding. This problem of achieving high density W- UO_2 composites using high density fuel particles had been experienced in previous work at GE-NMPO and led to the development of agglomerated fuel particles for improved sinterability. Past experience had shown that high density fueled cores could be prepared of agglomerated UO_2 - Y_2O_3 mixtures blended with tungsten powder and sintered at or above the solutioning temperature

CONFIDENTIAL

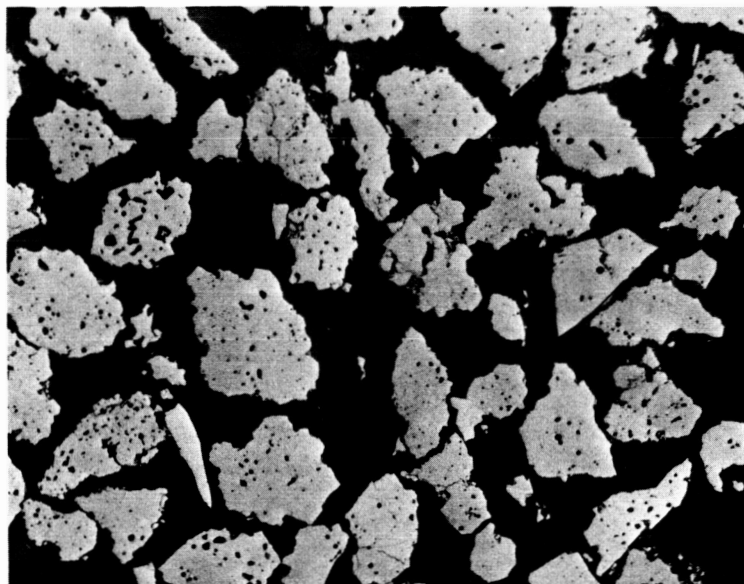


Figure B-1 - UO_2 - 10 mole percent Y_2O_3 , solutioned at 2000°C for 8 hours in H_2 . Crushed and screened to $-270/+400$ mesh. Particle range 30 to 180 microns. (Neg. 6148, 250X)

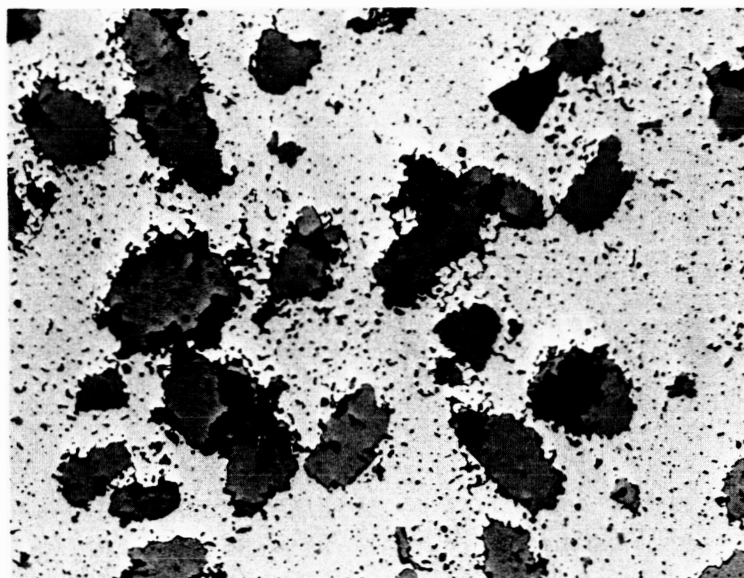


Figure B-2 - W - 20 v/o (UO_2 - Y_2O_3) core structure as sintered at 2200°C for 2 hours. Density was 92.3% of theoretical. (Neg. 6170, 250X)

CONFIDENTIAL

CONFIDENTIAL

TABLE B-1
SINTERED DENSITIES OF W- UO_2 - Y_2O_3 CORE COMPOSITES
CONTAINING HIGH FIRED FUEL PARTICLES

Core No.	Fuel Content, vol %	Sinter Cycle ^a	Green Weight, gms	Final Weight, gms	Density, Percent of Theoretical	
					Calculated	Exper.
A-1	10	D	643.5	639.8	92.6	92.6
B-1	20	A	645.2	641.5	87.6	87.9
B-2	20	A	638.3	634.7	86.1	87.9
B-3	20	A	638.5	635.5	86.2	87.7
B-4	20	B	622.8	620.9	92.3	91.8 ^b
B-5	20	C	678.9	676.6	89.1	90.9
B-6	20	C	679.3	676.7	89.1	90.7
B-7	20	C	679.3	676.9	90.8	— ^b
C-1	30	D	676.5	672.9	86.0	89.6
C-2	30	E	662.5	660.9	85.0	89.8
C-3	30	E	670.0	668.7	86.0	89.2
C-4	30	E	675.9	674.5	85.2	88.9
W-1	Tungsten Control	D	668.8	662.5	94.5	94.4

^aSintering Cycles (All cores presintered at 800°C – 1 hour in hydrogen)

A – 2400°C – 2 hr

B – 1200°C – 1.5 hr plus 2200°C – 2 hr; H₂ flow 12 cfh

C – 1200°C – 2 hr plus 2200°C – 2.5 hr; H₂ flow 16 cfh

D – 1200°C – 2 hr plus 1800°C – 2 hr plus 2200°C – 2 hr;

H₂ flow 20 cfh

E – 1200°C – 3 hr plus 1800°C – 14 hr plus 2200°C – 2 hr

^bSubsequently densified by autoclaving at 1750°C to 94.7 percent of theoretical density.

of UO_2 - Y_2O_3 . Furthermore, the fuel particles in a core prepared of agglomerated fuel are more rounded or pebble-shaped and the cores show less porosity when agglomerated fuel is used.

Agglomerated Fuel

To demonstrate the advantages of using agglomerated fuel particles in the large cores required, a new series of experimental fueled cores was prepared. A 2-kilogram batch of UO_2 – 8.5 weight percent Y_2O_3 was impact blended, isopressed, crushed, and screened to obtain -270/+400 mesh particles. This material was heated to 750°C in helium for 1 hour to strengthen the agglomerates and then was rescreened to remove fines. The net yield was about 27 percent.

This agglomerated fuel was blended with tungsten powder in batches of 10, 20, and 30 volume percent fuel. Core compacts were cold pressed in a 1.25-inch diameter steel die to form green cores 3.5 inches long weighing 675 grams. These cores were sintered at either 2200° or 2500°C for 2 hours and cooled in argon, sinter cycles F and G, respectively. The results of these experiments are shown in Table B-2. Densities well above 95 percent of theoretical were obtained for all the cores, regardless of fuel loading. The highest densities were obtained by sintering at 2500°C.

The cores had good fuel distribution and contained a few fines generated in blending. The fuel particles were generally round and of good density. The cores sintered at 2500°C had a somewhat coarser grain size develop in the tungsten matrix than that of the 2200°C sin-

TABLE B-2
SINTERED DENSITIES OF W-UO₂-Y₂O₃ CORE COMPOSITES
CONTAINING AGGLOMERATED FUEL PARTICLES

Core No.	Fuel Content, vol %	Sinter Cycle ^a	Green Weight, gms	Final Weight, gms	Density, Percent of Theoretical		
					Calculated	Exper.	As-Machined
A-5	10	G	669.3	667.4	95.8	96.5	96.4
A-6	10	G	678.5	676.5	96.8	96.6	96.4
A-7	10	G	678.5	676.5	96.6	96.6	96.5
B-9	20	G	675.0	673.8	96.5	97.1	—
B-10	20	G	673.5	672.3	96.7	97.2	—
B-11	20	G	673.9	672.7	97.1	97.2	—
C-5	30	F	673.8	672.0	95.7	95.6	95.2
C-6	30	F	675.8	674.0	96.2	95.5	95.2
C-7	30	G	676.5	674.6	97.6	96.9	96.9
C-8	30	G	677.0	673.9	97.5	96.9	96.8

^aAll cores presintered at 800°C — 1 hour in hydrogen.

F — RT to 1200°C — 1 hr; hold 1200°C — 1.5 hr; to 2200°C — 1 hr; hold 2200°C — 2 hr. Cool in argon.

G — Same as F except hold 2200°C — 1 hr; to 2500°C — 1 hr; hold 2500°C — 2 hr; cool to 2100°C in H₂ and then furnace cool in argon.

tered cores, but in general the core structures of the 2500°C sintered cores were superior. Only a trace of free uranium was detected in cores sintered either at 2200° or 2500°C.

X-ray diffraction analysis showed no unreacted UO₂ and a homogeneous solid solution of the UO₂-Y₂O₃ after the 2200°C sinter. After the 2500°C sinter, no free UO₂ or Y₂O₃ was detected, but two solid solution phases were present with A₁ = 5.450 Å and A₂ = 5.437 Å.

The results of these experiments with agglomerated fuel and comparative results obtained using the high-fired, high density fuel were presented to the NASA Technical Director during the second month of the contract. It was agreed that the use of the high-fired UO₂-Y₂O₃ fuel was undesirable for a number of obvious reasons. Technical Directive No. 1 was then issued by the NASA Technical Director authorizing the use of agglomerated fuel for preparation of the test specimens.

~~CONFIDENTIAL~~

APPENDIX C

GAS PRESSURE BONDING STUDIES

Initially it was planned to seal the tungsten sleeve to the W-Re-Mo end-plates by electron beam welding. Six specimens were fabricated in this manner and although five appeared to be gas-tight going into the hot gas pressure bonding operation (autoclave) only one specimen (B-11) was completely bonded as indicated by ultrasonic inspection. This specimen subsequently blistered when subjected to thermal cycle testing.

To avoid the need for welding of tungsten, an overclad of tantalum was employed. It was previously determined that during the autoclave operation the diffusion of tantalum into tungsten was no more than 2 microns. Eight assembled specimens were canned in tantalum and processed in the autoclave at 1730 °C for 1.5 hours under 10,000 psi helium pressure. The tantalum overclad was removed by hydriding at 300 °C. This was successful for one specimen; however, all others lost not only the tantalum but also the tungsten cladding which cracked severely, apparently as a result of stresses induced by the hydrided tantalum.

Molybdenum was then substituted for tantalum as overclad material and proved quite successful. Molybdenum was not selected initially because of anticipated difficulties in welding a gas-tight seal. However, molybdenum could be removed from the clad specimens chemically and was, therefore, attractive as an expendable overclad material.

With the exception of specimen C-8 which was bonded using a tantalum overclad, all of the 15 specimens used for thermal cycle testing were prepared using molybdenum overclad for gas pressure bonding of the tungsten sleeves and end-plates to the core matrix.

~~CONFIDENTIAL~~

~~CONFIDENTIAL~~

APPENDIX D
ALTERNATE FABRICATION PROCEDURES
FOR TYPE D SPECIMENS

The fabrication of the Type D specimens required for this program presented an unusual problem in the preparation of the thin-wall fueled sleeve. Several approaches were investigated before a procedure evolved that would provide a well-bonded, crack-free sleeve of the required dimensional tolerances.

Initially it was proposed that the sleeves be machined from full size fueled cores of high density and the bore be honed to such a diameter as to fit over the fueled core with a snug fit. The sleeve, which at this point would have a heavy wall, would be gas pressure bonded to the core and then be ground on the circumference to produce the required sleeve thickness of 0.020 inch.

This method was unsuccessful because of the inability to internally grind and hone the 3-inch long sleeve without breaking near the midpoint. It did appear feasible, however, for shorter length sleeves.

An alternate method investigated briefly was to isostatically press the sleeve material as a blended powder around the high density machined core, can in molybdenum, and densify by processing in the autoclave at 1750°C. This was not successful because the green fueled sleeve did not sinter or densify sufficiently in the autoclave to permit machining of the molybdenum can or the sleeve without sleeve breakage.

A new approach was suggested by the NASA Technical Director which had been tried at NASA Lewis Research Center and found to be feasible. This method consisted of the following steps:

1. Isostatically press W - 30 percent fuel blend at 50,000 psi to form a green core approximately 1 inch in diameter by 3.5 inches long. A binder of 2 percent stearic acid may be used.
2. Drill small hole in each end of green core compact to serve as centers and grind diameter to about 0.970 inch, calculated to shrink in sintering to approximately 0.840 inch diameter.
3. Center machined core in mold and pour W - 20 percent fuel blend around it.
4. Isostatically press at 35,000 psi to form fueled sleeve around core.
5. Sinter by established procedure to obtain at least 95 percent of theoretical density of both core and sleeve.
6. Cut section off each end and measure diameter of core accurately (± 0.001 inch).
7. Grind on centers to such a diameter that 0.020-inch thick fueled sleeve remains on the core. Thickness must be controlled within 0.001 inch.
8. Trim length to 2.75 inch (2.50 inch minimum).
9. Coat core-sleeve body with 0.0015 inch of tungsten by vapor deposition from tungsten hexachloride.

Eight full size core-sleeve specimens were prepared by this technique while investigating effects of variables in isostatic pressing pressures and the resulting dimensional control. It was shown that no binder material was necessary in cold pressing and that green pressed

~~CONFIDENTIAL~~

~~CONFIDENTIAL~~

compacts could be machined on centers to exact diameters without cracking. The shrinkage of the core during sintering could be predicted within 2 percent, provided slumping of the heavy compact did not occur at temperature. After machining on centers the sleeve thickness, as measured at each end of the core, varied from 0.018 to 0.022 inch. However, this measurement was difficult to make accurately because the interface between core and sleeve could not be sharply defined. If this method of fabricating Type D specimens was used, considerable relief on dimensional tolerance would be required.

Meanwhile, an effort was made to salvage some of the sleeve pieces that had broken during internal grinding in the initial work previously described. It was observed that sleeve lengths up to 1.5 inches could be machined successfully and finish ground to fit over the core which had been centerless ground to 0.785 inch. The sleeve wall thickness was about 0.080 inch at this point. Two pieces of the sleeve were fitted over a core and in so doing both cracked longitudinally. Nevertheless, the assembly was canned in a tantalum capsule and processed in the autoclave at 1750°C under 10,000 psi helium pressure. When the tantalum was ground away and the sleeve thickness reduced to 0.020 inch, it was found that the longitudinal cracks in the sleeve pieces had healed as had the joint between the two sections of sleeving. This was confirmed by dye penetrant inspection and provided sufficient evidence for the success of this method that it was accepted as the optimum approach to fabrication of Type D specimens. The fabrication procedure described in Section III was adopted on the basis of these findings.

~~CONFIDENTIAL~~

~~CONFIDENTIAL~~

APPENDIX E
THERMAL CYCLING TEST PROCEDURES
AND TEST DATA

THERMAL CYCLING TEST PROCEDURES

A typical heating element used in the high temperature thermal cycling furnace is shown in Figure E-1. This all tungsten element is 8 inches long, 2.5 inches in diameter, and is formed from 0.04 inch sheet. Using a split cylinder arrangement, the heating element is welded to a split 0.25 inch thick tungsten end-plate which in turn is welded to two 1.0 inch diameter molybdenum electrodes. A tungsten ring welded to the opposite end of the split tungsten heater provides electrical continuity. With this construction the heating element could be positioned vertically and supported from above. In this manner, the expansion of the heating element arising from high temperature operation is easily accommodated.

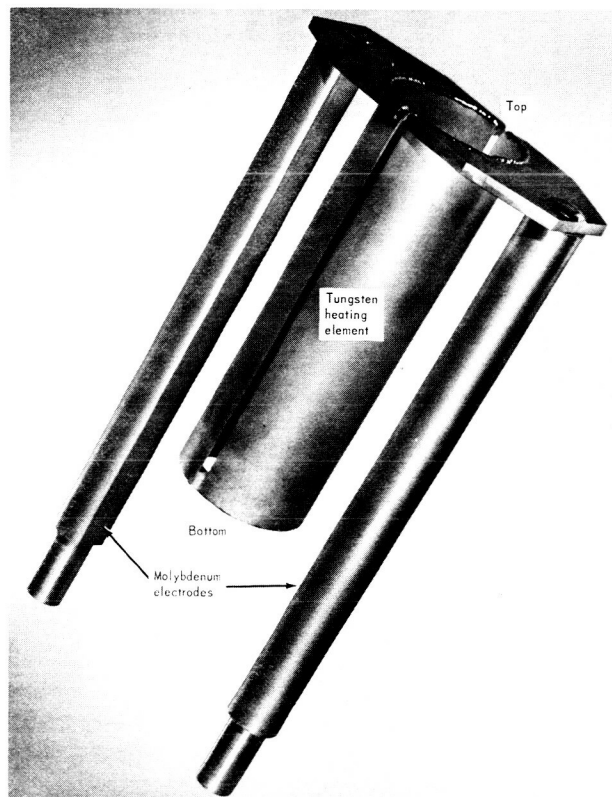


Figure E-1 - Tungsten heating element used in thermal cycling furnace
(Neg. P65-3-23C)

~~CONFIDENTIAL~~

CONFIDENTIAL

During installation, the heating element is held in place and the ends of the molybdenum electrodes are bolted to water-cooled copper terminal rods which penetrate the lower flange of the furnace shell through special insulating glands. Once the heating element is installed, a radiation shield assembly is positioned to encircle the heating element from end to end. In this assembly 10 concentric layers of 5 mil tungsten sheet are employed with a spacing of 0.06 inch. Similar assemblies are provided to function as upper and lower radiation shields to allow for improved thermal efficiency as well as improved temperature uniformity within the hot zone. An outer water-cooled stainless steel furnace shell bolted to the lower furnace flange provides a gas-tight enclosure for operation with various atmospheres.

A photograph of the high temperature thermal cycling furnace along with the associated equipment required in its operation is presented in Figure E-2. It will be observed that the furnace itself is fairly compact having overall external dimensions of 14 inches in diameter by 20 inches in length. Also shown in Figure E-2 is the vacuum system (consisting of mechanical and diffusion pumps) used either in vacuum tests or in pumpdown operations prior to back-filling the furnace with hydrogen or inert gas. Immediately beneath the test furnace is the step-down transformer which supplies up to 24 volts to the furnace heating element. Just to the left of the test furnace is the power control console which incorporates a controller, programmer, and amplifying driver units with a 440 volt saturable core reactor transformer which couples to the step-down transformer located beneath the furnace. The controller unit is a proportioning control system that has potentiometric circuitry which compares a reference d.c. millivoltage set point to a d.c. millivoltage sensor signal. Through the electrical arrangement of this unit and its associated components, the control circuit of the saturable reactor transformer is regulated and controlled. The sensor signal used for control purposes in the thermal cycling testing was obtained from a watts transducer (a thermal conversion device utilizing furnace voltage and current and yielding a

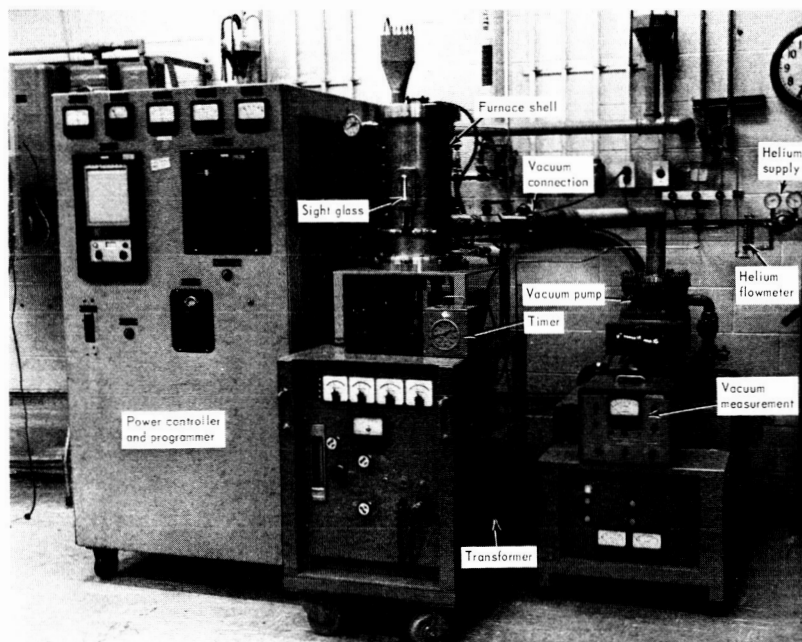


Figure E-2 - Photograph of high temperature thermal cycling furnace and associated equipment (Neg. P65-9-39A)

CONFIDENTIAL

~~CONFIDENTIAL~~

d. c. millivoltage as output signal). The programmer unit used a specially contoured cam to actuate mechanical linkages to adjust a potentiometer providing the reference d. c. millivoltage. By varying the millivoltage set point with time, any desired heating or cooling rate could be imposed. An auxiliary timer was incorporated to interrupt the cam drive circuit so that any dwell time at maximum temperature could be achieved. Also, a special timer switch allowed the furnace to be turned off automatically at the completion of any pre-set number of thermal cycles.

A special safety circuit was also built into the furnace control system to turn off the furnace power in the event of any interruption in main line power, loss of coolant water flow, coolant water over-temperature, low helium pressure, or furnace over-temperature.

It was possible to test three specimens simultaneously in these thermal cycling evaluations. All specimens were placed on a circular tungsten support plate to position them at the longitudinal center of the heating element. Each specimen was set on end with its longitudinal axis parallel to the axis of the heating element and the specimens were spaced to approximate an equilateral triangle within the heating element. Three 0.25 inch diameter tungsten rods served as supports for the 0.25 inch thick tungsten support plate. These tungsten support rods were seated in the lower furnace flange.

Temperature measurements were made by means of an optical pyrometer sighted through the sight-glass on the front of the furnace, through a narrow spacing in the longitudinal thermal shield assembly, through the longitudinal slit in the heating element, and onto a black body target rod. This rod was 0.25 inch in diameter and extended some 4 inches above the circular support plate. It was positioned along the axis of the heating element and at almost the exact center of the cluster of test specimens. Black body holes 0.03 inch in diameter and 0.16 inch in depth were positioned at various locations along the length of this target rod to allow true temperatures to be read at various longitudinal positions within the sample zone of the heating element.

Optical pyrometer calibration was effected in the usual manner by comparison with a standard pyrometer which was calibrated and certified by the National Bureau of Standards. This standard pyrometer is used only for such calibration work and is maintained in the Standards Laboratory of GE-NMPO. In calibrating a "working" pyrometer up to 2200°C, both it and the standard pyrometer were sighted on a tungsten strip lamp, also certified by NBS, and temperatures read simultaneously; for temperatures above 2200°C, a carbon arc was used. Absorption corrections for the quartz sight-glass were obtained in a similar manner in that the tungsten strip lamp temperatures were measured with and without the sight-glass in the optical path.

Before the thermal cycling furnace was put into use, the diffusion pump was actuated and the furnace chamber evacuated to 5×10^{-5} Torr. Furnace shell degassing was then effected by introducing hot water into the coolant passages. When the pressure again reached 5×10^{-5} Torr, the heating element was energized to achieve a hot zone temperature of 2500°C. Furnace degassing was then considered complete and after the furnace power and vacuum pump were turned off, helium was introduced to bring the furnace pressure to 5 psig.

Prior to testing, all specimens were cleaned in acetone to remove any contamination which might have been picked up during inspection and subsequent handling. In preparing for a test, the cleaned specimens were loaded through a 2-inch diameter opening in the top furnace flange and positioned on the tungsten support plate. During this loading operation, a helium flow was maintained to minimize the amount of air admitted to the furnace chamber. When loading was completed, the furnace port was closed with a quartz disc, and

~~CONFIDENTIAL~~

the mechanical pump was energized to yield a chamber pressure of 5×10^{-3} Torr. Hot water then was admitted into the furnace chamber walls. Following this operation, cold water was again admitted into the coolant channels. After the vacuum system was valved off a flow of helium was admitted to the furnace to raise the pressure to 5 psig and then was permitted to flow until the furnace volume had been displaced at least five (5) times. In this way, the furnace was made ready for cycling operations and the furnace control system was energized to impose the desired number of thermal cycles.

In a pre-test calibration run, three solid cylinders of tungsten were employed to simulate the test specimens to be used eventually. A typical thermal cycling test was performed to demonstrate that the desired operating conditions were being obtained and that the control system was functioning to provide completely automatic operation. Temperature measurements made during this particular check-out run led to the temperature-time relationship shown in Figure E-3. It is obvious that the cam employed had the desired shape to yield the proper test conditions. Not only is a 10-minute dwell time achieved but the heating and cooling rates are well within the limits required: in this study, it was specified that at least one hour be taken to heat the samples to 2500°C and that cooling to room temperature should take at least one hour. Based on the solid lines drawn in Figure E-3, the heating and cooling rates approximate 40 and $14.5^{\circ}\text{C}/\text{min.}$, respectively.

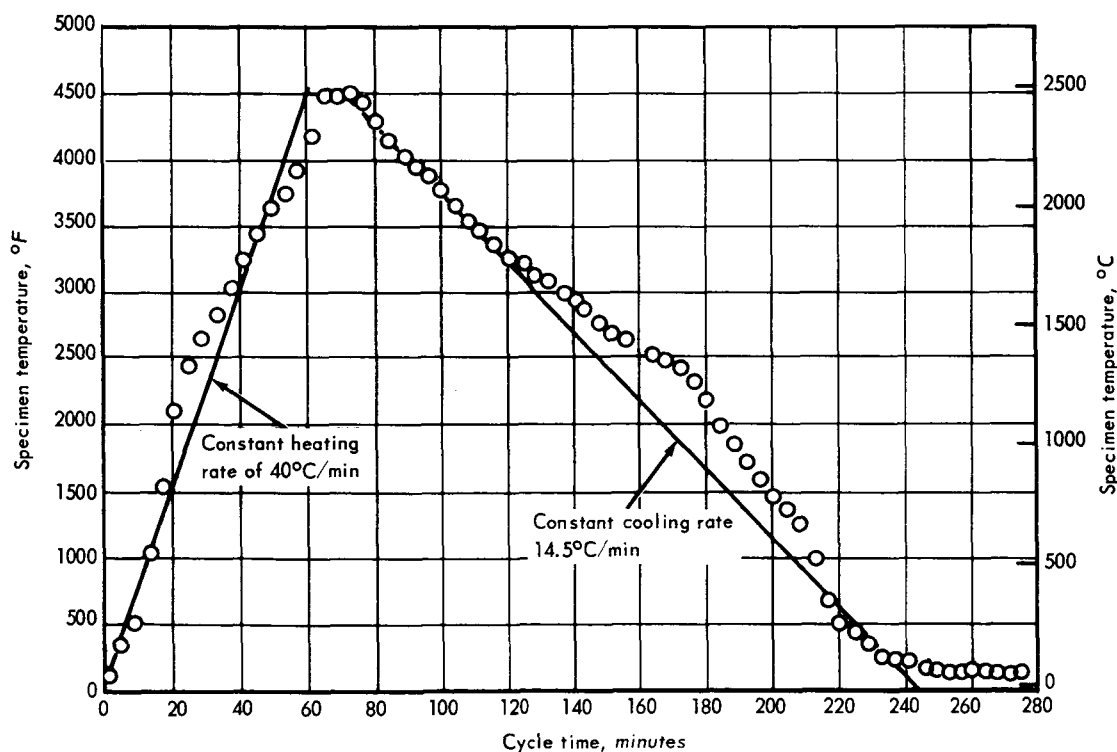


Figure E-3—Typical temperature-time relationship obtained during thermal cycling test with 10-minute dwell time at 2500°C (Temperatures above 1000°C measured optically; below 1000°C a Pt/Pt-10Rh thermocouple was employed)

Also demonstrated in the pre-test calibration run was the ability to consistently reproduce test specimen temperature when a certain millivoltage output of the watts transducer had

~~CONFIDENTIAL~~

been reached. Past experience at GE-NMPO with this type of high temperature furnace indicated that reliable results are obtainable in this manner but it was still considered desirable to reconfirm this operating technique for the type of specimens involved. Furthermore, throughout the thermal cycling test program, daily checks of this relationship were made by measuring the maximum specimen temperature optically, and no temperature deviations were noted. Hence, the use of the watts transducer output to establish a certain temperature was demonstrated to be a reliable approach.

One of the tungsten specimens used in the pre-test calibration runs contained three black body holes drilled at certain longitudinal locations. One hole was drilled at the exact longitudinal mid-point while the other two holes were one inch above and one inch below this middle hole. At a temperature of 2500°C, the specimen temperature was uniform within 35°C with the highest temperature being observed at the hole location near the bottom of the specimen. These temperature measurements were made with an optical pyrometer viewing the black body holes through a quartz window in the side of the furnace. Another temperature measurement was made by sighting the top ends of the three tungsten cylinders through a quartz window in the top of the furnace. Black body holes located at the ends of these specimens indicated the exact same temperature for all three specimens, although this end temperature was some 10°C lower than the value read in the upper black body hole drilled in the side of the one tungsten cylinder. Hence, at a maximum temperature of 2500°C longitudinal temperature uniformity for the specimens was achieved within about 50°C.

THERMAL CYCLING TEST DATA

Thermal cycling test data are presented in Table E-1.

~~CONFIDENTIAL~~

CONFIDENTIAL

TABLE E-1

SUMMARY OF INSPECTION RESULTS OBTAINED IN THERMAL CYCLING TESTS

Specimen	No. of Thermal Cycles	Cumulative Hours on Test	Percent Change in			
			Midpoint Diameter	Length	Volume	Weight
1) – Type Number 1, 10-minute Dwell Tests						
A-7	5	22.5	-0.08	0	-0.14	3×10^{-3}
	10	45.0	-0.14	-0.02	-0.26	6×10^{-3}
	15	67.5	a	a	a	a
	20	90.0	-0.17	0	-0.31	1.2×10^{-2}
	25 ^b	112.5	-0.19	0	-0.35	1.7×10^{-2}
	27	121.5	-0.21	0	-0.43	1.8×10^{-2}
	29	130.5	-0.21	0	-0.33	1.9×10^{-2}
	32	144.0	-0.23	0	-0.37	2.1×10^{-2}
	34	153.0	-0.24	0.01	-0.44	2.2×10^{-2}
	36	162.0	-0.23	0.02	-0.39	2.3×10^{-2}
	38	171.0	-0.24	0.03	-0.43	2.5×10^{-2}
	40 ^e	180.0	-0.25	0.03	-0.42	2.6×10^{-2}
	45	202.5	-0.26	0.05	-0.36	2.9×10^{-2}
	50	225.0	-0.26	0.06	-0.47 (-0.46) ^f	3.1×10^{-2}
B-12	5		-0.14	-0.04	-0.26	7×10^{-3}
	10		-0.23	-0.04	-0.44	1.2×10^{-2}
	15		a	a	a	a
	20		-0.35	0.07	-0.60	2.3×10^{-2}
	25 ^b		-0.41	0.05	-0.69	2.8×10^{-2}
	27	Same as above	-0.43	0.05	-0.81	2.9×10^{-2}
	29		-0.46	0.07	-0.74	2.8×10^{-2}
	32		-0.47	0.08	-0.71	3.1×10^{-2}
	34		-0.47	0.10	-0.77	3.2×10^{-2}
	36		-0.50	0.10	-0.74	3.3×10^{-2}
	38		-0.51	0.11	-0.77	3.4×10^{-2}
	40 ^e		-0.52	0.15	-0.77	3.5×10^{-2}
	45		-0.54	0.18	-0.69	3.7×10^{-2}
	50	-0.56	0.20	-0.87 (-0.92)	3.8×10^{-2}	
C-8	5		-0.03	0.05	0.07	-7×10^{-3}
	10		-0.02	0.14	0.13	-1.4×10^{-2}
	15		a	a	a	a
	20		-0.14	0.26	0.19	-1.9×10^{-2}
	25 ^b		-0.10	0.32	0.25	c
	27	Same as above	-0.17	c	0.07	-2.4×10^{-2}
	29		-0.19	0.34	0.14	c
	32		-0.19	0.36	0.16	-3.5×10^{-2}
	34		-0.21	0.38	-0.16	-2×10^{-3d}
	36		-0.21	0.38	-0.13	-2×10^{-3}
	38		-0.22	0.39	-0.16	-4×10^{-3}
	40 ^e		-0.23	0.38	-0.14	-7×10^{-3}
	45		-0.26	0.44	-0.11	-1.1×10^{-2}
	50	-0.25	0.47	-0.17 (-0.03)	-2.0×10^{-2}	

CONFIDENTIAL

~~CONFIDENTIAL~~

TABLE E-1 (Cont.)

SUMMARY OF INSPECTION RESULTS OBTAINED IN THERMAL CYCLING TESTS

Specimen	No. of Thermal Cycles	Cumulative Hours on Test	Percent Change in			
			Midpoint Diameter	Length	Volume	Weight
B-10	5	22.5	0.02	0.04	0.18	2×10^{-3}
	10	45.0	0.03	0.09	0.77	4×10^{-3}
	15	67.5	-0.03	0.13	0.07	6×10^{-3}
	20	90.0	-0.06	0.17	0.14	9×10^{-3}
	25	112.5	-0.10	0.19	0.16	1.2×10^{-2}
	30	135.0	-0.05	0.26	0.09	1.4×10^{-2}
	35	157.5	-0.11	0.28	0.19	1.7×10^{-2}
	40	180.0	-0.11	0.33	0.21	2.0×10^{-2}
	45	202.5	-0.13	0.36	0.26	2.5×10^{-2}
	50	225.0	-0.14	0.40	0.16 (0.12)	2.8×10^{-2}
C-7	5		0.01	0.07	0.17	4×10^{-3}
	10		0.01	0.05	0.04	6×10^{-3}
	15		0.01	0.09	0.10	8×10^{-3}
	20		0.01	0.12	0.22	9×10^{-3}
	25		0.00	0.12	0.23	9×10^{-3}
	30	Same as above	0.00	0.12	0.09	1.0×10^{-2}
	35		0.00	0.14	0.21	1.1×10^{-2}
	40		-0.01	0.15	0.22	1.1×10^{-2}
	45		0.00	0.19	0.27	1.3×10^{-2}
	50		-0.02	0.20	0.17 (0.16)	1.6×10^{-2}
A-15	5		-0.13	0.10	-0.06	5×10^{-3}
	10		-0.21	0.15	-0.16	7×10^{-3}
	15		-0.27	0.20	0.10	1×10^{-2}
	20		-0.32	0.23	-0.24	1.3×10^{-2}
	25		-0.35	0.27	-0.23	1.6×10^{-2}
	30	Same as above	-0.37	0.31	-0.32	1.8×10^{-2}
	35		-0.39	0.34	-0.29	2.0×10^{-2}
	40		-0.42	0.38	-0.27	2.3×10^{-2}
	45		-0.43	0.39	-0.25	2.6×10^{-2}
	50		-0.45	0.45	-0.36 (-0.45)	3.0×10^{-2}
2) - Type Number 2, 1-hour Dwell Tests						
A-8	5	26.66	-0.24	0.32	-0.01	-2×10^{-4}
	10	53.33	-0.32	0.43	-0.07	-9×10^{-3}
	15	80.00	-0.41	0.51	-0.13	-1×10^{-4}
	20	106.66	-0.46	0.56	-0.13	7×10^{-3}
	25	133.33	-0.49	0.64	-0.31	7×10^{-3}
	30	160.00	-0.53	0.65	-0.19	6×10^{-3}
	35	186.66	-0.54	0.78	-0.09	5×10^{-3}
	40	213.33	-0.56	0.75	-0.17	4×10^{-3}
	45	240.00	-0.59	0.84	-0.14	4×10^{-3}
	50	266.66	-0.59	0.83	-0.16 (-0.35)	4×10^{-3}

~~CONFIDENTIAL~~

CONFIDENTIAL

TABLE E-1 (Cont.)

SUMMARY OF INSPECTION RESULTS OBTAINED IN THERMAL CYCLING TESTS

Specimen	No. of Thermal Cycles	Cumulative Hours on Test	Percent Change in			
			Midpoint Diameter	Length	Volume	Weight
B-14	5		-0.28	-0.01	-0.47	6×10^{-3}
	10		-0.34	0	-0.63	9×10^{-3}
	15		-0.44	0	-0.81	2×10^{-2}
	20		-0.51	0.02	-0.89	2×10^{-2}
	25	Same as above	-0.55	0.05	-0.45	3×10^{-2}
	30		-0.61	0.06	-1.09	3×10^{-2}
	35		-0.66	0.10	-1.04	4×10^{-2}
	40		-0.71	0.12	-1.13	4×10^{-2}
	45		-0.73	0.15	-1.17	4×10^{-2}
	50		-0.75	0.19	-1.09 (-1.31)	4×10^{-2}
	51 ^h	337.00	-0.76	0.26	-1.18	6×10^{-2}
	56	363.66	-0.78	0.28	-1.09	6×10^{-2}
	61	390.33	-0.80	0.33	-1.20	6×10^{-2}
	66	416.00	-0.82	0.39	-1.20	7×10^{-2}
	71	442.66	-0.83	0.40	-1.19	7×10^{-2}
C-9	5		-0.14	0.42	0.13	1×10^{-2}
	10		-0.28	0.59	0.20	1×10^{-2}
	15		-0.31	0.59	0.16	2×10^{-2}
	20		-0.36	0.65	0.23	3×10^{-2}
	25	Same as A-8	-0.38	0.73	0.02	3×10^{-2}
	30		-0.42	0.77	0.16	4×10^{-2}
	35		-0.44	0.83	0.27	4×10^{-2}
	40		-0.47	0.89	0.22	4×10^{-2}
	45		-0.48	0.95	0.24	4×10^{-2}
	50		-0.50	1.0	0.36 (0)	5×10^{-2}
A-10	5		-0.13	0.04	-0.10	-5×10^{-4}
	10		-0.19	0.11	-0.26	2×10^{-4}
	15		-0.21	0.18	-0.09	-3×10^{-4}
	20		-0.29	0.22	-0.09	-9×10^{-4}
	25	Same as above	-0.29	0.28	-0.14	-2×10^{-3}
	30		-0.32	0.31	0	-2×10^{-3}
	35		-0.33	0.38	-0.04	-3×10^{-3}
	40		-0.35	0.41	-0.06	-7×10^{-3}
	45		-0.35	0.45	-0.06	-8×10^{-3}
	50		-0.35	0.49	-0.02 (-0.21)	-8×10^{-3}
B-19	5		-0.18	0.15	-0.03	6×10^{-4}
	10		-0.26	0.23	-0.10	-3×10^{-4}
	15		-0.34	0.30	-0.11	-1×10^{-3}
	20		-0.37	0.41	-0.12	-2×10^{-3}
	25	Same as above	-0.39	0.49	-0.23	-1×10^{-3}
	30		-0.42	0.54	-0.04	-3×10^{-3}
	35		-0.45	0.59	-0.09	-3×10^{-3}
	40		-0.44	0.66	-0.15	-4×10^{-3}
	45		-0.45	0.76	-0.01	-4×10^{-3}
	50		-0.47	0.81	-0.01 (-0.13)	-5×10^{-3}

CONFIDENTIAL

~~CONFIDENTIAL~~

TABLE E-1 (Cont.)

SUMMARY OF INSPECTION RESULTS OBTAINED IN THERMAL CYCLING TESTS

Specimen	No. of Thermal Cycles	Cumulative Hours on Test	Percent Change in			
			Midpoint Diameter	Length	Volume	Weight
C-10	5	Same as above	-0.18	0.22	-0.03	1×10^{-2}
	10		-0.29	0.34	-0.13	1×10^{-2}
	15		-0.35	0.43	-0.15	1×10^{-2}
	20		-0.48	0.52	-0.19	1×10^{-2}
	25		-0.50	0.45	-0.34	2×10^{-2}
	30		-0.56	0.66	-0.18	2×10^{-2}
	35		-0.61	0.91	-0.34	2×10^{-2}
	40		-0.65	0.79	-0.37	2×10^{-2}
	45		-0.67	0.83	-0.49	2×10^{-2}
	50		-0.71	0.88	-0.48 (-0.54)	2×10^{-2}
B-13	1 ^h	71.33	-0.41	0.06	-0.40	2×10^{-2}
T 0.85 ^j	6	98.00	-0.48	0.08	-0.38	2×10^{-2}
B -0.26	11	124.66	-0.53	0.24	-0.51	2×10^{-2}
	16	151.33	-0.56	0.25	-0.60	2×10^{-2}
	21	177.00	-0.60	0.28	-0.63	3×10^{-2}
W-1	5	26.66	-0.33	0.02	-1.05	-1×10^{-3}
(unclad tungsten)	10	53.33	-0.39	-0.03	-1.30	-2×10^{-3}
	15	80.00	-0.41	-0.04	-1.34	-4×10^{-3}
T -0.28	20	106.66	-0.43	-0.05	-1.35	-6×10^{-3}
B -0.46						
W-2	1	71.33	-0.35	-0.32	-4.67 ⁱ	-1×10^{-2}
(unclad tungsten)		(67-hour soak)				
T -0.27						
B -0.16						

3) - Type Number 1, 10-minute Dwell Tests of Type D Specimens

D-2	5	22.5	-0.01	0.11	0.07	-6×10^{-2}
	10	45.0	-0.01	0.11	0.14	-1×10^{-1}
	15	67.5	-0.02	0.07	0.03	-1×10^{-1}
	20	90.0	-0.02	0.08	-0.02	-1×10^{-1}
	25	112.5	-0.03	0.09	0	-1×10^{-1}
T 0.46	30	135.0	-0.04	0.10	-0.06	-2×10^{-1}
B 0.16	35	157.5	-0.05	0.10	-0.05	-2×10^{-1}
	40	180.0	-0.07	0.11	-0.04	-2×10^{-1}
	45	202.5	-0.08	0.13	-0.05	-2×10^{-1}
	50	225.0	-0.10	0.16	-0.05 (-0.04)	-2×10^{-1}

~~CONFIDENTIAL~~

~~CONFIDENTIAL~~

TABLE E-1 (Cont.)

SUMMARY OF INSPECTION RESULTS OBTAINED IN THERMAL CYCLING TESTS

Specimen	No. of Thermal Cycles	Cumulative Hours on Test	Percent Change in			
			Midpoint Diameter	Length	Volume	Weight
D-3	5	Same as above	-0.01	1.99	1.03	8×10^{-3}
	10		-0.04	2.99	1.38	6×10^{-3}
	15		0	3.40	1.56	1×10^{-2}
	20		0.12	3.73	1.80	1×10^{-2}
T 2.4	25		0.15	5.10	2.50	9×10^{-3}
B 0.15	30		0.18	5.66	2.70	9×10^{-3}
	35		0.22	5.80	2.80	8×10^{-3}
	40		0.28	6.14	2.91	8×10^{-3}
	45		0.31	5.85	3.23	5×10^{-3}
	50		0.33	5.81	3.10	6×10^{-3}
D-4	5	Same as above	0.02	0.26	0.08	-4×10^{-3}
	10		0.13	0.27	0.32	2×10^{-3}
	15		0.20	0.33	0.60	4×10^{-3}
	20		0.24	0.39	0.72	8×10^{-3}
T 0.61	25		0.28	0.42	0.90	1×10^{-2}
B 0.3	30		0.33	0.45	1.08	2×10^{-2}
	35		0.38	0.47	0.96	2×10^{-2}
	40		0.43	0.51	1.34	3×10^{-2}
	45		0.43	0.54	1.50	3×10^{-2}
	50		0.46	0.58	1.48	3×10^{-2}

^aNo inspection; automatic timer failed to interrupt test after 15 cycles.

^bProgram specified inspection after every two cycles following Cycle No. 20; automatic timer failed to interrupt test at end of Cycle No. 22; this difficulty with the automatic timer was eventually corrected.

^cNot measured.

^dNew weight taken after removing small piece of tantalum foil from end cap region. Subsequent values are cumulative from this point.

^eApproval received to inspect after every 5 thermal cycles rather than after every 2 cycles.

^fPercentage change in specimen volume estimated from diameter and length measurements corresponding to inspection results after 50 thermal cycles.

^gOne small blister (about 5 mils high and 0.4 inch in diameter) noted after 15 cycles; after 50 cycles blister increased in height to about 30 mils.

^hAfter 67-hour isothermal soak at 2500°C.

ⁱVolume measurements distorted by slight surface porosity of specimen.

^jPercentage change in specimen diameter at top and bottom given by T and B, respectively.

~~CONFIDENTIAL~~

~~CONFIDENTIAL~~

~~CONFIDENTIAL~~

~~CONFIDENTIAL~~

REPORT DISTRIBUTION LIST FOR
CONTRACT NO. NAS 3-6213

NASA Lewis Research Center (3)
21000 Brookpark Road
Cleveland, Ohio 44135
Attention: Neal T. Saunders

NASA Lewis Research Center (1)
21000 Brookpark Road
Cleveland, Ohio 44135
Attention: Technical Utilization Office,
MS 3-16

NASA Lewis Research Center (2)
21000 Brookpark Road
Cleveland, Ohio 44135
Attention: Library

U. S. Atomic Energy Commission (3)
Technical Reports Library
Washington, D. C.

AEC Headquarters (1)
Div. of Reactor Development
Washington, D. C.
Attention: J. Simmons

National Aeronautics and Space
Administration (2)
Washington, D. C. 20546
Attention: NPO

NASA Lewis Research Center (1)
21000 Brookpark Road
Cleveland, Ohio 44135
Attention: Office of Reliability and
Quality Assurance

NASA Ames Research Center (1)
Moffett Field, California 94035
Attention: Library

NASA Goddard Space Flight Center (1)
Greenbelt, Maryland 20771
Attention: Library

NASA Lewis Research Center (1)
21000 Brookpark Road
Cleveland, Ohio 44135
Attention: Thomas J. Flanagan
Contracting Officer
Mail Stop 500-210

NASA Scientific and Technical
Information Facility (6 and Reproducible)
Box 5700
Bethesda, Maryland
Attention: NASA Representative

NASA Lewis Research Center (1)
21000 Brookpark Road
Cleveland, Ohio 44135
Attention: Reports Control Office

U. S. Atomic Energy Commission (3)
Technical Information Service Extension
P. O. Box 62
Oak Ridge, Tennessee

National Aeronautics and Space
Administration (1)
Washington, D. C. 20546
Attention: G. Deutsch (RRM)

NASA Lewis Research Center
21000 Brookpark Road
Cleveland, Ohio 44135
Attention: (One copy each)
Nuclear Technology Office, MS 501-2
Neal Saunders, MS 105-1
S. Kaufman, MS 49-2
T. Moss, MS 500-309
J. Creagh, MS 500-309
H. Smreker, MS 501-2

NASA Flight Research Center (1)
P. O. Box 273
Edwards, California 93523
Attention: Library

~~CONFIDENTIAL~~

~~CONFIDENTIAL~~

Jet Propulsion Laboratory (1)
4800 Oak Grove Drive
Pasadena, California 91103
Attention: Library

NASA Langley Research Center (1)
Langley Station
Hampton, Virginia 23365
Attention: Library

NASA Marshall Space Flight Center (1)
Huntsville, Alabama
Attention: Library

Argonne National Laboratory (2)
9700 South Cass Avenue
Argonne, Illinois
Attention: J. Schumar
R. Noland

Oak Ridge Gaseous Diffusion Plant (1)
Oak Ridge, Tennessee
Attention: P. Huber

Battelle Memorial Institute (1)
505 King Avenue
Columbus, Ohio 43201
Attention: E. Hodge

Sylvania Electric Products (1)
Chemical and Metallurgical Div.
Towanda, Pennsylvania
Attention: M. MacInnis

United Nuclear Corp. (1)
New Haven, Conn.
Attention: Library

General Atomic Division (1)
General Dynamics Corp.
P. O. Box 608
San Diego, California 92112
Attention: A. Weinberg

General Electric Co.
Vallecitos Atomic Laboratory
P. O. Box 846
Pleasanton, California
Attention: A. Kaznoff

Los Alamos Scientific Laboratory
Los Alamos, New Mexico
Attention: J. Taub

NASA Manned Spacecraft Center (1)
Houston, Texas 77001
Attention: Library

NASA Western Operations (1)
150 Pico Boulevard
Santa Monica, California 90406
Attention: Library

Battelle Northwest Laboratories
P. O. Box 999
Richland, Washington 99352
Attention: D. R. deHalas

Nuclear Materials and Equipment Corp.
Apollo, Pennsylvania
Attention: B. Vondra

Westinghouse Electric Corp. (1)
Astronuclear Laboratory
Box 10864
Pittsburgh, Pennsylvania 15236
Attention: D. Thomas

Union Carbide Corp. (1)
Nuclear Products Department
Lawrenceburg, Tennessee
Attention: W. Eatherly

Atomics International Division (1)
North American Aviation
8900 Desota Avenue
Canoga Park, California
Attention: S. Carneglia

Martin-Marietta Corp.
Nuclear Division
Baltimore, Maryland 21203
Attention: J. Monroe

Lawrence Radiation Laboratory
Livermore, California
Attention: A. Rothman

~~CONFIDENTIAL~~

DISTRIBUTION

INTERNAL

J. Barnard (NTD)
H. C. Brassfield
R. W. Briskin
L. P. Bupp (NTD-VAL)
V. P. Calkins
K. P. Cohen (APO)
J. F. Collins (2)
P. K. Conn
J. B. Conway (2)
D. H. Culver
N. P. Fairbanks
E. W. Filer
A. B. Greninger (NTD)
G. F. Hamby
L. D. Jordan
G. Kortan
L. McEwen (IPO)
J. E. McConnelee
J. A. McGurty
G. T. Muehlenkamp
S. Naymark
W. E. Niemuth
G. Pomeroy
R. B. Richards (APED)
F. C. Robertshaw
D. G. Salyards
J. E. Van Hoomissen (NTD-SPNSO)
W. R. Yario
J. F. Young (NED)
Library (6)

~~CONFIDENTIAL~~